

CT
87
19

note technical note techn

COPY 2

Microwave Landing System Area Navigation (MLS RNAV) Transformation Algorithms and Accuracy Testing

Barry R. Billman
James H. Remer
Min. J. C.
~~FEDERAL AVIATION ADMINISTRATION~~

NOV 18 Rec'd

TECHNICAL CENTER LIBRARY
ATLANTIC CITY, N.J. 08405

May 1987

DOT/FAA/CT-TN87/19

This document is available to the U.S. public
through the National Technical Information
Service, Springfield, Virginia 22161.



U.S. Department of Transportation
Federal Aviation Administration
Technical Center
Atlantic City International Airport, N.J. 08405

NOTICE

This document is disseminated under the sponsorship of the Department of Transportation in the interest of information exchange. The United States Government assumes no liability for the contents or use thereof.

The United States Government does not endorse products or manufacturers. Trade or manufacturer's names appear herein solely because they are considered essential to the object of this report.

1. Report No. DOT/FAA/CT-TN87/19		2. Government Accession No.		3. Recipient's Catalog No.	
4. Title and Subtitle MICROWAVE LANDING SYSTEM AREA NAVIGATION (MLS RNAV) TRANSFORMATION ALGORITHMS AND ACCURACY TESTING				5. Report Date July 1987	
				6. Performing Organization Code ACT-140	
7. Author(s) Barry R. Billmann, James H. Remer, and Min-Ju Chang				8. Performing Organization Report No. DOT/FAA/CT-TN87/19	
9. Performing Organization Name and Address Department of Transportation Federal Aviation Administration Technical Center Atlantic City International Airport, N.J. 08405				10. Work Unit No. (TRAIS)	
				11. Contract or Grant No. T0701G	
12. Sponsoring Agency Name and Address Department of Transportation Federal Aviation Administration Program Engineering and Maintenance Service Washington, D.C. 20590				13. Type of Report and Period Covered Technical Note	
				14. Sponsoring Agency Code APM-450	
15. Supplementary Notes Helicopter Program					
16. Abstract Microwave Landing System Area Navigation (MLS RNAV) is a technique which affords the ability to perform precision navigation in the terminal area of a heliport or airport. It utilizes the signal coverage provided by the MLS angle data transmitters and associated precision distance measuring equipment (DME/P). Navigation performed using an MLS RNAV system is not limited to approaches along a runway centerline or azimuth radial, but may assume any conceivable flightpath within MLS coverage. Examples of these types of approaches would include curves, segmented and oblique offset (parasite), as well as computed centerline (offset) approaches. The work presented herein treats MLS RNAV from a theoretical perspective. MLS RNAV transformation algorithms are developed and tested under real world and laboratory conditions. Anticipated system accuracy is computed under various anticipated operational scenarios. These scenarios include parasite and computed centerline approaches, including the effects of signal source error. The effects on total system accuracy of offsetting the conical elevation transmitter from the runway centerline are presented. The errors associated with computed centerline approaches when the azimuth is offset from the runway centerline is presented.					
17. Key Words Area Navigation (RNAV) Helicopter Microwave Landing System (MLS) Heliport			18. Distribution Statement This Document is Available to the U.S. Public Through the National Technical Information Service, Springfield, Va. 22161		
19. Security Classif. (of this report) Unclassified		20. Security Classif. (of this page) Unclassified		21. No. of Pages 148	22. Price

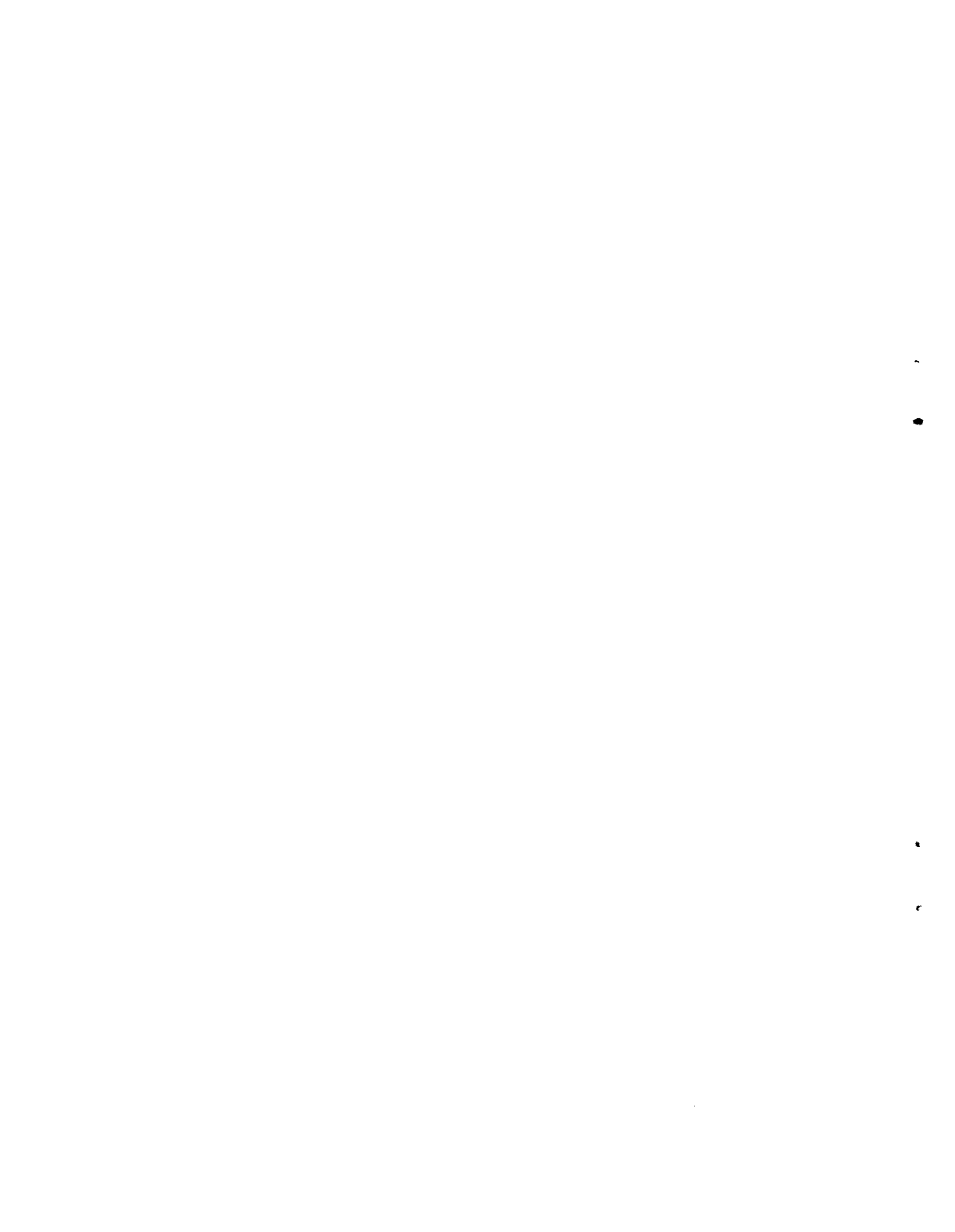
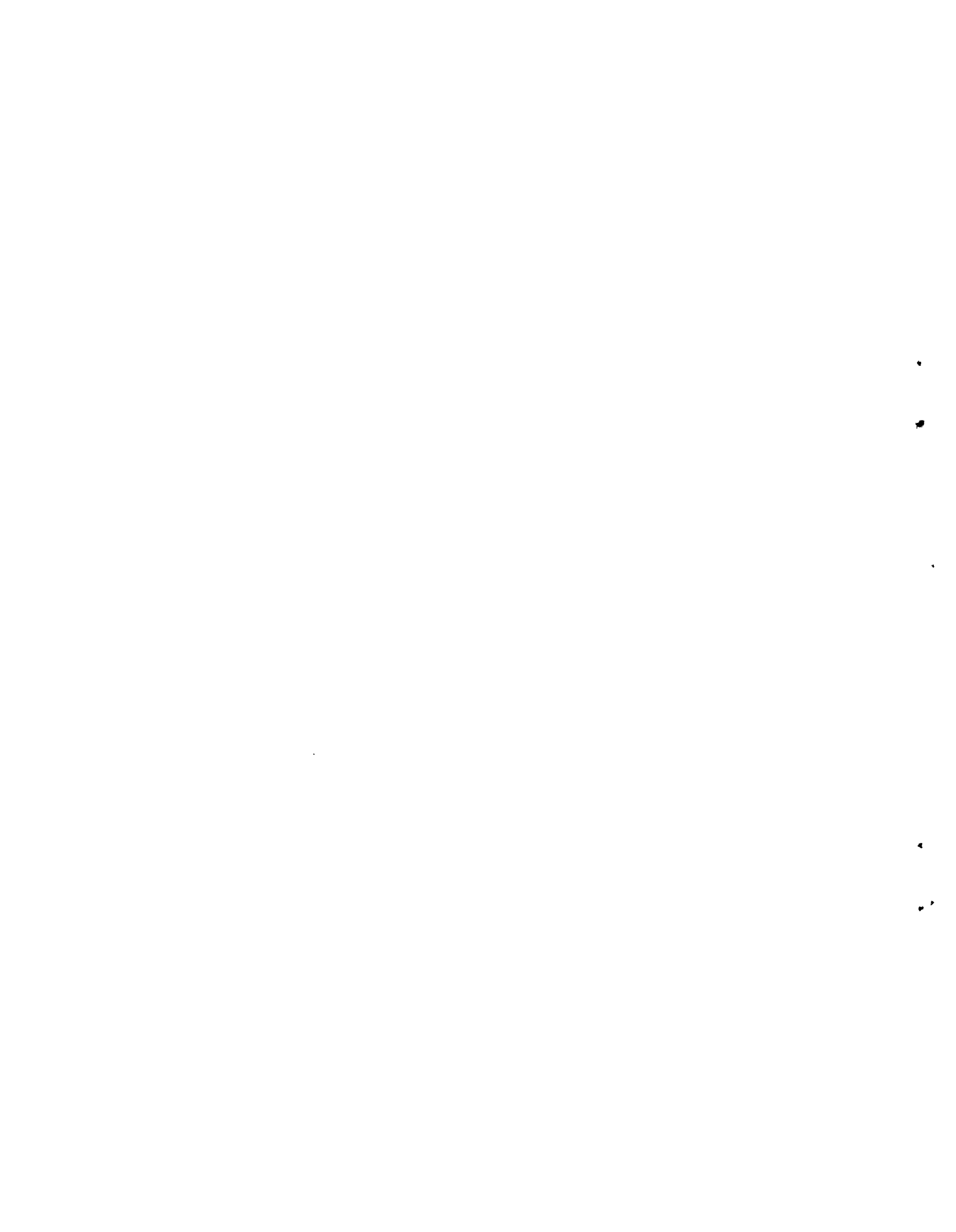


TABLE OF CONTENTS

	Page
EXECUTIVE SUMMARY	xiii
INTRODUCTION	1
Purpose	1
Background	1
DISCUSSION	2
MLS Coordinate Transformation Algorithms	2
MLS Coordinate Transformation Algorithm Descriptions	3
Transformation Algorithm Philosophy and Usage	3
Coordinate Transformation Algorithm Test Procedure	29
Grid Point Testing	29
MLS RNAV Flight Simulations (Synthesized Input Data)	60
MLS RNAV Flight Simulations (Actual Flight Data)	71
Signal Source Error Simulations for Computed Centerline Approaches	76
Signal Source Error Simulations for Parasite Approaches	92
Parasite Approach Measures of Skewness and Kurtosis	98
Conical Elevation Induced Errors	107
SUMMARY OF RESULTS	118
CONCLUSIONS	127
BIBLIOGRAPHY	129
APPENDIXES	
A - Cartesian to MLS Coordinate Transformations	
B - MLS Signal Accuracy Degradation	
C - Parasite Approach Studies Measures of Skewness and Kurtosis	
D - Conic Elevation Induced Error Computations	



LIST OF ILLUSTRATIONS

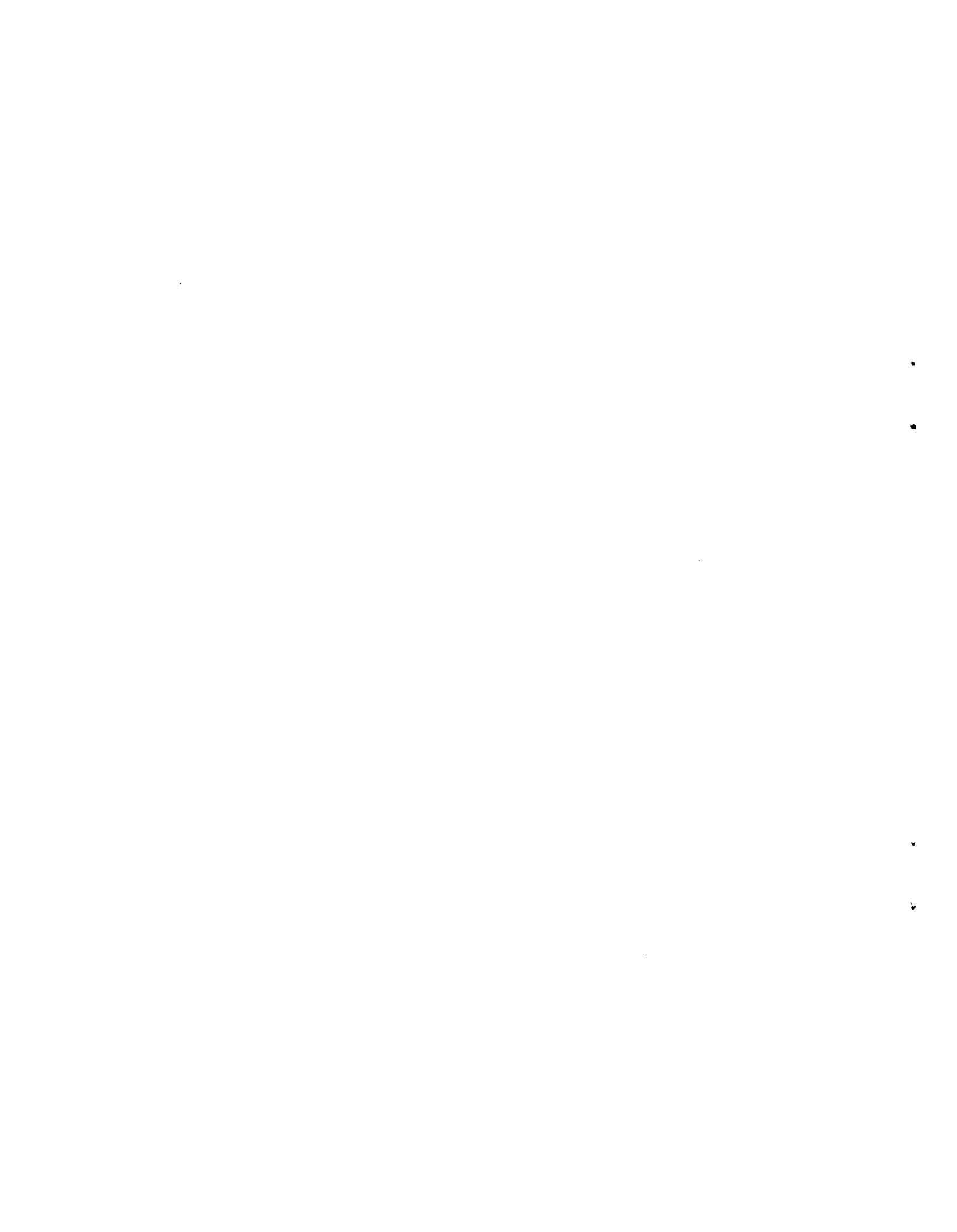
Figure		Page
1	Conical Graphical Solution	4
2	Planar Graphical Solution	5
3	Case I, Geometry	10
4	Case II, Geometry	14
5	Case III, Geometry	17
6	Case IV, Geometry	20
7	Case V, Geometry	24
8	Case VI, Geometry	28
9	Case VII, Geometry	34
10	Case VIII, Geometry	37
11	Case IX, Geometry	42
12	Case X, Geometry	47
13	Case XI, Geometry	52
14	Case XII, Geometry	59
15	Lab Simulation 1, Along-Track Error, Shreeves Algorithm, 10° Azimuth, 6° Glidepath	61
16	Lab Simulation 1, Crosstrack Error, Shreeves Algorithm, 10° Azimuth, 6° Glidepath	62
17	Lab Simulation 1, Height Error Shreeves Algorithm, 10° Azimuth, 6° Glidepath	63
18	Lab Simulation 2, Along-Track Error, Shreeves Algorithm, 30° Azimuth, 9° Glidepath	65
19	Lab Simulation 2, Crosstrack Error, Shreeves Algorithm, 30° Azimuth, 9° Glidepath	66
20	Lab Simulation 2, Height Error, Shreeves Algorithm, 30° Azimuth, 9° Glidepath	67
21	Lab Simulation 3, Along-Track Error, Thedford Algorithm, 10° Azimuth, 6° Glidepath	68

LIST OF ILLUSTRATIONS (CONTINUED)

Figure		Page
22	Lab Simulation 3, Crosstrack Error, Thedford Algorithm, 10° Azimuth, 6° Glidepath	69
23	Lab Simulation 3, Height Error, Thedford Algorithm, 10° Azimuth, 6° Glidepath	70
24	Lab Simulation 4, Along-Track Error, Thedford Algorithm, 30° Azimuth, 9° Glidepath	72
25	Lab Simulation 4, Crosstrack Error, Thedford Algorithm, 30° Azimuth, 9° Glidepath	73
26	Lab Simulation 4, Height Error, Thedford Algorithm, 30° Azimuth, 9° Glidepath	74
27	MLS RNAV System Software Block Diagram	75
28	Example of MLS RNAV Offset Azimuth Computed Centerline Approach	78
29	Monte Carlo Determination of MLS RNAV Position Error	80
30	Signal Source Error Simulation Results, Crosstrack Error, Elevation Transmitter to Azimuth Transmitter Distance, 3,000 to 9,000 ft	89
31	Signal Source Error Simulation Results, Crosstrack Error, Elevation Transmitter to Azimuth Transmitter Distance, 3,500 to 9,000 ft	90
32	Signal Source Error Simulation Results, Crosstrack Error, Elevation Transmitter to Azimuth Transmitter Distance, 4,000 to 10,000 ft	91
33	Signal Source Error Simulation Results, Along-Track Error, Elevation Transmitter to Azimuth Transmitter Distance, 3,000 to 9,000 ft	93
34	Signal Source Error Simulation Results, Along-Track Error, Elevation Transmitter to Azimuth Transmitter Distance, 4,000 to 10,000 ft	94

LIST OF ILLUSTRATIONS (CONTINUED)

Table		Page
35	Signal Source Error Simulation Results, Along-Track Error, Elevation Transmitter to Azimuth Transmitter Distance, 3,500 to 9,500 ft	95
36	MLS RNAV Approach to Noninstrumented Runway	96
37	MLS RNAV Approach to an On-Field Heliport	97
38	Parasite Approach Cross and Along-Track Error Plots	105
39	Parasite Approach Vertical Track Error Plots	106
40	Glidepath Error for Offset Elevation (EL = 3°)	115
41	Glidepath Error for Offset Elevation (EL = 6°)	116
42	Glidepath Error for Offset Elevation (EL = 9°)	117



LIST OF TABLES

Table		Page
1	MLS Reconstruction Algorithms	6
2	Test Parameters for MLS RNAV Lab Simulations	64
3	Total MLS RNAV System Error in Position Determination	77
4	Crosstrack Error due to Azimuth Offset, DH = 200 ft, Glidepath Angle = 3°	81
5	Along-track Error Due to Azimuth Offset, DH = 200 ft, Glidepath Angle = 3°	82
6	Crosstrack Error Due to Azimuth Offset, DH = 250 ft, Glidepath Angle = 4.5°	83
7	Along-Track Error Due to Azimuth Offset, DH = 250 ft Glidepath Angle = 4.5°	84
8	Crosstrack Error Due to Azimuth Offset, DH = 300 ft Glidepath Angle = 6.0°	85
9	Along-Track error Due to Azimuth Offset, DH = 300 ft Glidepath Angle = 6.0°	86
10	Crosstrack Error Due to Azimuth Offset, DH = 350 ft Glidepath Angle = 9.0°	87
11	Along-Track Error Due to Azimuth Offset, DH = 350 ft Glidepath Angle = 9.0°	88
12	Parasite Approach Simulation, 45° Course Angle, Decision Height = 200 ft	99
13	Parasite Approach Simulation, 315° Course Angle, Decision Height = 200 ft	100
14	Parasite Approach Simulation, 45° Course Angle, Decision Height = 250 ft	101
15	Parasite Approach Simulation, 315° Course Angle, Decision Height = 250 ft	102
16	Parasite Approach Simulation, 45° Course Angle, Decision Height = 300 ft	103
17	Parasite Approach Simulation, 315° Course Angle, Decision Height = 300 ft	104

LIST OF TABLES (CONTINUED)

Table		Page
18	Skewness and Kurtosis for Parasite Approach Simulation for 45° Approach at DH = 200 ft	108
19	Skewness and Kurtosis for Parasite Approach Simulation for 315° Approach at DH = 200 ft	109
20	Skewness and Kurtosis for Parasite Approach Simulation for 45° Approach at DH = 250 ft	110
21	Skewness and Kurtosis for Parasite Approach Simulation for 315° Approach at DH = 250 ft	111
22	Skewness and Kurtosis for Parasite Approach Simulation for 45° Approach at DH = 300 ft	112
23	Skewness and Kurtosis for Parasite Approach Simulation for 315° Approach at DH = 300 ft	113
24	Vertical Position Error (Feet) Due to Offset of Conic Elevation	114
25	Part I, MLS Threshold Crossing Errors (ft), EL Angle = 2.5°	119
26	Part I, MLS Threshold Crossing Errors (ft), EL Angle = 3.0°	119
27	Part I, MLS Threshold Crossing Errors (ft), EL Angle = 3.5°	120
28	Part I, MLS Threshold Crossing Errors (ft), EL Angle = 4.0°	120
29	Part I, MLS Threshold Crossing Errors (ft), EL Angle = 2.5°, EL Phase Center Height = 8.0 ft	121
30	Part I, MLS Threshold Crossing Errors (ft), EL Angle = 3.0°, EL Phase Center Height = 8.0 ft	121
31	Part I, MLS Threshold Crossing Errors (ft), EL Angle = 3.5°, EL Phase Center Height = 8.0 ft	122
32	Part I, MLS Threshold Crossing Errors (ft), EL Angle = 4.0°, EL Phase Center Height = 8.0 ft	122
33	Part II, MLS Threshold Crossing Errors (Degrees) EL Angle = 2.5°	123
34	Part II, MLS Threshold Crossing Errors (Degrees) EL Angle = 3.0°	123
35	Part II, MLS Threshold Crossing Errors (Degrees) EL Angle = 3.5°	124
36	Part II, MLS Threshold Crossing Errors (Degrees) EL Angle = 4.0°	124

LIST OF TABLES (CONTINUED)

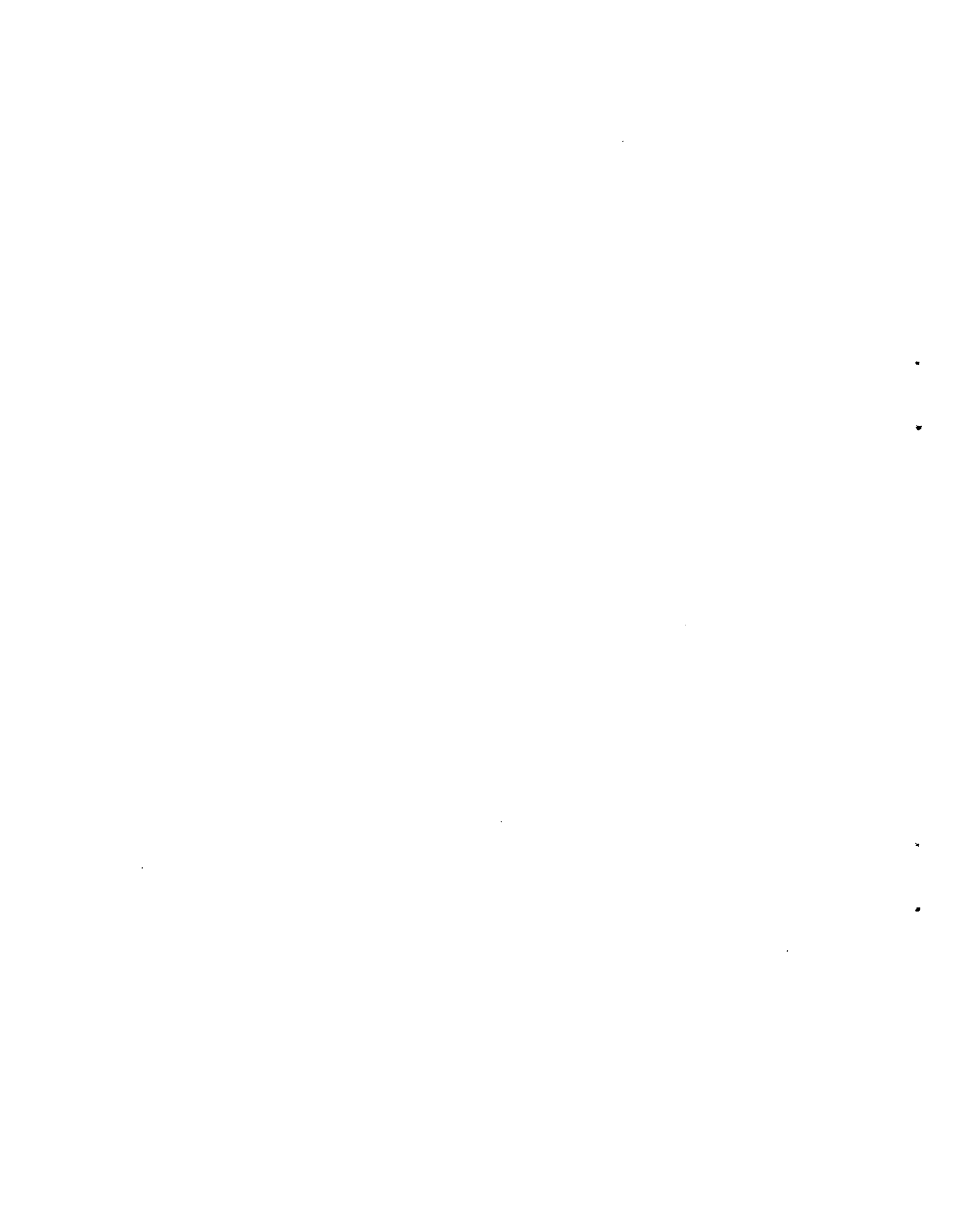
Table		Page
37	Part III, MLS Threshold Equivalent Elevation Angles (Degrees) EL Angle = 2.5°	125
38	Part III, MLS Threshold Equivalent Elevation Angles (Degrees) EL Angle = 3.0°	125
39	Part III, MLS Threshold Equivalent Elevation Angles (Degrees) EL Angle = 3.5°	126
40	Part III, MLS Threshold Equivalent Elevation Angles (Degrees) EL Angle = 4.0°	126



EXECUTIVE SUMMARY

This report details the system design and theoretical studies identifying accuracies associated with a Microwave Landing System Area Navigation (MLS RNAV) system. An MLS RNAV system makes use of the signal coverage volume afforded by the MLS to provide precision navigation within the airport terminal area. This allows randomly oriented linear flightpaths, complex curved flightpaths and complex combinations thereof to be executed. A subset of these flightpaths, namely the computed centerline and parasite approaches, are considered here.

This report describes the derivation, analysis, and testing of MLS to cartesian coordinate transformation algorithms. Simulated flight profiles employing this software are tested using both clinical and live flight derived input data. In addition, anticipated system accuracy is computed under various anticipated operational scenarios. These simulations are performed for the computed centerline and parasite approaches. The errors attributable to the MLS signal sources are factored into these analyses. Regions of acceptable Category I accuracy can be extracted from these results. Also, the effects on total system accuracy of offsetting the conical beam elevation transmitter from the runway centerline are presented.



INTRODUCTION

PURPOSE.

The purpose of this report is to document the plans, conduct, and results of the analytical studies performed as an integral part of the Microwave Landing System Area Navigation (MLS RNAV) project. These analytical studies were conducted in order to define the limitations and capabilities of performance of an MLS RNAV system in an airborne environment prior to, and in the absence of, the availability of RNAV system flight data. A principal purpose for these simulations of MLS RNAV system performance was that of comparison with and contribution to the Radio Technical Commission for Aeronautics (RTCA), Special Committee 151, Minimum Operational Performance Standards (MOPS). Additionally, the purpose of these studies was to develop and validate the MLS to cartesian coordinate transformation algorithms needed for the development of an MLS RNAV system.

BACKGROUND.

The Time Reference Scanning Beam (TRSB) MLS was selected as the new international standard approach and landing guidance system by the International Civil Aviation Organization (ICAO) on April 19, 1978. Presently being implemented at airports around the world, the new generation MLS will be in use as the standard precision landing system well into the next century. Consisting of azimuth and elevation, and precision distance measuring equipment (DME/P) transponder, MLS makes possible precision approach and landing operations under IFR conditions. Azimuth angle (θ) coverage is available over a nominal $\pm 40^\circ$ sector out to a range of 20 nautical miles (nmi) and elevation angle (ϕ) coverage is available from 0.9° to 15° at the same range. DME/P coverage is available out to a range of 22 nmi from the ground transponder. Given this wide area of MLS coverage in the terminal and final approach areas and given the proper airborne computer and display equipment, it is possible to perform three dimensional RNAV in the terminal and/or final approach areas.

In essence, area navigation consists of executing nonradially defined flight profiles relative to radio navigation aids (MLS, very high frequency omni directional range (VOR), etc.). Examples of this may include final landing approaches which are simply offset from and parallel to the 0° course of an MLS azimuth unit (computed centerline approaches) as well as nonparallel and nonradial (parasite) approaches to heliports. More sophisticated RNAV flight profiles would include precision navigation to a waypoint using random single segment paths as well as multiwaypoint and complex curved paths. Numerous benefits should accrue from the implementation of area navigation in the terminal and final approach areas. Among these are increased aircraft safety, obstacle avoidance, separation, increased airport efficiency and operations rates, as well as the performance of instrument approaches to non-MLS equipped runways.

Work performed at the Federal Aviation Administration (FAA) Technical Center at the Atlantic City International Airport, New Jersey, has addressed the myriad

tasks inherent in the successful development and implementation of an MLS RNAV system. Principally, the work falls into two areas: (1) analytical studies and (2) experimentation. The present report is concerned with the analytical studies.

Analytical studies in MLS RNAV comprise numerous topics. Six of these topics which were studied and are covered in detail in this report are:

1. The development and testing of 12 various iterative and exact closed form solution algorithms which effect the transformation from MLS angle and range coordinates to rectangular cartesian coordinates.
2. The simulation of RNAV flight profiles using the algorithms of task 1 and computer generated noiseless angular and range input data.
3. The simulation of RNAV flight profiles using the full RNAV software suite and live flight angle and range input data.
4. The simulation of centerline approaches in the presence of an offset azimuth unit when the input data includes the effects of MLS signal source error.
5. The simulation of parasite approaches for a general ground equipment siting which includes the effects of MLS signal source error.
6. The calculation of glidepath error due to the offset of a conic elevation unit.

DISCUSSION

MLS COORDINATE TRANSFORMATION ALGORITHMS.

The three ground based MLS transmitting units: azimuth, elevation, and precision distance measuring equipment define a generalized MLS coordinate system with the triple (θ, ϕ, ρ) . Knowing the triple and the relative positions of the ground units, it is possible to locate the position of the aircraft in space.

With a three-dimensional (3D) MLS RNAV it is possible to determine position independently of the conventional MLS selected reference azimuth and elevation approach course. Practicality and simplicity dictate that a cartesian coordinate (X, Y, Z) reference system be employed. In our development, the origin of this coordinate system can assume any position in space. The x-axis is aligned parallel to the 0° azimuth. In order to obtain aircraft position in this coordinate system it was necessary to develop a set of equations to convert the coordinate triple (θ, ϕ, ρ) into the new cartesian coordinate triple. For obvious reasons this transformation must be unique in the region of application. These equations, when implemented on a digital computer, are known as the MLS transformation algorithms. These algorithms run the gamut from a simple exact solution for (x, y, z) to a complex, fully general iterative solution. The degree of sophistication is dependent on the ground unit geometry, with most sophistication required when the ground units are sited in different z-planes. In the most general case, any location of MLS azimuth, elevation, and DME/P equipment in cartesian space is allowed. These conditions vastly complicated

the transformation problem. Fortunately, for many cases, only a subset of these conditions need be considered. When certain simplifying assumptions are made (e.g., collocated azimuth and DME/P equipment), exact solutions to the transformation problem are made available.

The approach to the MLS transformation problem solution is illustrated in figures 1 and 2. These figures present the mathematical representation and not the physical representation of the signal patterns. As illustrated, the MLS azimuth unit defines a plane at angle θ , referenced to boresight (planar azimuth) or a cone of exterior angle θ , (conical azimuth) with origin located at (X_a, Y_a, Z_a) . The elevation unit defines a cone of exterior angle ϕ , centered at its location (X_e, Y_e, Z_e) . The prototype DME/P defines a sphere of radius ρ , whose center is located at (X_d, Y_d, Z_d) . These three surfaces intersect at a maximum of four points. Three of these points can be discarded based on prior knowledge of the geometry. A total of 12 different transformation algorithms have been developed at the FAA Technical Center. A description of the siting geometry, the signal propagation pattern, and the method of solution of these algorithms are contained in table 1.

In several of the cases, the origin of the coordinate system has been situated to coincide with one or more of the MLS signal sources. The recommended origin for MLS coordinate transformation is the MLS datum point. This point is located abeam the elevation unit on the runway centerline. For the special cases presented herein which do not use the MLS datum as the origin, conformance will necessitate the use of simple x, y, and z linear translations to the MLS datum point.

All of the algorithms presented herein have been written in Fortran 77 and run on a Digital Equipment VAX 11/750 computer under the VMS version 4.2 operating system. They have been tested successfully at azimuth angles from $+40^\circ$ to -40° , elevation angles of $+2^\circ$ to 20° , and DME/P ranges from 2 to 20 nmi. Those who use these algorithms outside of these limits should independently verify that iterative solution algorithms are applied in a proper region of convergence.

MLS COORDINATE TRANSFORMATION ALGORITHM DESCRIPTIONS.

A total of 12 different MLS to cartesian coordinate transformation algorithms have been developed. These algorithms are tailored to address varying degrees of complexity and conditions in the coordinate transformation process. As noted in table 1, some of the pertinent complexity issues are method of solution (exact closed form or iterative), type of azimuth signal (planar or conical), collocated or separated signal sources, coplanar Z plane location or separate Z plane locations, and cartesian location of the signal sources. Specific descriptions of each algorithm are covered in the following narrative, as well as in the derivations of each individual case.

TRANSFORMATION ALGORITHM PHILOSOPHY AND USAGE.

GENERAL COMMENTS (APPLY TO ALL CASES). In a completely general sense, MLS reconstruction consists of transforming MLS angular and DME/P range data into cartesian coordinates. Furthermore, in the most general case, any location of MLS azimuth, elevation, and DME/P stations in cartesian space is allowed. These conditions vastly complicate the transformation problem. Fortunately, for many cases, only a subset of these conditions need be considered. With conic azimuth propagation only Case III, IV, VI, VIII, IX, and XII need to be considered.

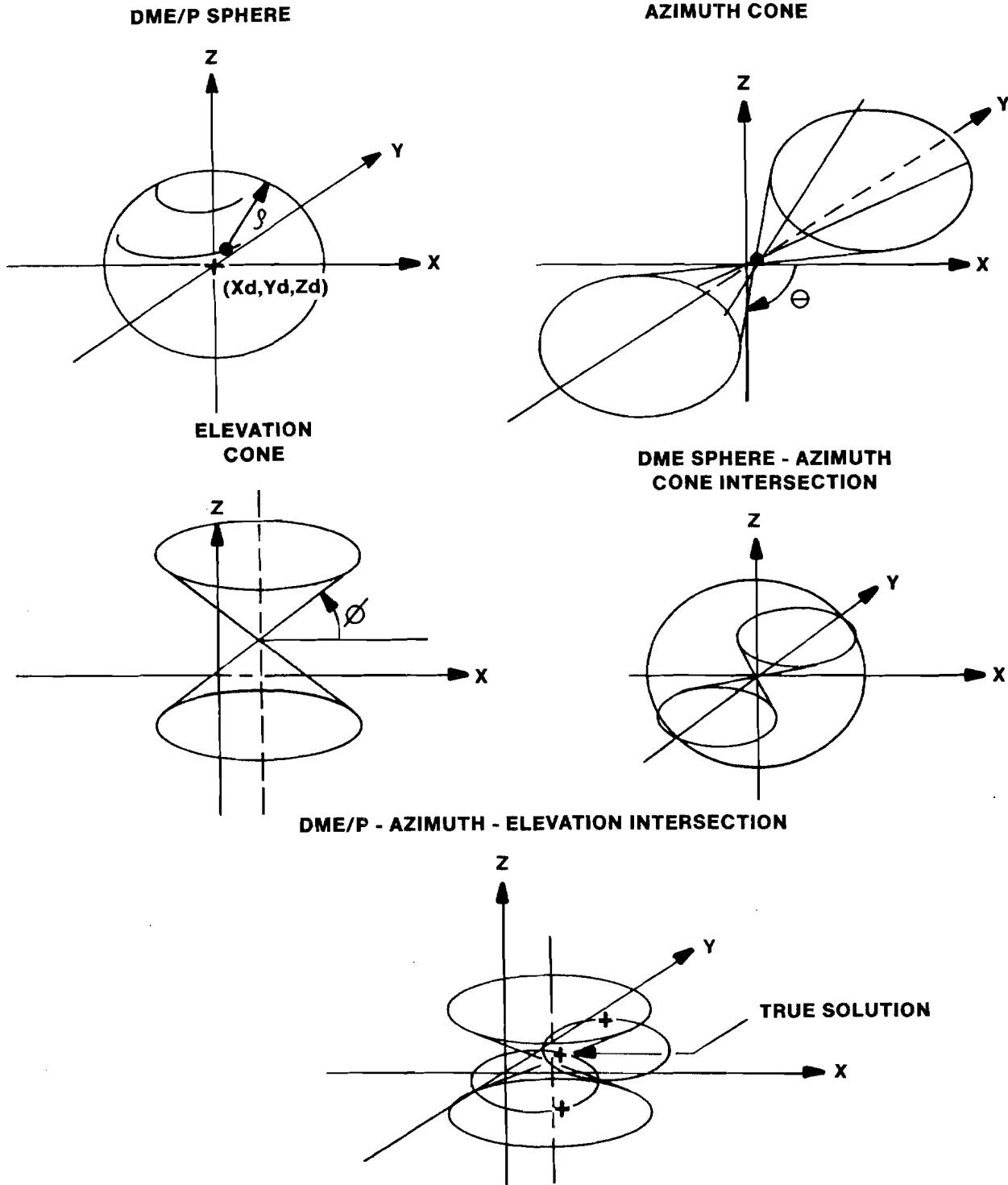
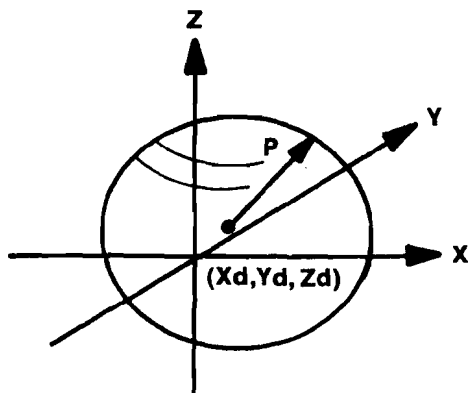
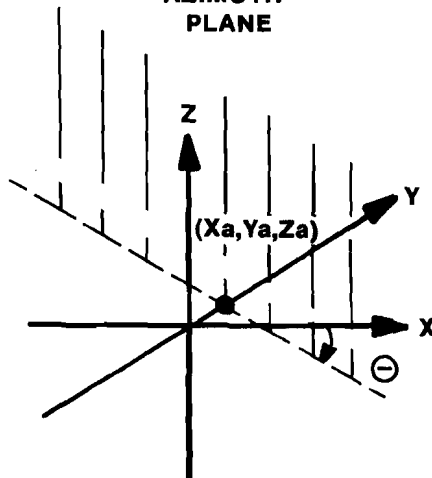


FIGURE 1 CONICAL GRAPHICAL SOLUTION

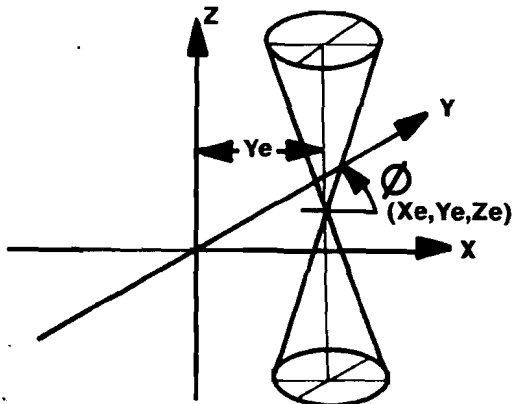
DME/P SPHERE



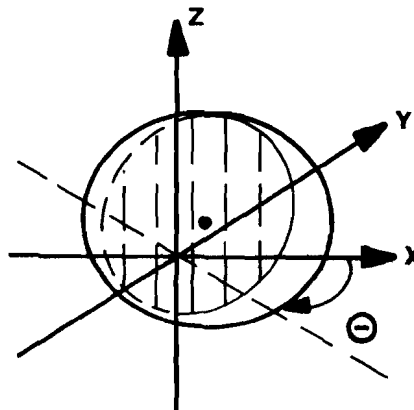
AZIMUTH PLANE



ELEVATION CONE



DME SPHERE-AZIMUTH PLANE INTERSECTION



DME-AZIMUTH-ELEVATION INTERSECTION

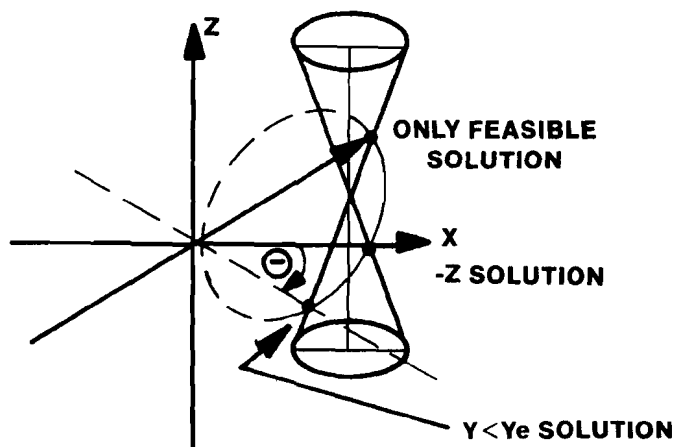


FIGURE 2 PLANAR GRAPHICAL SOLUTION

TABLE 1. MLS RECONSTRUCTION ALGORITHMS

Case	Description	Solution
1	DME & AZ COLLOCATED, PLANAR AZ AZ & EL COLINEAR, SAME Z PLANE	EXACT
2	DME & AZ COLLOCATED, PLANAR AZ AZ & EL OFFSET, SAME Z PLANE	EXACT
3	DME & AZ COLLOCATED, CONICAL AZ AZ & EL COLINEAR, SAME Z PLANE	EXACT
4	DME & AZ COLLOCATED, CONICAL AZ AZ & EL OFFSET, SAME Z PLANE	EXACT
5	DME & AZ COLLOCATED, PLANAR AZ AZ & EL COLINEAR, DIFFERENT Z PLANES	ITERATIVE
6	DME & AZ COLLOCATED, CONICAL AZ AZ & EL COLINEAR, DIFFERENT Z PLANES	ITERATIVE
7	COMPLETE GENERAL SOLUTION PLANAR AZ, GENERAL AZ, EL & DME POSITIONS "THEDFORD" TYPE ALGORITHM	ITERATIVE
8	"THEDFORD ALGORITHM" EXTENSION CONICAL AZ, DME & AZ COLLOCATED	ITERATIVE
9	COMPLETELY GENERAL SOLUTION CONICAL AZ NONLINEAR SEIDEL ITERATION	ITERATIVE
10	COMPLETELY GENERAL SOLUTION PLANAR AZ NONLINEAR SEIDEL ITERATION	ITERATIVE
11	"THEDFORD ALGORITHM" PLANAR AZ, DME REFERENCE FRAME AZ & EL POSITIONS COMPLETE GENERAL	ITERATIVE
12	"SHREEVES ALGORITHM" CONIC AZ & EL COMPLETE GENERAL AZ, EL & DME POSITIONS	NEWTON/RAPHSON JACOBIAN ITERATION

DME = Precision DME Antenna
 AZ = Azimuth Antenna
 EL = Elevation

The algorithm descriptions address diverse cases by considering geometries of progressively increasing complication. Each case presented includes the mathematical development, the FORTRAN code used, and an illustration identifying reference measures used as input.

The transformation algorithms numbered 1 through 4 are simple ones which comprise exact solutions to the transformation problem. This simplicity is made possible by assuming the collocation at the cartesian origin of the azimuth and DME/P units and by not allowing any relative displacement in the z-direction between the elevation and other ground units. Case II differs from I and case IV differs from III in that cases IV and II permit a lateral (y-direction) displacement of the elevation unit from the azimuth DME/P units. Also, cases I and II use planar and cases III and IV use conic azimuth. These 4 algorithms will probably find use running on relatively unsophisticated computers in applications such as computing a parallel offset course.

Cases V and VI introduce an additional level of sophistication beyond the first four cases in that the elevation unit is displaced in the Z direction from the collocated azimuth and DME/P units, which define the coordinate system origin. This relative displacement greatly complicates the resulting mathematics, leading to quartic polynomials in X which must be solved using an iterative technique. Case V addresses planar and case VI addresses conic azimuth. Although a split site configuration is allowed under these cases, the two sites are assumed to lie along a common line parallel to the runway centerline. These algorithms would most probably be used for geometries which have significant z-plane differences (e.g., sloped runways). A computer of moderate sophistication would be required to run these programs.

CASE I:

This case assumes that both the azimuth and DME/P ground units are collocated and reside in the same horizontal z-plane as the elevation unit. Also, the elevation and azimuth and DME/P units are assumed to be located along a common line, which is parallel to, but offset from the runway centerline. The azimuth beam is assumed to be planar. The azimuth and DME/P units are located at the origin of the cartesian coordinate system. A closed form solution results.

The equations which result are:

$$\text{From DME/P} = x^2 + y^2 + z^2 = \rho^2 \quad (1)$$

$$\text{From Azimuth: } y = -x \tan \theta \quad (2)$$

$$\text{From Elevation: } y^2 + (x - x_e)^2 = z^2 \cot^2 \phi \quad (3)$$

These equations are solved for y and a quadratic in y results as follows:

Substitute (2) into (1) to eliminate y:

$$x^2 \tan^2 \theta + x^2 + z^2 = \rho^2 \quad (4)$$

or:

$$x^2(1 + \tan^2 \theta) + z^2 = \rho^2 \quad (5)$$

Substituting (2) into (3) to eliminate y:

$$x^2 \tan^2 \theta + (x - x_e)^2 = z^2 \cot^2 \phi \quad (6)$$

Substituting (5) into (6) to eliminate z yields:

$$x^2 \tan^2 \theta + (x - x_e)^2 = ((\rho^2 - x^2(1 + \tan^2 \theta)) \cot^2 \phi) \quad (7)$$

Rearranging and collecting terms:

$$x^2(\tan^2 \theta + \cot^2 \phi + \tan^2 \theta \cot^2 \phi + 1) - 2xx_e - \rho^2 \cot^2 \phi + x_e^2 = 0 \quad (8)$$

Using the quadratic formula (8) has solutions:

$$x = \frac{2x_e \pm (4x_e^2 - 4(\tan^2 \theta + \cot^2 \phi + \tan^2 \theta \cot^2 \phi + 1)(x_e^2 - \rho^2 \cot^2 \phi))^{1/2}}{2(\tan^2 \theta + \cot^2 \phi + \tan^2 \theta \cot^2 \phi + 1)} \quad (9)$$

The larger value of x is chosen

The x value from equation 9 is then substituted into equations (2) and (1) respectively to obtain x and z.

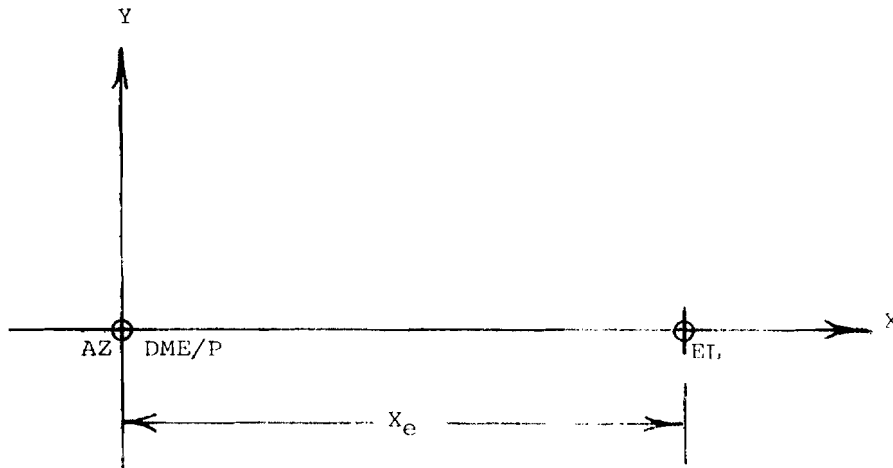
$$y = -x \tan \theta \quad (2)$$

$$z = (\rho^2 - y^2 - x^2)^{1/2} \text{ from} \quad (1)$$

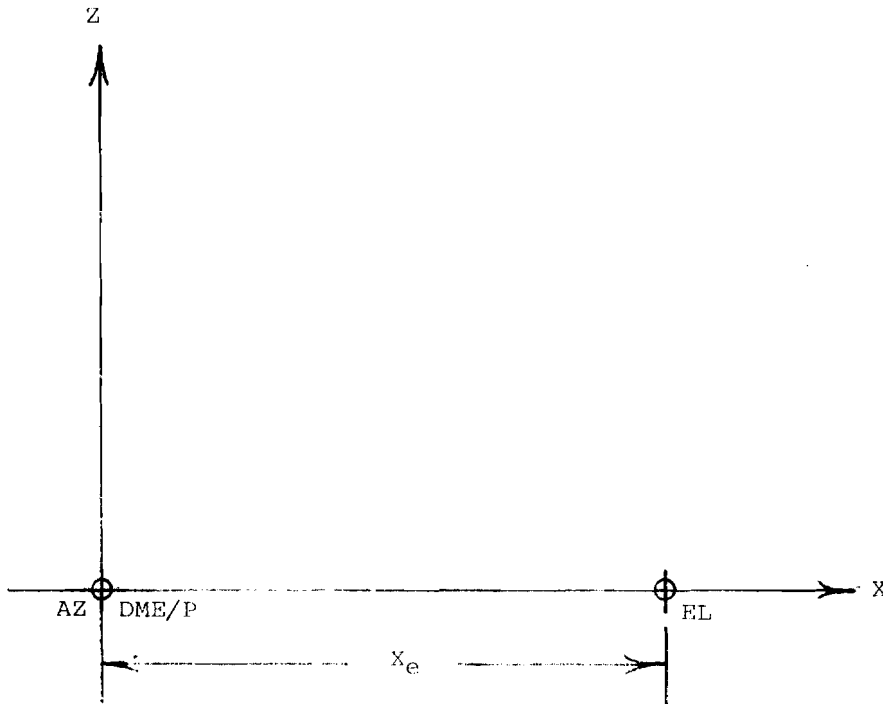
MLS RECONSTRUCTION ALGORITHM
CASE I FORTRAN SUBROUTINE

```
      SUBROUTINE CASE1(THET,PHI,RHOD,XE,X,Y,Z)
C***** SUBROUTINE CALCULATES CARTESIAN COORDINATES FROM
C      MLS ANGLE AND DME/P DATA
C      THET=RCVR AZ (RADIANS)
C      PHI =RCVR EL(RADIANS)
C      RHOD = DME/P DISTANCE (FEET)
C      XE=AZ TO EL SEPARATION (FEET)
C
C      DETERMINE THE SQUARES OF TAN AND COT OF THET AND PHI
C
      TAN2TH=(SIN(THET)/COS(THET))*(SIN(THET)/COS(THET))
      COT2PH = (COS(PHI)/SIN(PHI))*(COS(PHI)/SIN(PHI))
C***** DETERMINE QUADRATIC PARAMETERS
      A = 1.0+TAN2TH+COT2PH+TAN2TH*COT2PH
      B = 2.0*XE
      C = XE*XE - RHOD*RHOD*COT2PH
C***** SOLVE QUADRATIC AND PICK LARGER SOLUTION FOR X
C
      X = (-B+SQRT(B*B-4.0*A*C))/(2.0*A)
      Y = -X*TAN(THET)
      Z = SQRT (RHOD*RHOD-Y*Y-X*X)
      RETURN
      END
```

CASE I



PLAN VIEW



ELEVATION VIEW

FIGURE 3. CASE I, GEOMETRY

CASE II:

This case assumes that both the azimuth and DME/P ground units are collocated and reside in the same horizontal z-plane as the elevation unit. However, the azimuth and DME/P units are assumed to be separated from the elevation unit by a distance x_e along a line parallel to the runway centerline, and by a distance y_e transverse to the runway centerline. The azimuth and DME/P units are located at the origin of the coordinate system. The azimuth beam is assumed to be planar. A closed form solution results.

The equations which result are:

$$\text{From DME/P} = x^2 + y^2 + z^2 = \rho^2 \quad (1)$$

$$\text{From Azimuth: } y = -x \tan \theta \quad (2)$$

$$\text{From Elevation: } (x - x_e)^2 + (y - y_e)^2 = z^2 \cot^2 \phi \quad (3)$$

Substitute (2) into (1) to eliminate y :

$$x^2 \tan^2 \theta + x^2 + z^2 = \rho^2 \quad (4)$$

or:

$$x^2(1 + \tan^2 \theta) + z^2 = \rho^2 \quad (5)$$

Substituting (2) into (3) to eliminate y :

$$(x \tan \theta + y_e)^2 + (x - x_e)^2 = z^2 \cot^2 \phi \quad (6)$$

Rearranging (5)

$$z^2 = \rho^2 - x^2(1 + \tan^2 \theta) \quad (7)$$

Substituting (7) into (6) to eliminate z :

$$(x \tan \theta + y_e)^2 + (x - x_e)^2 = (\rho^2 - x^2(1 + \tan^2 \theta)) \cot^2 \phi \quad (8)$$

Expanding and collecting terms:

$$\begin{aligned} & x^2(\tan^2 \theta + \cot^2 \phi + \cot^2 \phi \tan^2 \theta + 1) \\ & + x(2y_e \tan \theta - 2x_e) \\ & + (x_e^2 + y_e^2 - \rho^2 \cot^2 \phi) \end{aligned} \quad (9)$$

Equation 9 is a quadratic which can be solved by the quadratic formula:

$$x = \frac{-B \pm (B^2 - 4AC)^{1/2}}{2A} \quad (10)$$

Wherein:

$$A = \tan^2 \theta + \cot^2 \phi + \cot^2 \phi \tan^2 \theta + 1 \quad (11)$$

$$B = +2y_e \tan \theta - 2x_e \quad (12)$$

$$C = x_e^2 + y_e^2 - \rho^2 \cot^2 \phi \quad (13)$$

Choose the larger value of X obtained from (10)

The value of y is gotten from:

$$y = -x \tan \theta \quad (2)$$

z is obtained from recasting equation (1):

$$z = (\rho^2 - x^2 - y^2)^{1/2} \quad (1a)$$

MLS RECONSTRUCTION ALGORITHM
CASE II FORTRAN SUBROUTINE

```
      SUBROUTINE CASE2(THET,PHI,RHOD,XE,YE,X,Y,Z)
C***** THIS SUBROUTINE USED THE MLS ANGLE AND DME/P DATA IN
C        CONJUNCTION WITH OFFSET DISTANCES TO COMPUTE CARTESIAN
C        X,Y AND Z COORDINATES.
C        THET = RCVR AZ ANGLE (RADIAN)
C        PHI = RCVR EL ANGLE (RADIAN)
C        RHOD = DME/P DISTANCE (FT)
C        XE = OFFSET BETWEEN AZ AND EL IN X DIRECTION (FT)
C        YE = OFFSET BETWEEN AZ AND EL IN Y DIRECTION (FT)
C
C        DETERMINE SQUARES OF TAN AND COT OF THET AND PHI
      TANTH=SIN(THET)/COS(THET)
      TAN2TH = (SIN(THET)/COS(THET))*(SIN(THET)/COS(THET))
      COT2PH = (COS(PHI)/SIN(PHI))*(COS(PHI)/SIN(PHI))
C***** DETERMINE QUADRATIC PARAMETERS
      A = 1.0 + TAN2TH + COT2PH + COT2PH*TAN2TH
      B = +2.0*YE*TANTH-2.0*XE
      C = XE*XE+YE*YE-RHOD*RHOD*COT2PH
C        SOLVE QUADRATIC AND PICK LARGER SOLUTION
      X =(-B+SQRT(B*B-4*A*C))/(2*A)
      Y=-X*TANTH
      Z=SQRT(RHOD*RHOD-X*X-Y*Y)
      RETURN
      END
```

CASE II

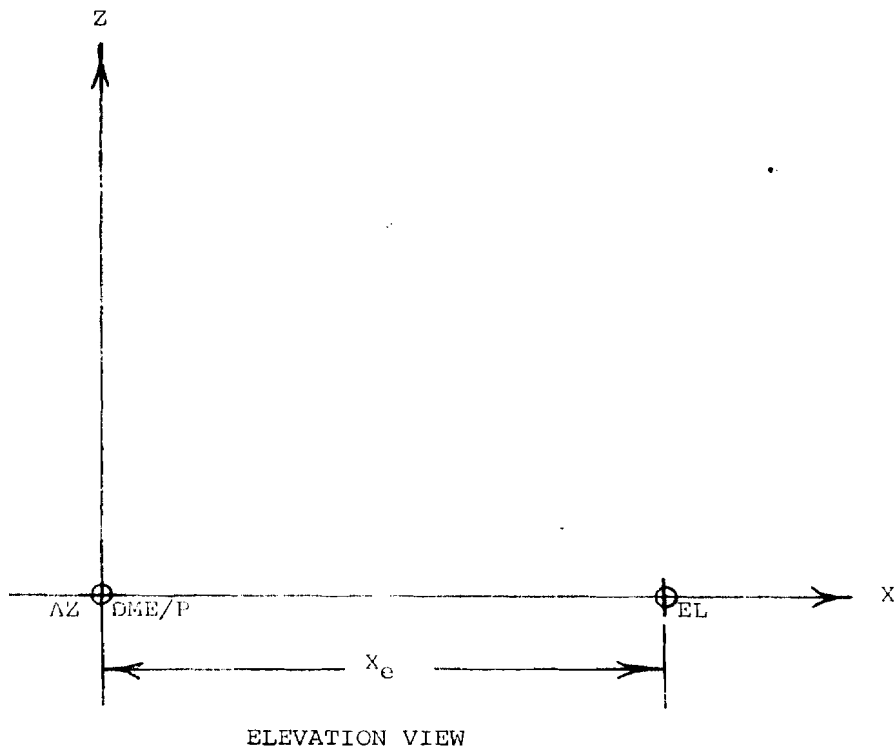
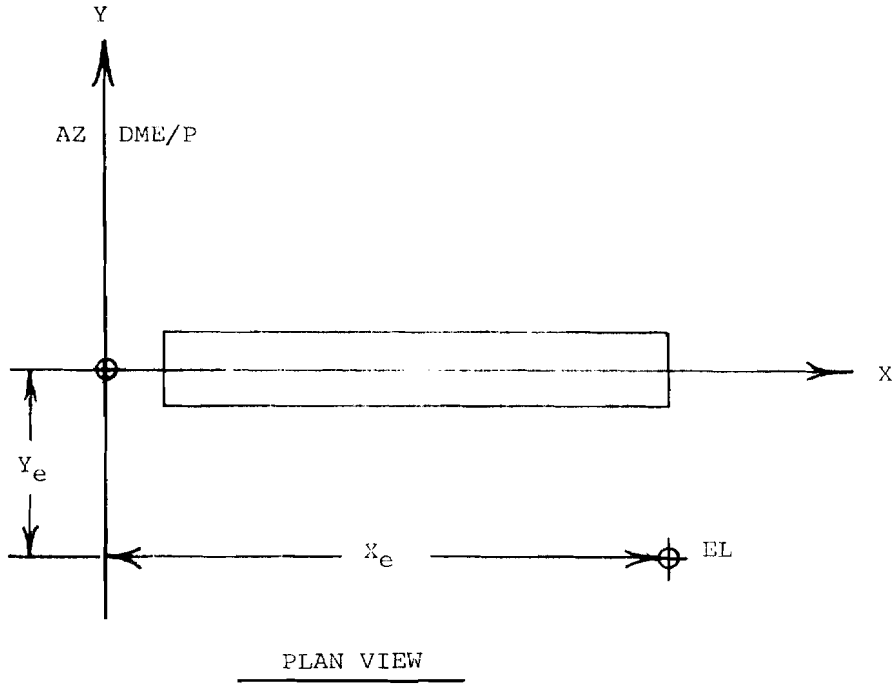


FIGURE 4. CASE II, GEOMETRY

CASE III:

This case assumes that both the azimuth and DME/P ground units are collocated and reside in the same horizontal z-plane as the elevation unit. The azimuth and DME/P units are separated, however, by a distance x_e along a line parallel to the runway centerline. The azimuth and DME/P units are located at the origin of the coordinate system. The azimuth beam forms a cone with exterior angle θ . A closed form solution results.

The equations which result are:

$$\text{From DME/P, a sphere: } x^2+y^2+z^2 = \rho^2 \quad (1)$$

$$\text{From Azimuth, a cone: } \rho \sin \theta = -y \quad (2)$$

$$\text{From Azimuth, a cone: } x^2+z^2=y^2 \cot^2 \theta \quad (3)$$

$$\text{From Elevation, a cone: } y^2+(x-x_e)^2=z^2 \cot^2 \phi \quad (4)$$

$$\text{Square (2): } y^2 = \rho^2 \sin^2 \theta \quad (5)$$

$$\text{Substitute (5) into (3): } x^2+z^2 = \rho^2 \sin^2 \theta \cot^2 \theta \quad (6)$$

$$\text{From trigonometry: } \sin^2 \theta \cot^2 \theta = \cos^2 \theta \quad (7)$$

$$\text{Therefore: } x^2+z^2 = \rho^2 \cos^2 \theta \quad (8)$$

$$\text{Solve for z: } z^2 = \rho^2 \cos^2 \theta - x^2 \quad (9)$$

$$\text{Substitute (9) into (4): } y^2+(x-x_e)^2=(\rho^2 \cos^2 \theta - x^2) \cot^2 \phi \quad (10)$$

Substitute (5) for y^2 in (10):

$$\rho^2 \sin^2 \theta + (x-x_e)^2 = (\rho^2 \cos^2 \theta - x^2) \cot^2 \phi \quad (11)$$

Multiplying out and collecting any terms yields a quadratic:

$$x^2(1+\cot^2 \phi) - 2x x_e + x_e^2 + \rho^2 \sin^2 \theta - \rho^2 \cos^2 \theta \cot^2 \phi = 0 \quad (12)$$

The quadratic parameters are:

$$A = (1+\cot^2 \phi) \quad (13)$$

$$B = -2x_e \quad (14)$$

$$C = x_e^2 + \rho^2 \sin^2 \theta - \rho^2 \cos^2 \theta \cot^2 \phi \quad (15)$$

Using the quadratic formula:

$$x = \frac{-B \pm (B^2 - 4AC)^{1/2}}{2A} \quad (16)$$

Choose the larger value of x

From (2) obtain Y :

$$y = -\rho \sin \theta \quad (2)$$

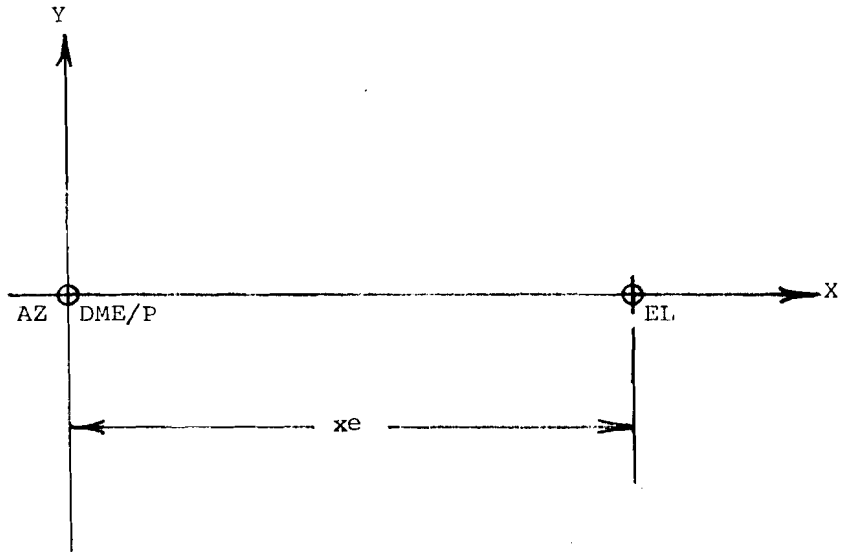
From (1) obtain z :

$$z = (\rho^2 - x^2 - y^2)^{1/2} \quad (17)$$

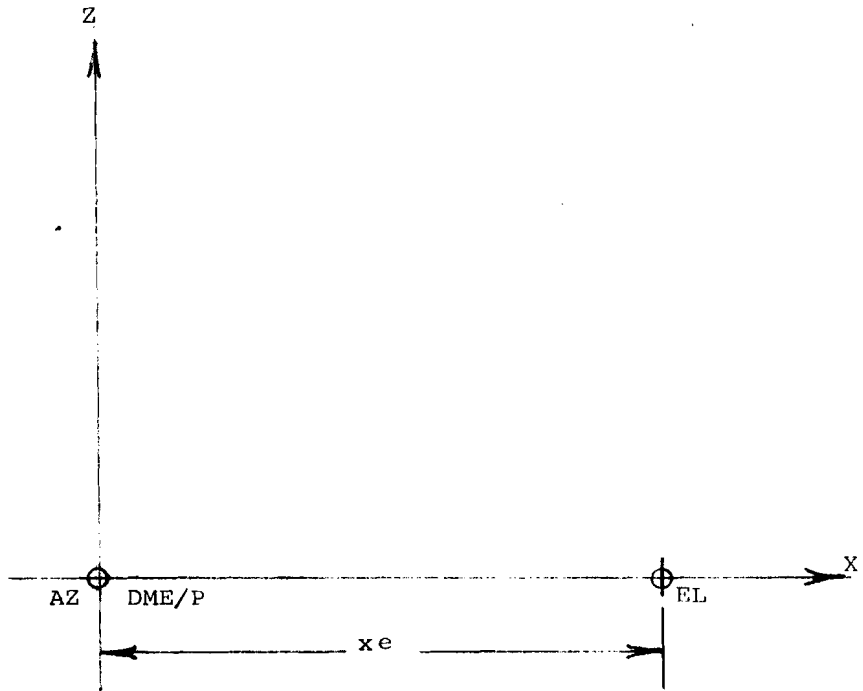
MLS RECONSTRUCTION ALGORITHM
CASE III FORTRAN SUBROUTINE

```
      SUBROUTINE CASE3(THET,PHI,RHOD,XE,X,Y,Z)
C***** THIS SUBROUTINE USES THE MLS ANGLE AND DME/P DATA
C        TOGETHER WITH OFFSET DISTANCE YE TO COMPUTE CARTESIAN
C        X,Y AND Z COORDINATES.
C        THET = RCVR AZ ANGLE (RADIANS)
C        PHI = RCVR EL ANGLE (RADIANS)
C        RHOD = DME/P DISTANCE (FT)
C        YE = OFFSET BETWEEN AZ AND EL IN Y DIRECTION (FT)
C
C        DETERMINE SQUARES OF TAN AND COT OF THET AND PHI
      TAN2TH = (SIN(THET)/COS(THET))*(SIN(THET)/COS(THET))
      COT2PH = (COS(PHI)/SIN(PHI))*(COS(PHI)/SIN(PHI))
C***** DETERMINE QUADRATIC PARAMETERS
      A = 1.0+COT2PH
      B = -2.0*XE
      C = XE*XE+RHOD*RHOD*SIN(THET)*SIN(THET)-
      &    RHOD*RHOD*COS(THET)*COS(THET)*COT2PH
C***** SOLVE QUADRATIC AND PICK LARGER SOLUTION
      X=(-B+SQRT(B*B-4.0*A*C))/(2.0*A)
      Y=-1.0*RHOD*SIN(THET)
      Z=SQRT(RHOD*RHOD-X*X-Y*Y)
      RETURN
      END
```

CASE III



PLAN VIEW



ELEVATION VIEW

FIGURE 5. CASE III, GEOMETRY

CASE IV:

This case assumes that both the azimuth and DME/P ground units are collocated and reside in the same horizontal z-plane as the elevation unit. However, the azimuth and DME/P units are assumed to be separated from the elevation unit by a distance x_e along a line parallel to the runway centerline, and by a distance y_e transverse to the runway centerline. The azimuth and DME/P units are located at the origin of the coordinate system. The azimuth beam is assumed to be conical. A closed form solution results.

The equations which result are:

$$\text{From DME/P, } x^2 + y^2 + z^2 = \rho^2 \quad (1)$$

$$\text{From Azimuth, } \rho \sin \theta = -y \quad (2)$$

$$x^2 + z^2 = y^2 \cot^2 \theta \quad (3)$$

$$\text{From Elevation } (x - x_e)^2 + (y - y_e)^2 = z^2 \cot^2 \phi \quad (4)$$

Substitute (2) into (4) to eliminate y :

$$(\rho \sin \theta + y_e)^2 + (x - x_e)^2 = z^2 \cot^2 \phi \quad (5)$$

$$\text{Square (2): } \rho^2 \sin^2 \theta = y^2 \quad (6)$$

$$\text{Substitute (6) into (3): } x^2 + z^2 = \rho^2 \sin^2 \theta \cot^2 \theta \quad (7)$$

$$\text{From trigonometry: } \sin^2 \theta \cot^2 \theta = \frac{\sin^2 \theta \cos^2 \theta}{\sin^2 \theta} = \cos^2 \theta \quad (8)$$

$$\text{Therefore: } x^2 + z^2 = \rho^2 \cos^2 \theta \quad (9)$$

$$z^2 = \rho^2 \cos^2 \theta - x^2 \quad (10)$$

Substitute (10) into (5):

$$(\rho \sin \theta + y_e)^2 + (x - x_e)^2 = (\rho^2 \cos^2 \theta - x^2) \cot^2 \phi \quad (11)$$

Simplifying and collecting terms:

$$x^2(1 + \cot^2 \phi) - 2x x_e + (y_e^2 + x_e^2 + 2y_e \rho \sin \theta + \rho^2 \sin^2 \theta - \rho^2 \cos^2 \theta \cot^2 \phi) = 0 \quad (12)$$

This is a quadratic which can be solved for x as:

$$x = \frac{-B \pm (B^2 - 4AC)^{1/2}}{2A} \quad (13)$$

The larger value of x is chosen in (13).

$$\text{Where: } A = 1 + \cot^2 \phi \quad (14)$$

$$B = -2x_e \quad (15)$$

$$C = y_e^2 + x_e^2 + 2y_e \rho \sin \theta + \rho^2 \sin^2 \theta - \rho^2 \cos^2 \theta \cot^2 \phi = 0 \quad (16)$$

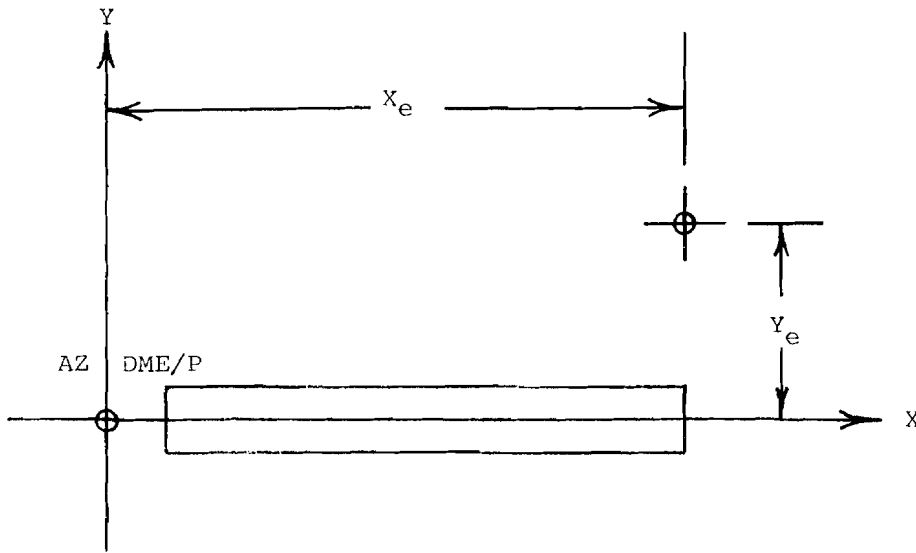
$$\text{Obtain } x \text{ from (2): } y = -\rho \sin \theta \quad (2)$$

$$\text{Solve (1) for } z: z = (\rho^2 - x^2 - y^2)^{1/2} \quad (17)$$

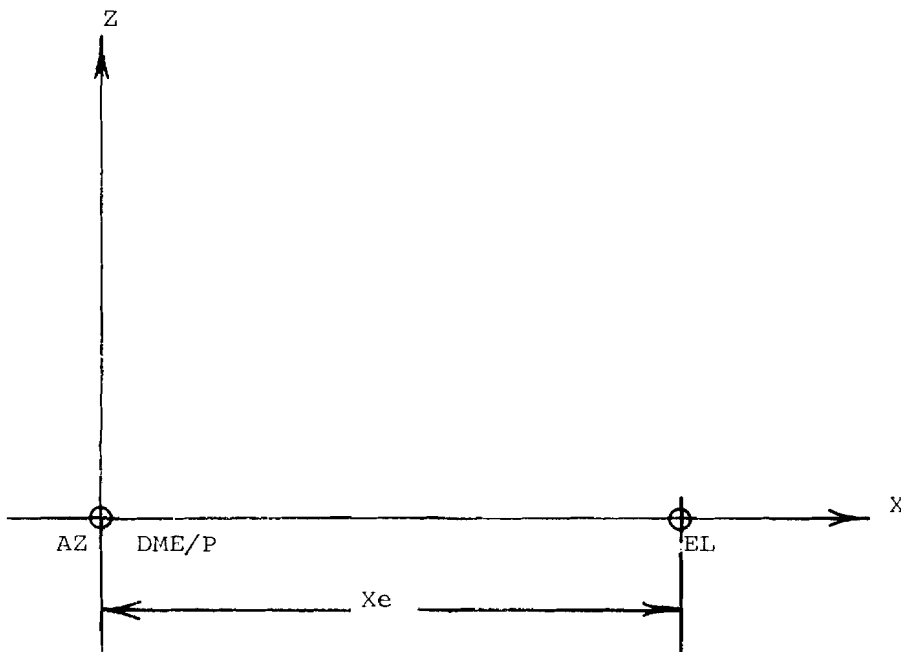
MLS RECONSTRUCTION ALGORITHM
CASE IV FORTRAN SUBROUTINE

```
      SUBROUTINE CASE4(THET,PHI,RHOD,YE,XE,X,Y,Z)
C***** THIS SUBROUTINE USES THE MLS ANGLE AND DME/P DATA
C        TOGETHER WITH OFFSET DISTANCE YE TO COMPUTE CARTESIAN
C        X,Y AND Z COORDINATES.
C        THET = RCVR AZ ANGLE (RADIAN)
C        PHI = RCVR EL ANGLE (RADIAN)
C        RHOD = DME/P DISTANCE (FT)
C        YE = OFFSET BETWEEN AZ AND EL IN Y DIRECTION (FT)
C        XE = OFFSET BETWEEN AZ AND EL IN X DIRECTION (FT)
C        DETERMINE SQUARES OF TAN AND COT OF THET AND PHI
      TAN2TH = (SIN(THET)/COS(THET))*(SIN(THET)/COS(THET))
      COT2PH = (COS(PHI)/SIN(PHI))*(COS(PHI)/SIN(PHI))
C***** DETERMINE QUADRATIC PARAMETERS
      A = 1.+COT2PH
      B = -2.0*XE
      C = YE*YE+XE*XE+2.0*YE*RHOD*SIN(THET)
      +RHOD*RHOD*SIN(THET)*SIN(THET)
      -RHOD*RHOD*COS(THET)*COS(THET)*COT2PH
C***** SOLVE QUADRATIC AND PICK LARGER SOLUTION
      X=(-B+SQRT(B*B-4*A*C))/(2.0*A)
      Y= - RHOD*SIN(THET)
      Z=SQRT(RHOD*RHOD-X*X-Y*Y)
      RETURN
      END
```

CASE IV



PLAN VIEW



ELEVATION VIEW

FIGURE 6. CASE IV, GEOMETRY

CASE V:

This case assumes that both the azimuth and DME/P ground units are collocated and reside at the origin of the coordinate system in the $z=0$ plane. The elevation unit does not reside in this plane, but rather, it lies in the vertically displaced plane $z=z_e$. Furthermore, the elevation unit is displaced by a distance x_e along the x axis from the azimuth and DME/P units. There is assumed to be no relative displacement between any of the units in the y direction. Planar azimuth is used in the derivation. A closed form expression does not result, but rather, a quartic polynomial in x results. An iterative solution (Newton-Raphson) running on a digital computer is recommended.

The equations which result are:

$$\text{From DME/P: } x^2 + y^2 + z^2 = \rho^2 \quad (1)$$

$$\text{From Azimuth: } y = -x \tan \theta \quad (2)$$

$$\text{From Elevation: } y^2 + (x - x_e)^2 = (z - z_e)^2 \cot^2 \phi \quad (3)$$

$$\text{Square (2): } y^2 = x^2 \tan^2 \theta \quad (4)$$

$$\text{Substitute (4) into (1): } x^2 \tan^2 \theta + x^2 + z^2 = \rho^2 \quad (5)$$

$$\text{Rearranging (5) yields: } z^2 = \rho^2 - x^2(1 + \tan^2 \theta) \quad (6)$$

$$\text{Taking the positive square root of (6): } z = +(\rho^2 - x^2(1 + \tan^2 \theta))^{1/2} \quad (7)$$

Substituting (7) into (3) yields:

$$y^2 + (x - x_e)^2 = ((\rho^2 - x^2(1 + \tan^2 \theta))^{1/2} - z_e)^2 \cot^2 \phi \quad (8)$$

Substituting (4) into (8) yields:

$$x^2 \tan^2 \theta + (x - x_e)^2 = ((\rho^2 - x^2(1 + \tan^2 \theta))^{1/2} - z_e)^2 \cot^2 \phi \quad (9)$$

Multiplying out and collecting terms:

$$x^2 \tan^2 \theta + (x - x_e)^2 - (\rho^2 - x^2(1 + \tan^2 \theta)) \cot^2 \phi - z_e^2 \cot^2 \phi = -2z_e(\rho^2 - x^2(1 + \tan^2 \theta))^{1/2} \cot^2 \phi \quad (10)$$

Square both sides:

$$4z_e^2(\rho^2 - x^2(1 + \tan^2 \theta)) = x^4 \tan^4 \theta + 2x^2 \tan^2 \theta - 2x^2 \tan^2 \theta (\rho^2 - x^2(1 + \tan^2 \theta)) \cot^2 \phi - 2x^2 \tan^2 \theta z_e^2 \cot^2 \phi + (x - x_e)^4 - 2(x - x_e)^2 (\rho^2 - x^2(1 + \tan^2 \theta)) \cot^2 \phi - 2(x - x_e)^2 z_e^2 \cot^2 \phi + (\rho^2 - x^2(1 + \tan^2 \theta))^2 \cot^4 \phi - 2(\rho^2 - x^2(1 + \tan^2 \theta)) \cot^4 \phi z_e^2 + z_e^4 \cot^4 \phi \quad (11)$$

$$\text{This equation is of the form: } Ax^4 + Bx^3 + Cx^2 + Dx + E = 0 \quad (12)$$

$$\text{Where: } A = \tan^4 \theta + 2 \tan^2 \theta (1 + \tan^2 \theta) \cot^2 \phi + 2(1 + \tan^2 \theta) \cot^2 \phi + (1 + \tan^2 \theta)^2 \cot^4 \phi + 1 \quad (13)$$

$$B = -4x_e - 4x_e(1 + \tan^2 \theta) \cot^2 \phi \quad (14)$$

$$C = 2 \tan^2 \theta - 2 \rho^2 \tan^2 \theta \cot^2 \phi - 2 \tan^2 \theta z e^2 \cot^2 \phi + 6 x e^2 - 2 \rho^2 \cot^2 \phi - 2 z e^2 \cot^2 \phi + 2 x e^2 (1 + \tan^2 \theta) \cot^2 \phi - 2 \rho^2 (1 + \tan^2 \theta) \cot^4 \phi + 2 (1 + \tan^2 \theta) \cot^4 \phi z e^2 + 4 z e^2 (1 + \tan^2 \theta) \quad (15)$$

$$D = -4 x e^3 + 4 x e \rho^2 \cot^2 \phi + 4 x e z e^2 \cot^2 \phi \quad (16)$$

$$E = -2 x e^2 \rho^2 \cot^2 \phi - 2 x e^2 z e^2 \cot^2 \phi + \rho^4 \cot^4 \phi - 2 \rho^2 \cot^4 \phi z e^2 + z e^4 \cot^4 \phi + x e^4 - 4 z e^2 \rho^2 \quad (17)$$

There should be 4 real roots which correspond to the four points of intersection. An iterative procedure such as Newton-Raphson should work provided care is taken to insure convergence to the proper point.

The equation employed in this method is:

$$x_{n+1} = x_n - \frac{f(x_n)}{f'(x_n)} \quad (18)$$

Where $f(x_n)$ is equation (12) above and:

$$f'(x) = 4Ax^3 + 3Bx^2 + 2Cx + D \quad (19)$$

The positive value of x closest to the elevation station is desired if $z e$ is positive. If $z e$ is negative, the intersection point farthest from elevation is desired.

Once x is known, y is obtained by:

$$y = -x \tan \theta \quad (20)$$

z is obtained via (1) and x and y :

$$z = (\rho^2 - x^2 - y^2)^{1/2} \quad (21)$$

MLS RECONSTRUCTION ALGORITHM
CASE V FORTRAN SUBROUTINE

```

SUBROUTINE CASE5(THET,PHI,RHOD,XE,ZE,X,Y,Z,LIM)
C***** SUBROUTINE CALCULATES CARTESIAN COORDINATES FROM
C      MLS ANGLE AND DME/P DATA
C      THET=RCVR AZ (RADIANS)
C      PHI=RCVR EL(RADIANS)
C      XE=AZ TO EL SEPARATION (FEET)
C
C      DETERMINE THE POWERS OF TAN AND COT OF
C      THET AND PHI, RHOD, XE AND ZE
C      TAN2TH=(SIN(THET)/COS(THET))*(SIN(THET)/COS(THET))
C      COT2PH = (COS(PHI)/SIN(PHI))*(COS(PHI)/SIN(PHI))
C      COT4PH=COT2PH*COT2PH
C      RHOD2=RHOD*RHOD
C      ZE2=ZE*ZE
C      XE2=XE*XE
C***** DETERMINE QUARTIC PARAMETERS
C      A = TAN2TH*TAN2TH+2.0*TAN2TH*(1.0+TAN2TH)*COT2PH+2.0*(1.0+TAN2TH)*COT2PH
C      1+(1.0+TAN2TH)*(1.0+TAN2TH)*COT4PH+1.0
C      B = -4.0*XE-4.0*XE*(1.0+TAN2TH)*COT2PH
C      C = 2.0*TAN2TH-2.0*RHOD2*TAN2TH*COT2PH-2.0*TAN2TH*ZE2*COT2PH
C      1+6.0*XE2-2.0*RHOD2*COT2PH-2.0*ZE2*COT2PH+2.0*XE2*
C      1(1.0+TAN2TH)*COT2PH-2.0*RHOD2*(1.0+TAN2TH)*COT4PH+
C      12.0*(1.0+TAN2TH)*COT4PH*ZE2+4.0*ZE2*ZE2*
C      1(1.0+TAN2TH)
C      D = -4.0*XE2*XE+4.0*XE*RHOD2*COT2PH+4.0*XE*ZE2*COT2PH
C      E = -2.0*XE2*RHOD2*COT2PH-2.0*XE2*ZE2*COT2PH+RHOD2*RHOD2*
C      1COT4PH-2.0*RHOD2*COT4PH*ZE2+ZE2*ZE2*COT4PH+XE2*XE2
C      1-4.0*ZE2*RHOD2
C
C      START NEWTON RAPHSON ITERATION HERE
C      COMPUTE START POINT X (XE IF ZE >0, RHOD IF ZE<0)
C      IF(ZE.GT.0.0) X=XE
C      IF(ZE.LT.0.0) X=RHOD
C
C      COMPUTE QUARTIC X FUNCTION F
C      10 F = A*X*X*X*X+B*X*X*X+C*X*X+D*X+E
C      COMPUTE DERIVATIVE OF F=FDIV
C      FDIV=4.0*A*X*X*X+3.0*B*X*X+2.0*C*X+D
C
C      COMPUTE NEW ITERATIVE POINT XN
C      XN=X-F/FDIV
C      COMPARE THE DIFFERENCE BETWEEN OLD
C      AND NEW Y VALUES TO TOLERANCE LIMIT=LIM
C      IF(ABS(XN-X).LT.LIM)GO TO 20
C      X=XN
C      GO TO 10
C      20 Y=-X*TAN(THET)
C      Z=SQRT(RHOD2-X*X-Y*Y)
C      RETURN
C      END

```

CASE V

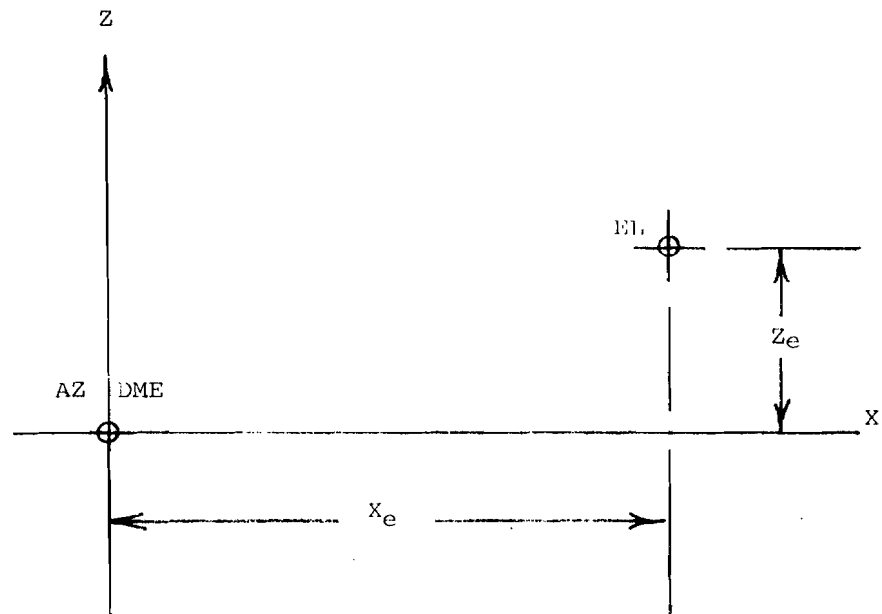
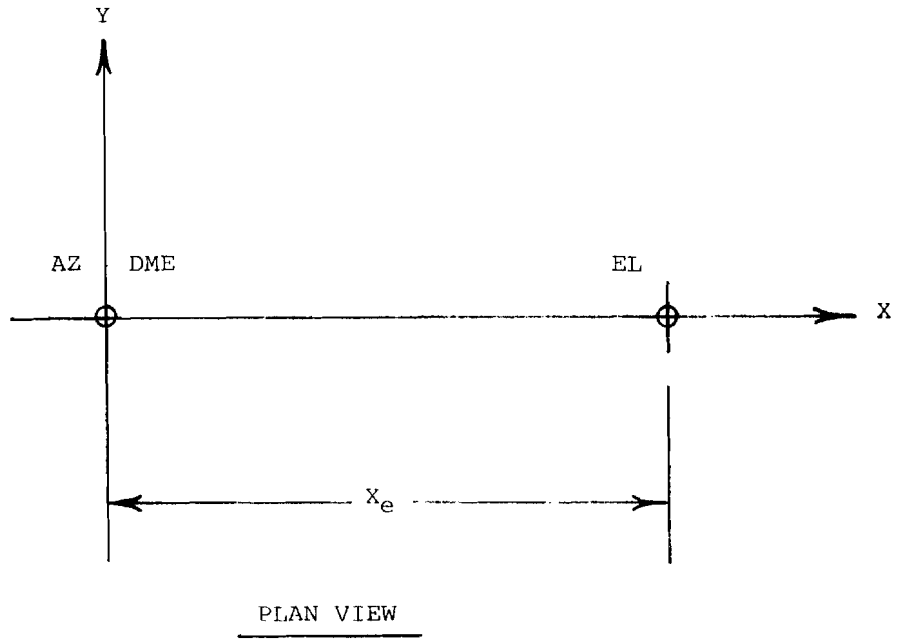


FIGURE 7. CASE V, GEOMETRY

CASE VI:

This case assumes that both the azimuth and DME/P ground units are collocated and reside at the origin of the coordinate system in the Z=0 plane (see figure). The elevation unit does not reside in this plane, but rather, it lies in the vertically displaced plane z=ze. Furthermore, the elevation unit is displaced by a distance xe along the x axis from the azimuth and DME/P units. There is assumed to be no relative displacement between any of the units in the y direction. The azimuth beam is assumed to be conical. A closed form expression does not result, but rather, a quartic polynomial in x results. An iterative solution (Newton-Raphson) running on a digital computer is recommended.

The equations which result are:

$$\text{From DME/P: } x^2 + y^2 + z^2 = \rho^2 \quad (1)$$

$$\text{From Azimuth: } y = -\rho \sin \theta \quad (2)$$

$$\text{From Elevation: } y^2 + (x - x_e)^2 = (z - z_e)^2 \cot^2 \phi \quad (3)$$

Substitute (2) into (1):

$$\rho^2 \sin^2 \theta + x^2 + z^2 = \rho^2 \quad (4)$$

$$\text{Rearranging and using } 1 - \sin^2 \theta = \cos^2 \theta \quad (5)$$

$$x^2 + z^2 = \rho^2 \cos^2 \theta \quad (6)$$

$$x = (\rho^2 \cos^2 \theta - z^2)^{1/2} \quad (7)$$

Substituting (2) and (7) into (3) to get:

$$\rho^2 \sin^2 \theta + ((\rho^2 \cos^2 \theta - z^2)^{1/2} - x_e)^2 = (z - z_e)^2 \cot^2 \phi \quad (8)$$

Multiplying out the terms:

$$\rho^2 \sin^2 \theta + \rho^2 \cos^2 \theta - z^2 - 2x_e(\rho^2 \cos^2 \theta - z^2)^{1/2} + x_e^2 = (z - z_e)^2 \cot^2 \phi \quad (9)$$

Rearranging:

$$-2x_e(\rho^2 \cos^2 \theta - z^2)^{1/2} = (z - z_e)^2 \cot^2 \phi + z^2 - \rho^2 - x_e^2 \quad (10)$$

Square both sides to clear fractional powers:

$$4x_e^2(\rho^2 \cos^2 \theta - z^2) = (z - z_e)^4 \cot^4 \phi + 2(z^2 - \rho^2 - x_e^2)(z - z_e)^2 \cot^2 \phi + (z^2 - \rho^2 - x_e^2)^2 \quad (11)$$

Multiplying out and collecting terms yields a quartic polynomial in Z:

$$Az^4 + Bz^3 + Cz^2 + Dz + E \quad (12)$$

$$\text{Where: } A = \cot^4 \phi + 2\cot^2 \phi + 1 \quad (13)$$

$$B = -4z_e \cot^4 \phi - 4z_e \cot^2 \phi \quad (14)$$

$$C = 6z_e^2 \cot^4 \phi + 2(z_e^2 - \rho^2 - x_e^2) \cot^2 \phi - 2\rho^2 + 2x_e^2 \quad (15)$$

$$D = -4z_e^3 \cot^4 \phi + 2(2\rho^2 z_e + 2x_e^2 z_e) \cot^2 \phi \quad (16)$$

$$E = x_e^4 + 2\rho^2 x_e^2 + \rho^4 - 2z_e^2 x_e^2 \cot^2 \phi - 2\rho^2 z_e^2 \cot^2 \phi + z_e^4 \cot^4 \phi - 4x_e^2 \rho^2 \cos^2 \theta \quad (17)$$

There should be 4 real roots which result, corresponding to the 4 points of intersection. Newton-Raphson iteration would be one technique which could be used for solution provided that care is taken to insure convergence to the proper point.

The equation employed in this method is:

$$z_{n+1} = z_n - \frac{f(z_n)}{f'(z_n)} \quad (18)$$

Where $f(z_n)$ is equation (12) above and:

$$f(z_n) = 4Az^3 + 3Bz^2 + 2Cz + D \quad (19)$$

The positive value of z closest to the elevation station is desired if z_e is positive. If z_e is negative, the intersection point farthest from the elevation is desired.

Once z is known, y is obtained by:

$$y = -\rho \sin \theta \quad (20)$$

$$x \text{ is obtained via (1) knowing } y \text{ and } z \quad (21)$$

$$x = (\rho^2 - z^2 - y^2)^{1/2} \quad (22)$$

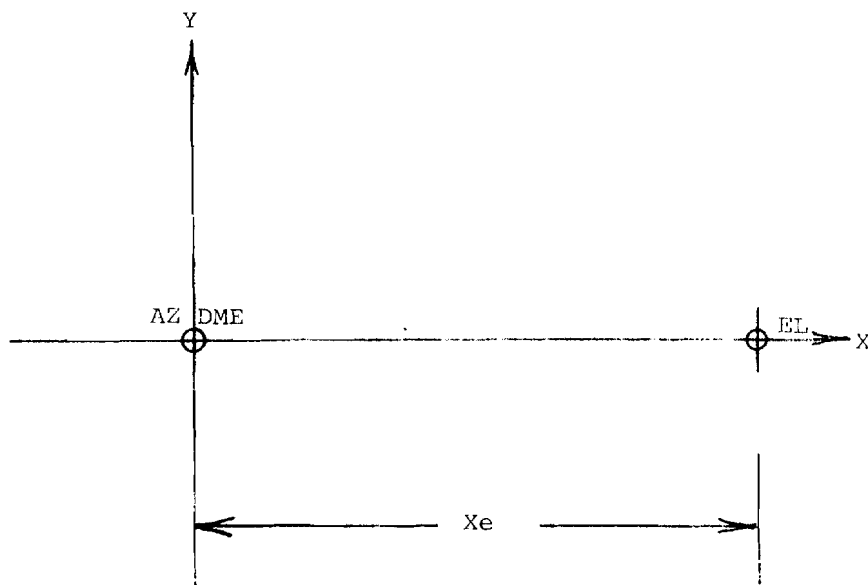
MLS RECONSTRUCTION ALGORITHM
CASE VI FORTRAN SUBROUTINE

```

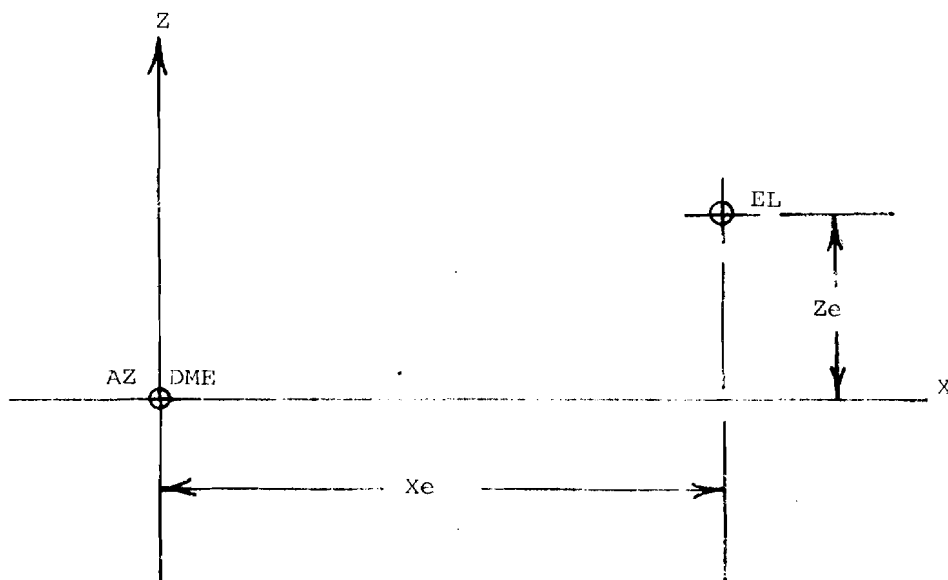
SUBROUTINE CASE6(THET,PHI,RHOD,XE,ZE,X,Y,Z,LIM)
C***** SUBROUTINE CALCULATES CARTESIAN COORDINATES FROM
C        MLS ANGLE AND DME/P DATA
C        THET=RCVR AZ (RADIANS)
C        PHI=RCVR EL(RADIANS)
C        RHOD=DME/P (FEET)
C        XE=AZ TO EL SEPARATION (FEET)
C        LIM=ITERATION LIMIT
C        DETERMINE THE POWERS OF COS AND COT OF
C        THET AND PHI, RHOD, XE AND ZE
        COS2TH = COS(THET)*COS(THET)
        COT2PH=COS(PHI)*COS(PHI)/(SIN(PHI)*SIN(PHI))
        COT4PH=COT2PH*COT2PH
        RHOD2=RHOD*RHOD
        XE2=XE*XE
        ZE2=ZE*ZE
C***** DETERMINE QUARTIC PARAMETERS
        A = COT4PH+2.0*COT2PH+1.0
        B = -4.0*ZE*COT4PH-4.0*ZE2*COT2PH
        C = 6.0*ZE2*COT4PH+2.0*(ZE2-RHOD2-XE2)*COT2PH-2.0*RHOD2+2.0*XE2
        D = -4.0*ZE2*ZE*COT4PH+2.0*(2.0*RHOD*ZE+2.0*XE2*ZE)*COT2PH
        E = XE2*XE2+2.0*RHOD2*XE2+RHOD2*RHOD2-2.0*ZE2*XE2*COT2PH
        1-2.0*RHOD2*ZE2*COT2PH+ZE2*ZE2*COT4PH-4.0*XE2*RHOD2*COS2TH
C
C        START NEWTON RAPHSON ITERATION HERE
C        COMPUTE START POINT Z HERE
        Z = (*RHOD-XE)*SIN(PHI)+ZE
C
C        COMPUTE QUARTIC Y FUNCTION F
10      F = A*Z*Z*Z*Z+B*Z*Z*Z+C*Z*Z+D*Z+E
C        COMPUTE DERIVATIVE OF F=FDIV
        FDIV=4.0*A*Z*Z*Z+3.0*B*Z*Z+2.0*C*Z+D
C
C        COMPUTE NEW ITERATIVE POINT ZN
        ZN=Z-F/FDIV
C        COMPARE THE DIFFERENCE BETWEEN OLD AND NEW Y VALUES TO DETERMINE
C        CONVERGENCE TO WITHIN LIMIT DELTA = LIM
        IF(ABS(ZN-Z).LT.LIM)GO TO 20
        Z=ZN
        GO TO 10
20      Y=-RHOD*SIN(THET)
        X=SQRT(RHOD2-Z*Z-Y*Y)
        RETURN
        END

```

CASE VI



PLAN VIEW



ELEVATION VIEW

FIGURE 8. CASE VI, GEOMETRY

Cases VII, VIII, and XI can be grouped together and are referred to as "Thedford" type algorithms after their originator, Dr. William Thedford. These algorithms iterate using a quadratic derived from the three MLS defining equations. Case VII is the most general of the three in that it covers an arbitrary placement of the three signal sources. It, along with case XI, employs planar azimuth. Case XI which uses the DME/P as the reference frame, requires a linear translation for use of a non-DME/P centered reference frame. Case VIII uses a collocated azimuth/DME/P referenced coordinate system as well as conic azimuth. It is the simplest of the three, and would be used for closely spaced signal sources. All three of the algorithms are relatively simple and converge within three iterations, which takes less than 20 milliseconds on a PDP 11/34 computer, a typical target machine.

Cases IX and X are very similar implementations of a Seidel-like iterative technique. The prime difference between them is that case IX addresses conic azimuth, whereas case X addresses planar azimuth. Completely arbitrary signal source geometries are allowed in both cases. The code required for these general solutions is minimal. The tradeoff for the aforementioned benefits is that a greater number of iterations are required for convergence. These algorithms are useful for the full 3D MLS RNAV implementation for general ground siting. However, these areas should be run on computers capable of fast processing.

Case XII is another conic azimuth case which is designed for completely arbitrary ground siting geometry. It employs Newton Raphson iteration in three dimensions on linear Taylor Series approximations to the three defining equations. It is applicable to full 3D MLS RNAV designs using any ground equipment siting. Convergence is rapid (usually within a few iterations). Code size is the largest of all the algorithms. Based on this fact, a computer with adequate memory and processing power is required with this application.

COORDINATE TRANSFORMATION ALGORITHM TEST PROCEDURE.

All 12 of the MLS transformation algorithms were subjected to various levels of validation testing. These tests were of three types:

1. Point by point validation of the transformation process throughout MLS coverage.
2. Simulated RNAV flights along various straight line single segment flight-paths using computer generated input data.
3. Simulated RNAV approaches and departures to and from the primary instrumented runway using live flight MLS triples as input data. A more detailed discussion of each of these tests follow.

GRID POINT TESTING.

All 12 of the MLS transformation algorithms were subjected to point by point validation testing over an MLS coverage volume spanning 20 nmi in DME/P, $\pm 40^\circ$ in azimuth and $+2^\circ$ to $+20^\circ$ in elevation. These tests entailed generating cartesian triples (x,y,z) over the MLS coverage volume, and then converting these to the equivalent MLS triple (θ, ϕ, ρ). The resulting MLS triple was input to the MLS

CASE VII:

This MLS Reconstruction Algorithm, referred to as "Case VII," is an extension to the "Thedford Algorithms" of Case XI. In concept, this algorithm is very similar to the Thedford Algorithm implementation. It differs from it principally in that the origin of the MLS cartesian coordinate system (0,0,0) is not located at the phase center of the DME/P ground transponder. Thus, the DME/P unit may assume any location (xd,yd,zd) in cartesian space. The azimuth ground transmitter is assumed here to produce a planar beam. Its phase center is located at (xa,ya,za). The elevation unit phase center is located at (xe,ye,ze), and produces a conical beam whose axis is parallel to the z axis. A closed form solution for the cartesian coordinates does not result, but rather, an iterative technique is employed to do the reconstruction. $Z_i = i^{th}$ approximation to Z.

The equations which result are as follows:

$$\text{From DME/P: } (x-xd)^2+(y-yd)^2+(z-zd)^2 = \rho^2 \quad (1)$$

$$\text{From planar azimuth: } \tan\theta = -(y-ya)/(x-xa) \quad (2)$$

$$\text{From elevation: } z_{i+1} - ze = \sin\phi((x-xe)^2+(y-ye)^2+(z-ze)^2)^{1/2} \quad (3)$$

$$\text{or: } z_{i+1} = ze + \sin\phi((x-xe)^2+(y-ye)^2+(z-ze)^2)^{1/2} \quad (4)$$

$$\text{Solve (2) for x: } x = xa - (y-ya)\cot\theta \quad (5)$$

Substitute (5) into (1):

$$(xa - (y-ya)\cot\theta - xd)^2 + (y-yd)^2 + (z-zd)^2 = \rho^2 \quad (6)$$

Multiplying out (6) and collecting terms yields:

$$y^2(1+\cot^2\theta) + y(2(xa\cot\theta - xacot\theta - yacot^2\theta - ya)) + (xa^2 + xd^2 + yd^2 + zd^2 + z^2 - \rho^2 + 2(xayacot\theta - zzd - xaxd) + ya^2\cot^2\theta) = 0 \quad (7)$$

Knowing the siting parameters, θ and z , and assuming a starting value for z , we have a quadratic equation which can be solved for y using:

$$y = \frac{-B \pm (B^2 - 4AC)^{1/2}}{2A} \quad (8)$$

$$\text{Where: } A = 1 + \cot^2\theta \quad (9)$$

$$B = 2(xd\cot\theta - xacot\theta - yacot^2\theta - ya) \quad (10)$$

$$C = xa^2 + xd^2 + yd^2 + zd^2 + z^2 - \rho^2 + 2(xayacot\theta - zzd - xaxd) + ya^2\cot^2\theta \quad (11)$$

Knowing y , θ , and the siting parameters, x can be obtained via (5):

$$x = xa - (y-ya)\cot\theta \quad (12)$$

The foregoing equations are incorporated into an algorithm which proceeds as follows:

$$\text{Pick a starting value for } z_i: z_i = \rho \sin\phi \quad (13)$$

Calculate A, B, and C:

$$A = 1 + \cot^2\theta \quad (9)$$

$$B = 2(xd\cot\theta - xacot\theta - yacot^2\theta - ya) \quad (10)$$

$$C = xa^2 + xd^2 + yd^2 + zd^2 + z^2 - \rho^2 + 2(xayacot\theta - zzd - xaxd) + ya^2\cot^2\theta \quad (11)$$

Use A,B, and C to calculate y:

$$y_i = -B + (B^2 - 4AC)^{1/2} / 2A \quad (8)$$

Calculate x from (5):

$$x_i = x_a - (y_i - y_a) \cot \theta \quad (5)$$

Calculate the next value of z:

$$z_{i+1} = z_e + \sin \phi \left((x - x_e)^2 + (y - y_e)^2 + (z - z_e)^2 \right)^{1/2} \quad (4)$$

Compute an error box for stopping:

$$\left| z_{i+1} - z_i \right| + \left| y_{i+1} - y_i \right| + \left| x_{i+1} - x_i \right| < \xi \quad (13)$$

If ξ is less than the limit, then stop iterating. If not, return to (8) and repeat the process.

Please note, that the angle ϕ is measured in a clockwise direction from the x axis, and singularities result when $\theta = 0$. To avoid this, logic must be included to let $y = y_a$ in this case, with x being calculated from (1).

On the first pass through the iteration, two successive values of z are assigned, but only one for x and y. Two values of x and y are required for the error test. They can be assigned by letting:

$$x_0 = \rho \cos \phi \cos \theta \quad (14)$$

$$y_0 = -\rho \cos \phi \sin \theta \quad (15)$$

FORTRAN SUBROUTINE FOR
MLS RECONSTRUCTION ALGORITHM
CASE VII

```

SUBROUTINE CASE13(THET,PHI,RHOD,XA,YA,ZA,XD,YD,
1 ZD,X,Y,Z,LIM)
C***** THIS ALGORITHM PROVIDES CARTESIAN X,Y,Z COORDINATE OUTPUT FOR
C MLS ANGLE AND DME/P INPUTS
C
C THET=RCVR AZ (RADIANS)
C PHI=RCVR EL(RADIANS)
C RHOD=DME/P (FEET)
C XA = AZ UNIT X COORDINATE
C YA = AZ UNIT Y COORDINATE
C ZA = AZ UNIT Z COORDINATE
C
C XE = EL UNIT X COORDINATE
C YE = EL UNIT Y COORDINATE
C ZE = EL UNIT Z COORDINATE
C
C LIM=ERROR TOLERANCE
C
C XD = DME UNIT X COORDINATE
C YD = DME UNIT Y COORDINATE
C ZD = DME UNIT Z COORDINATE
C
C CALCULATE POWERS AND TRANSCENDENTAL FUNCTIONS
C
C RHOD2=RHOD*RHOD
C COTTH=COS(THET)/SIN(THET)
C XD2=XD*XD
C YD2=YD*YD
C ZD2=ZD*ZD
C COT2TH=COTTH*COTTH
C XA2=XA*XA
C YA2=YA*YA
C
C CALCULATE FIRST VALUES OF X AND Y
C X = RHOD*COS(PHI)*COS(THET)
C Y = -1.0*RHOD*COS(PHI)*SIN(THET)
C
C CALCULATE Z STARTING POINT
C Z = RHOD*SIN(PHI)
C CALCULATE QUADRATIC FOR NEXT Y VALUE, YN
C
10 A = 1.0+COT2TH
C B = 2.0*(XD*COTTH-XA*COTTH-YA*COT2TH-YA)
C C = XA2+XD2+YD2+ZD2+Z*Z-RHOD2+2.0*(XA*YA*COTTH-
1 Z*ZD-XA*XD)+YA2*COT2TH
C
C YN=(-B+SQRT(B**2-4.0*A*C))/(2.0*A)
C
C CALCULATE XN, THE NEXT VALUE OF X
C

```

```

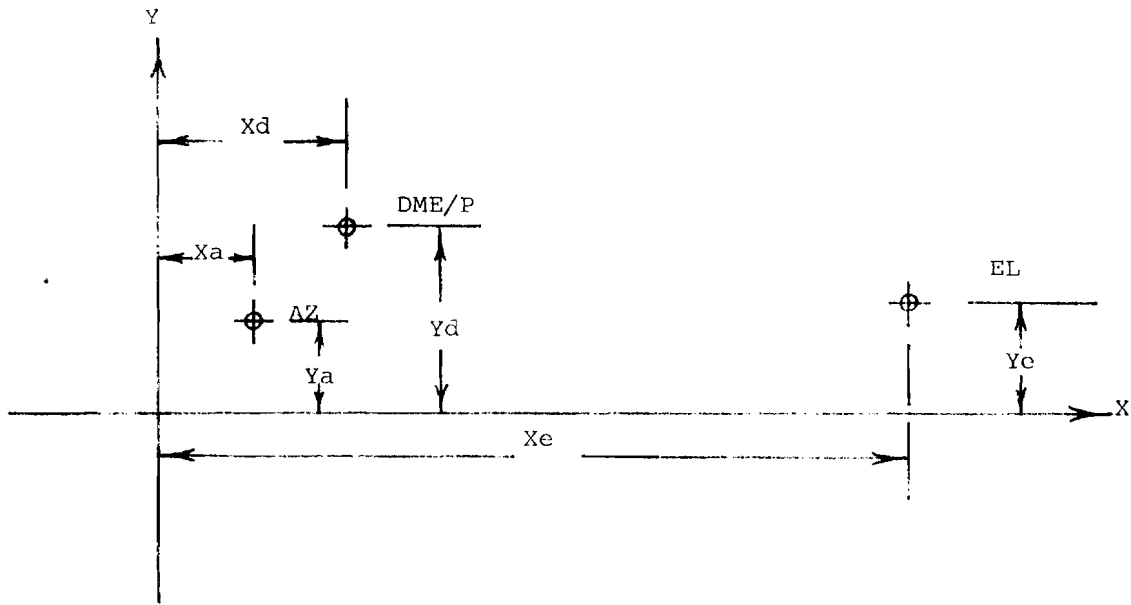
IF (THET.EQ.0.0) GO TO 20
XN=XA-(Y-YA)*COTTH
GO TO 30
C   CALCULATE 0 DEG THETA X VALUE
20  XN=XD+SQRT(RHOD2-(Z-ZD)**2-(YA-YD)**2)

C   CALCULATE NEXT Z VALUE, ZN
C
ZN=ZE+SIN(PHI)*SQRT((XN-XE)**2+(YN-YE)**2+(Z-ZE)**2)
C
C   COMPUTE ERROR BOX
C
EPS=ABS(ZN-Z)+ABS(YN-Y)+ABS(XN-X)
Z=ZN
Y=YN
X=XN

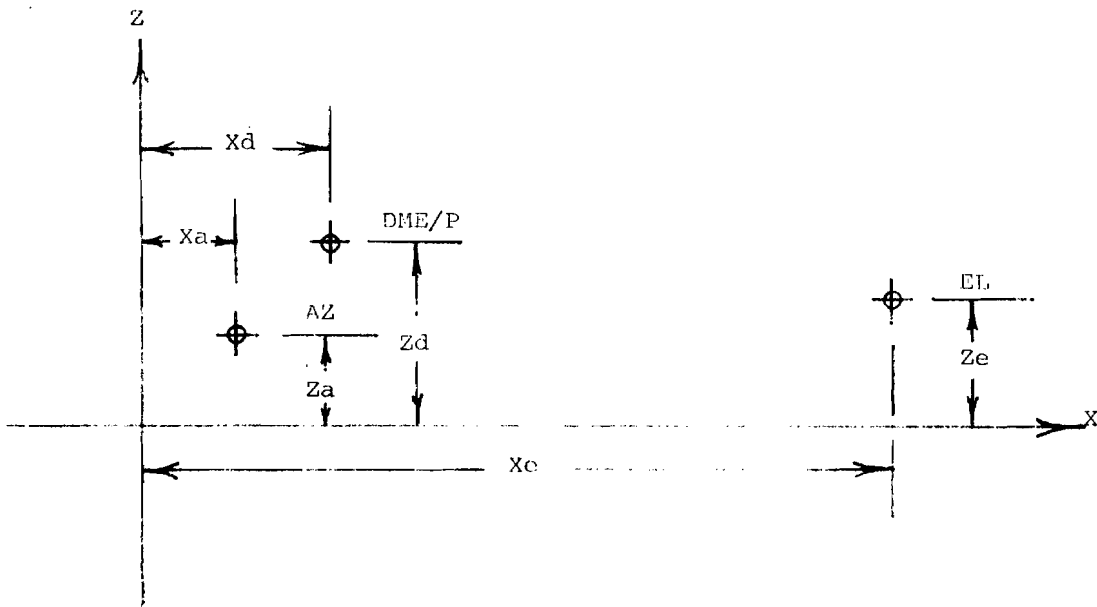
C
C   TEST FOR CONVERGENCE
C
IF (EPS.GE.LIM) GO TO 10
RETURN
END

```

CASE VII



PLAN VIEW



ELEVATION VIEW

FIGURE 9. CASE VII, GEOMETRY

CASE VIII:

This case is a simplification of case VII, the conical azimuth "Thedford Algorithm." However, it entails a simplification of the geometry to the collocated azimuth and DME/P configuration. This collocated site is taken as the origin of the coordinate system. The elevation station may be situated anywhere in space at the cartesian coordinates (x_e, y_e, z_e) . The equations which result are nonlinear, and an iterative solution is used to find the reconstructed (x, y, z) coordinates.

The equations which result are:

$$\text{From DME/P: } x^2 + y^2 + z^2 = \rho^2 \quad (1)$$

$$\text{From conical azimuth: } y = -\rho \sin \theta \quad (2)$$

$$\text{From elevation: } (z_{i+1} - z_e) = \sin \phi ((x - x_e)^2 + (y - y_e)^2 + (z_i - z_e)^2)^{1/2} \quad (3)$$

Where z_i is the last z estimate of current aircraft position.

$$\text{Substituting (2) into (1): } \rho^2 \sin^2 \theta + x^2 + z^2 = \rho^2 \quad (4)$$

$$\text{Rearranging (4): } x^2 = \rho^2 (1 - \sin^2 \theta) - z^2 \quad (5)$$

Taking the square root of both sides of (5) and using the identity

$$(1 - \sin^2 \theta) = \cos^2 \theta \quad (6)$$

$$x = \pm (\rho^2 \cos^2 \theta - z^2)^{1/2} \quad (7)$$

Note: Use the positive value, assuming there is no back azimuth.

The computation proceeds as follows:

Start with an initial value of z :

$$z_i = \rho \sin \phi + z_e \quad (8)$$

Use (8) to compute a value of x from (7):

$$x_i = (\rho^2 \cos^2 \theta - z_i^2)^{1/2} \quad (9)$$

From (2) calculate a value of y :

$$y_i = -\rho \sin \theta \quad (10)$$

Calculate an updated value of z from (3):

$$z_{i+1} = z_e + \sin \phi ((x_i - x_e)^2 + (y_i - y_e)^2 + (z_i - z_e)^2)^{1/2} \quad (11)$$

Check the differential change in z :

If the following holds then stop:

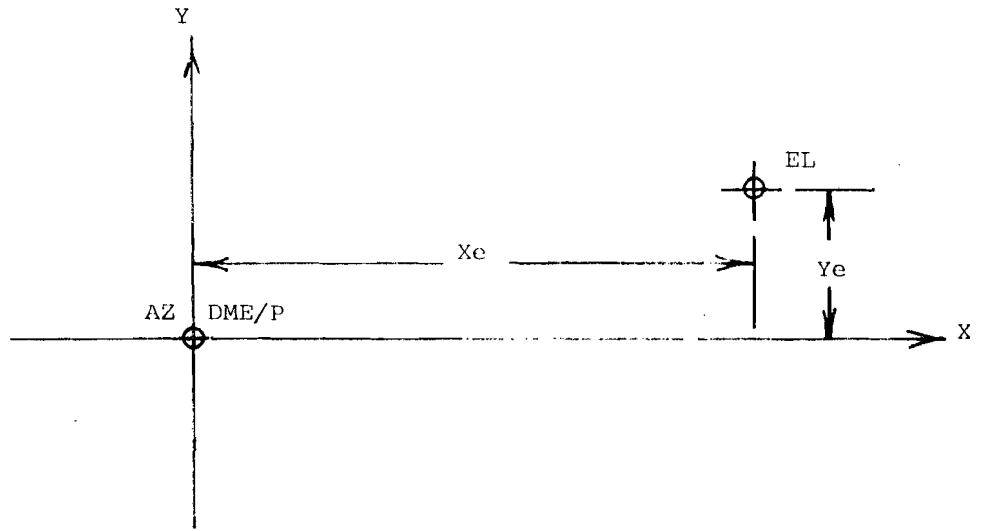
$$z_{\text{error}} = |z_{i+1} - z_i| < \xi \quad (12)$$

If not, return to (9) and repeat the computations.

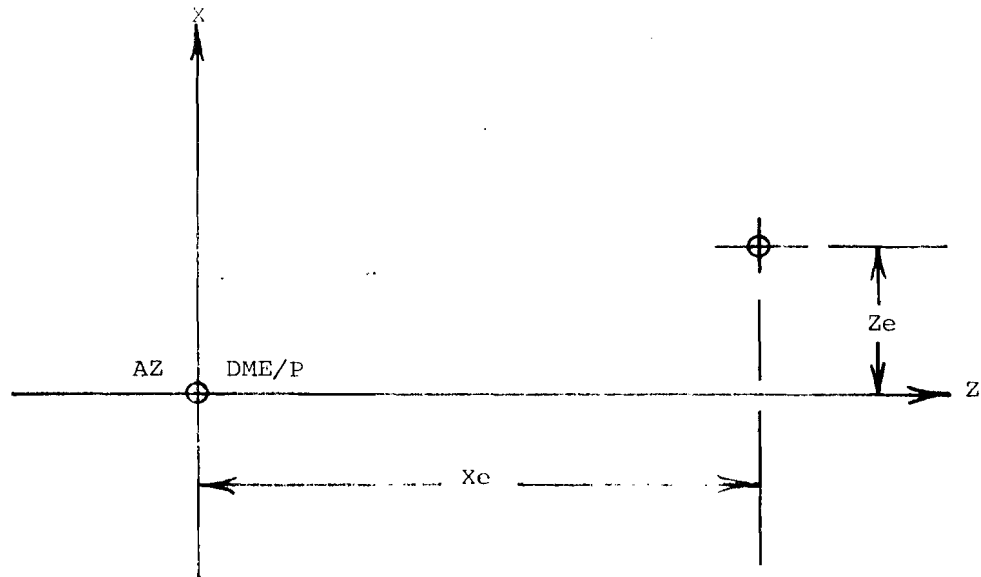
MLS RECONSTRUCTION ALGORITHM
CASE VIII FORTRAN

```
      SUBROUTINE CASE8(THET,PHI,RHOD,XE,ZE,X,Y,Z,LIM)
C***** SUBROUTINE CALCULATES CARTESIAN COORDINATES FROM
C      MLS ANGLE AND DME/P DATA
C      THET=RCVR AZ (RADIANS)
C      PHI=RCVR EL(RADIANS)
C      RHOD=DME/P (FEET)
C      AZIMUTH AND DME/P ARE COLLOCATED AT ORIGIN
C      XE = X COORDINATE OF ELEVATION (FEET)
C      YE = Y COORDINATE OF ELEVATION (FEET)
C      ZE = Z COORDINATE OF ELEVATION (FEET)
C
C      RHOD2=RHOD*RHOD
C      START ITERATION WITH INITIAL Z
C      Z = RHOD*SIN(PHI)+ZE
10     X = SQRT (RHOD2*COS(THET)*COS(THET)-Z*Z)
C      Y = -1.0*RHOD*SIN(THET)
C      CALCULATE NEW ZN
C      ZN=ZE+SIN(PHI)*SQRT((X-XE)**(X-XE)+(Y-YE)**(Y-YE)
1     1+(Z-ZE)**(Z-ZE))
C      TEST ITERATION CONVERGENCE
C      IF (ABS(ZN-Z).LT.LIM) GO TO 20
C      Z=ZN
C      GO TO 10
20     RETURN
C      END
```

CASE VIII



PLAN VIEW



ELEVATION VIEW

FIGURE 10. CASE VIII, GEOMETRY

CASE IX:

This case assumes a completely general geometry for the locations of the ground based azimuth, elevation, and DME/P stations. The azimuth unit is sited at cartesian coordinates (x_a, y_a, z_a) . The elevation unit is located at (x_e, y_e, z_e) . The DME/P coordinates are (x_d, y_d, z_d) . Conical azimuth and conical elevation are used in the derivation. Three nonlinear equations result. A closed form solution is not obtained. Instead, a nonlinear Seidel-like iteration procedure is employed in order to obtain a solution for x , y and z .

The equations which result are:

$$\text{From DME/P: } (x-x_d)^2+(y-y_d)^2+(z-z_d)^2 = \rho^2 \quad (1)$$

$$\text{From azimuth: } (x-x_a)^2+(z-z_a)^2=(y-y_a)^2 \cot^2 \theta \quad (2)$$

$$\text{From elevation: } (x-x_e)^2+(y-y_e)^2=(z-z_e)^2 \cot^2 \phi \quad (3)$$

Rearranging (3) to the form $z = f(x, y, \phi)$:

$$z = z_e + \tan \phi ((x-x_e)^2 + (y-y_e)^2)^{1/2} \quad (4)$$

Rearranging (2) to the form $y = f(x, z, \theta)$ yields:

$$y = y_a + \tan \theta ((x-x_a)^2 + (z-z_a)^2)^{1/2} \quad (5)$$

Rearranging (1) to the form $x = f(y, z, \rho)$ yields:

$$x = x_d + (\rho^2 - (y-y_d)^2 - (z-z_d)^2)^{1/2} \quad (6)$$

Three nonlinear iteration equations (4,5 and 6) have been derived. The computation of x , y and z proceeds as follows:

Pick a starting value for x :

$$x = \rho \cos \theta \quad (7)$$

Pick a starting value for y :

$$y = -\rho \sin \theta \quad (8)$$

Compute the next value of z , z_{i+1} :

$$z_{i+1} = z_e + \tan \phi ((x-x_e)^2 + (y-y_e)^2)^{1/2} \quad (9)$$

Compute the next value of y , y_{i+1} :

$$y_{i+1} = y_a + \tan \theta ((x-x_a)^2 + (z-z_a)^2)^{1/2} \quad (10)$$

Compute the next value of x , x_{i+1} :

$$x_{i+1} = x_d + (\rho^2 - (y-y_d)^2 - (z-z_d)^2)^{1/2} \quad (11)$$

Compare the new values x_{i+1} , y_{i+1} , z_{i+1} to the previous values:

$$|x_{i+1} - x_i| < \xi \quad (12)$$

$$|y_{i+1} - y_i| < \xi \quad (13)$$

$$|z_{i+1} - z_i| < \xi \quad (14)$$

If any of the above errors are out of bounds, then recompute using x_{i+1} , y_{i+1} , z_{i+1} as the new starting point.

MLS RECONSTRUCTION ALGORITHM
CASE IX FORTRAN

```

SUBROUTINE CASE9(THET,PHI,RHOD,XA,YA,ZA,XD,YD,ZD,
1 XE,YE,ZE,LIMX,LIMY,LIMZ,X,Y,Z,IFLAG,ITER)
C***** SUBROUTINE CALCULATES CARTESIAN COORDINATES FROM MLS
C ANGLE AND DME/P DATA
C THET=RCVRAZ (RADIANS)
C PHI=RCVREL(RADIANS)
C RHOD=DME/P (FEET)
C XA = AZ X COORDINATE (FEET)
C YA = AZ Y COORDINATE (FEET)
C ZA = AZ Z COORDINATE (FEET)
C XD = DME X COORDINATE (FEET)
C YD = DME Y COORDINATE (FEET)
C ZD = DME Z COORDINATE (FEET)
C XE = EL X COORDINATE (FEET)
C YE= EL Y COORDINATE (FEET)
C ZE = EL Z COORDINATE (FEET)
C LIMX = X ITERATION LIMIT
C LIMY = Y ITERATION LIMIT
C LIMZ = Z ITERATION LIMIT
C
C IFLAG = 0 ITERATED OUTCOME SUCCESSFULL
          = 1 ITERATIONS EXCEEDED
          = 2 SQRT ARG < 0
NOTE:   NUMBER OF ITERATIONS MAY VARY FROM 10 TO 90 FOR .1 FOOT TOLERANCE
IFLAG = 0

C DETERMINE THE STARTING VALUES, INCLUDING A PSEUDO VALUE FOR Z
C
Y = -1.0*RHOD*SIN(THET)
Z = 50.
X = RHOD*COS(THET)
ITER=0
10 ITER=ITER+1

C RECORD SAMPLE POINT WITH EXCESSIVE ITERATIONS

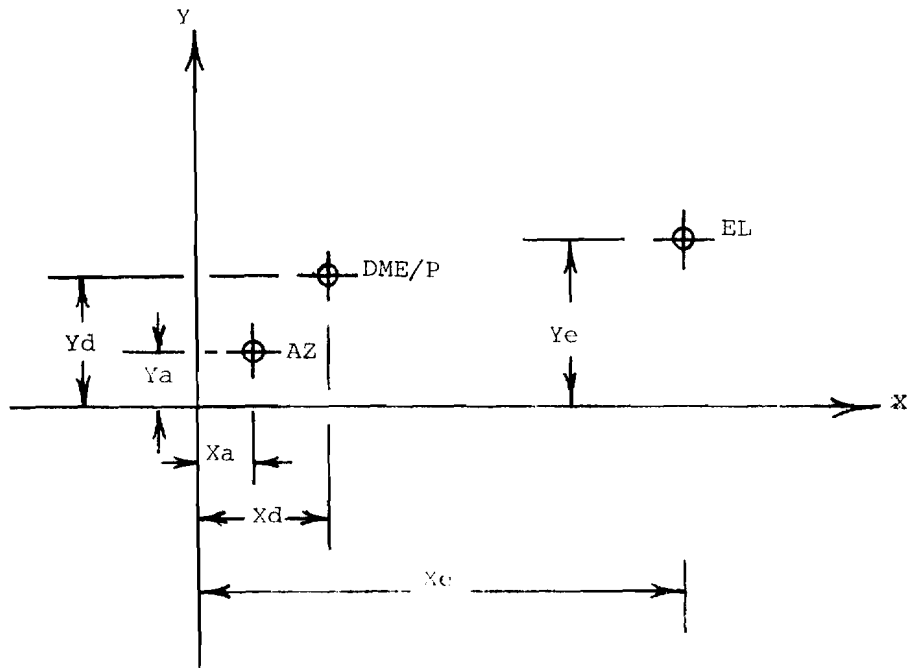
IF (ITER.GT.10) THEN
IFLAG=1
GO TO 99
ENDIF

C
Z1 = ZE+TAN(PHI)*SQRT((X-XE)**2+(Y-YE)**2)
Y1 = YA-TAN(THET)*SQRT((X-XA)**2+(Z1-ZA)**2)
R = RHOD**2-(Y1-YD)**2-(Z1-ZD)**2
IF(R.LT.0)THEN
IFLAG=2
GO TO 99
ENDIF

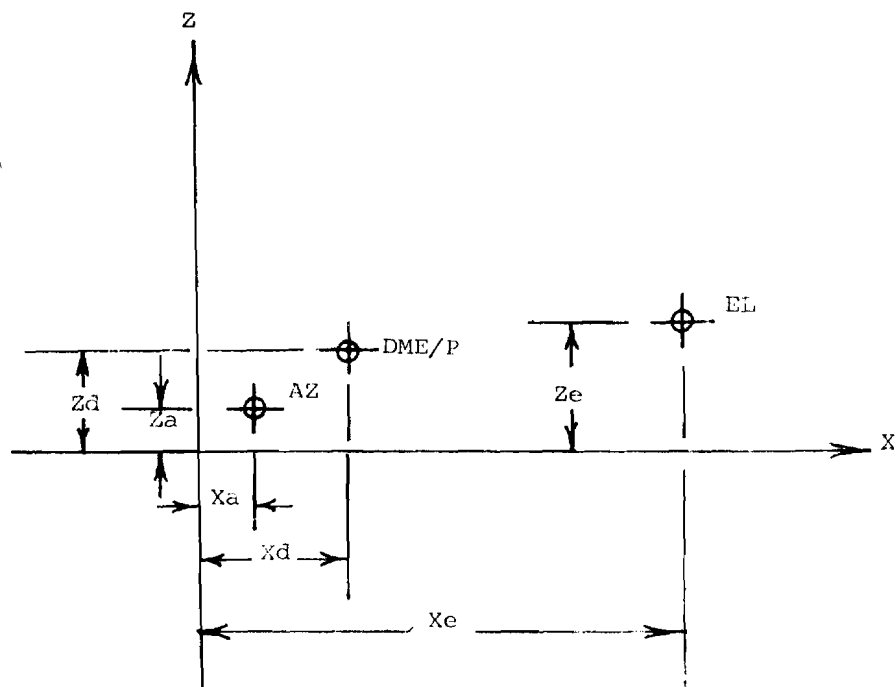
```

```
      X1=XD+SQRT(R)
C
C      TEST TOLERANCE
      IF(ABS(X1-X).GT.LIMX) GO TO 20
      IF(ABS(Y1-Y).GT.LIMY) GO TO 20
      IF(ABS(Z1-Z).GT.LIMZ) GO TO 20
C
C      BRING NEXT ITERATION PARAMETERS
C
20     X=X1
      Y=Y1
      Z=Z1
      GO TO 10
C
99     RETURN
      END
```

CASE IX



PLAN VIEW



ELEVATION VIEW

FIGURE 11. CASE IX, GEOMETRY

CASE X:

This case assumes a completely general geometry for the locations of the ground based azimuth, elevation, and DME/P stations. The azimuth unit is sited at cartesian coordinates (x_a, y_a, z_a) . The elevation unit is located at (x_e, y_e, z_e) . The DME/P coordinates are (x_d, y_d, z_d) . Planar azimuth and conical elevation are used in the derivation. Three nonlinear equations result. A closed form solution is not obtained. Instead, a nonlinear Seidel iteration procedure is employed in order to obtain a solution for x , y , and z . [See note 1]

The equations which result are:

$$\text{From DME/P: } (x-x_d)^2 + (y-y_d)^2 + (z-z_d)^2 = \rho^2 \quad (1)$$

$$\text{From azimuth: } (y-y_a) = -(x-x_a)\tan\theta \quad (2)$$

$$\text{From elevation: } (x-x_e)^2 + (y-y_e)^2 = (z-z_e)^2 \cot^2\phi \quad (3)$$

Rearranging (2) to obtain the form $y = f(x, \theta)$:

$$y = y_a + (x - x_a)\tan\theta \quad (4)$$

Rearranging to the form $z = f(x, y, \phi)$:

$$z = z_e + \frac{(x-x_e)^2 + (y-y_e)^2}{\cot^2\phi} \quad (5)$$

Rearranging (1) to the form $x = f(y, z, \rho)$:

$$x = x_d + \left[\rho^2 - (y-y_d)^2 - (z-z_d)^2 \right]^{1/2} \quad (6)$$

Three nonlinear iteration equations (4, 5 and 6) have been derived. The algorithm for computation of x , y and z proceeds as follows:

Pick a starting value for x :

$$x = \rho \cos\theta \cos\phi + x_d \quad (7)$$

Compute a value for y :

$$y = y_a + (x - x_a)\tan\theta \quad (8)$$

Compute a value for z :

$$z = z_e + \frac{(x-x_e)^2 + (y-y_e)^2}{\cot^2\phi} \quad (9)$$

Compute x_{i+1} :

$$x_{i+1} = x_d + \left[\rho^2 - (y - y_d)^2 - (z - z_d)^2 \right]^{1/2} \quad (10)$$

Compute y_{i+1} :

$$y_{i+1} = y_a + (x_a - x_{i+1}) \tan \theta \quad (11)$$

Compute z_{i+1} :

$$z_{i+1} = z_e + \frac{\left[(x_{i+1} - x_e)^2 + (y_{i+1} - y_e)^2 \right]^{1/2}}{\cot^2 \theta} \quad (12)$$

The iteration is repeated until the transformed coordinates begin to converge to their final values, as measured by the following test:

$$|y_{i+1} - y_i| < \xi \quad (13)$$

$$|x_{i+1} - x_i| < \xi \quad (14)$$

$$|z_{i+1} - z_i| < \xi \quad (15)$$

If these tests do not hold, then the process is repeated from step (10).

[1] Note: At values of the MLS triple near the limits of coverage, a large number of iterations (greater than 20) may be needed to assure convergence.

FORTRAN SUBROUTINE FOR MLS
RECONSTRUCTION ALGORITHM CASE X

```

C      SUBROUTINE TO CONVERT MLS ANGLES AND DME SLANT RANGE
C      INTO X,Y,Z, CARTESIAN COORDINATES USING ITERATIVE
C      PROCEDURES.
C
C      THET=RCVR AZ ANGLE (RADIANS)
C      PHI=RCVR EL ANGLE (RADIANS)
C      RHOD=SLANT RANGE (FEET)
C      XA=AZ X COORDINATE (FEET)
C      YA=AZ Y COORDINATE
C      ZA=AZ Z COORDINATE
C      XE=EL X COORDINATE
C      YE=EL Y COORDINATE
C      ZE=EL Z COORDINATE
C      XD=DME X COORDINATE
C      YD=DME Y COORDINATE
C      ZD=DME Z COORDINATE
C
C      SUBROUTINE CASE10(THET,PHI,RHOD,RNM,XA,YA,ZA,XE,YE,ZE,
C      &                  XD,YD,ZD,X,Y,Z,DELTA,IERR)
C
C      INTEGER      I,N
C
C      C**** INITIALIZE
C
C      N = 100
C      DELTA = .1
C      IERR = 0
C
C      C**** CALCULATE TRANSCENDENTAL FUNCTIONS
C      COTPH(COS(PHI))/(SIN(PHI))
C      COT2PH=COTPH*COTPH
C      TANTH=TAN(THET)
C
C      C**** CHOOSE FIRST VALUE FOR XI
C
C      XI = XD + RHOD * COS(THET)*COS(PHI)
C
C      C**** CHOOSE FIRST VALUE FOR YI
C
C      YI = YA+(XA-XI)*TANTH
C
C      C**** CHOOSE FIRST VALUE FOR ZI
C      ARG=((XI-XE)**2+(YI-YE)**2)/COT2PH
C      ZI = ZE+SQRT(ARG)
C
C      C**** ITERATIVE PROCEDURE
C

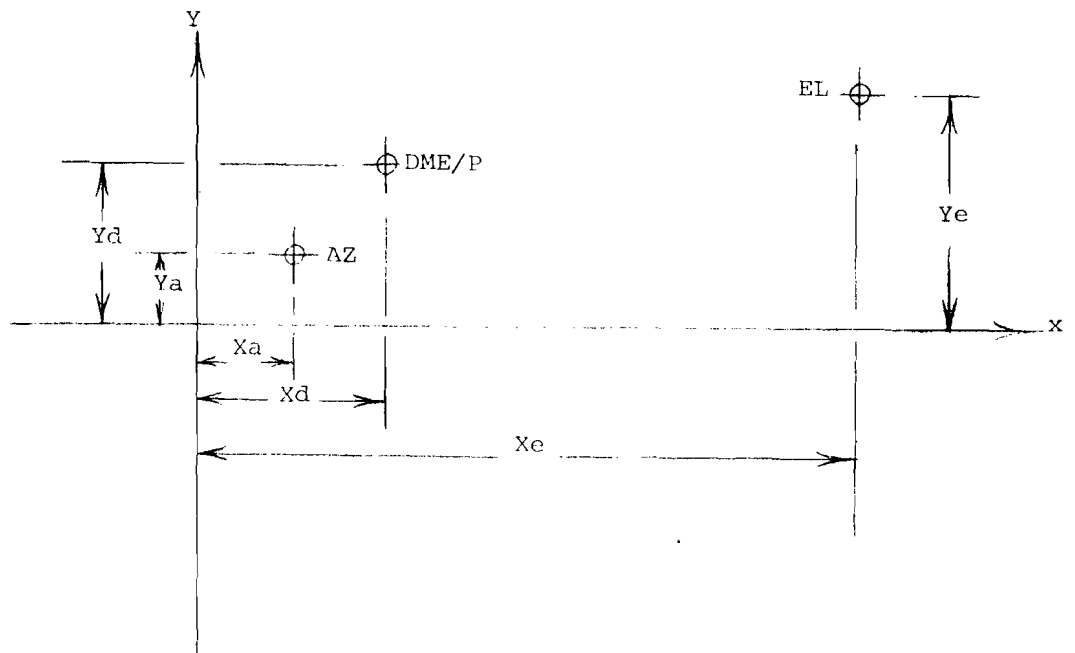
```

```

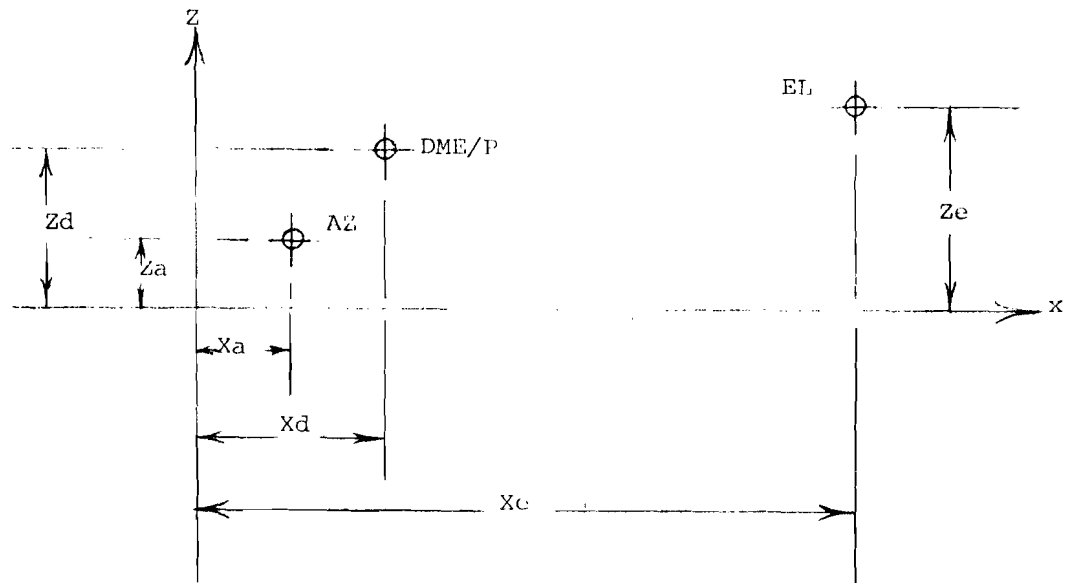
C
C
DO 1000, I = 1, N
X11 = XD+SQRT(RHOD**2-(YI-YD)**2-(ZI-ZD)**2)
Y11 = YA + (XZ - X11) * TANTH
ARG = ((X11-XE)**2+(Y11-YE)**2)/COT2PH
Z11 = ZE+SQRT(ARG)
IF((ABS(X11 - XI) .LE. DELTA) .AND. (ABS(Y11 - YI) . LE. DELTA)
& .AND. (ABS(Z11 - ZI) .LE. DELTA)) THEN
  X = X11
  Y = Y11
  Z = Z11
  GO TO 3000
ELSE
C
  XI = X11
  YI = Y11
  ZI = Z11
  END IF
1000 CONTINUE
C
C**** RECORD ERROR
WRITE (3,900) THET,PHI,RNM,XI,YI,ZI
900 FORMAT (6E12.4)
C
  IERR = 1
C
C**** FILL X,Y,Z WITH -999 IF AN ERROR OCCURS
C
  X = -999.
  Y = -999.
  Z = -999.
C
3000 CONTINUE
C
RETURN
END

```

CASE X



PLAN VIEW



ELEVATION VIEW

FIGURE 12. CASE X, GEOMETRY

CASE XI:

This case, referred to as the "Thedford Algorithm," is the counterpart to Case VII, the general extension to the "Thedford Algorithm," As such, it is in principle similar to the former case, but differs from it in that the azimuth is taken to be planar, as opposed to conical. The elevation unit also produces a conical beam. The three MLS units may assume any location, but the origin of the cartesian coordinate system, (0,0,0), is placed at the DME/P unit. The azimuth unit coordinates are (xa,ya,za), and the elevation unit coordinates are (xe,ye,ze). A closed form solution for the cartesian coordinates does not result, but rather an iterative technique is employed to do the reconstruction.

The equations which result are as follows:

$$\text{From DME/P: } x^2 + y^2 + z^2 = \rho^2 \quad (1)$$

$$\text{From planar azimuth: } \tan \theta = (y-ya)/(x-xa) \quad (2)$$

$$\text{From elevation: } z_{i+1}-ze = \sin \phi ((x-xe)^2+(y-ye)^2+(z-ze)^2)^{1/2} \quad (3)$$

$$\text{or: } z_{i+1}=ze + \sin \phi ((x-xe)^2+(y-ye)^2+(z-ze)^2)^{1/2} \quad (4)$$

$$\text{Solve (2) for y: } y=ya-(x-xa)\tan \theta \quad (5)$$

Substitute (5) into (1) to solve for x:

$$x^2+(ya-(x-xa)\tan \theta)^2+z^2 = \rho^2 \quad (6)$$

Multiplying out (6) and collecting terms yields:

$$x^2(1+\tan^2 \theta)+x(-2yat \tan \theta -2xat \tan^2 \theta)+(z^2-\rho^2+xa^2 \tan^2 \theta +2xayat \tan \theta +ya^2)=0 \quad (7)$$

This is a quadratic equation which may be solved for x using:

$$x = \frac{-B \pm (B^2 - 4AC)^{1/2}}{2A} \quad (8)$$

$$\text{Where: } A = 1 + \tan^2 \theta \quad (9)$$

$$B = -2yat \tan \theta - 2xat \tan^2 \theta \quad (10)$$

$$C = z^2 - \rho^2 + xa^2 \tan^2 \theta + 2xayat \tan \theta + ya^2 \quad (11)$$

Knowing x,z and ρ, y can be obtained via (5):

$$y = ya - (x-xa)\tan \theta \quad (5)$$

The foregoing equations are incorporated into an algorithm which proceeds as follows:

$$\text{Pick a starting value } z_i: z_i = \rho \sin \phi \quad (12)$$

$$\text{Calculate A, B and C: } A = 1 + \tan^2 \theta \quad (9)$$

$$B = -2yat \tan \theta - 2xat \tan^2 \theta \quad (10)$$

$$C = z^2 - \rho^2 + xa^2 \tan^2 \theta + 2xayat \tan \theta + ya^2 \quad (11)$$

Use A, B, and C to calculate x:

$$x_i = \frac{-B \pm (B^2 - 4AC)^{1/2}}{2A} \quad (8)$$

Calculate y from (5):

$$y_i = y_a - (x - x_a) \tan \theta \quad (5)$$

Calculate the next value of z:

$$z_{i+1} = z_e + \sin \phi \left((x - x_e)^2 + (y - y_e)^2 + (z_i - z_e)^2 \right)^{1/2} \quad (4)$$

Compute an error box for stopping:

$$\xi = |z_{i+1} - z_i| + |y_{i+1} - y_i| + |x_{i+1} - x_i| \quad (13)$$

If ξ is less than the limit, then stop iterating. If not, return to (8) and repeat the process.

Please note, that in order to avoid singularities, the angle θ is measured in a clockwise direction from the x axis.

On the first pass through the iteration, two successive values of z are assigned, but only one for x and y. Two values of x and y are required for the error test. They can be assigned by letting:

$$x_0 = \rho \cos \phi \cos \theta \quad (14)$$

$$y_0 = -\rho \cos \phi \sin \theta \quad (15)$$

FORTRAN SUBROUTINE FOR MLS
RECONSTRUCTION ALGORITHM CASE XI

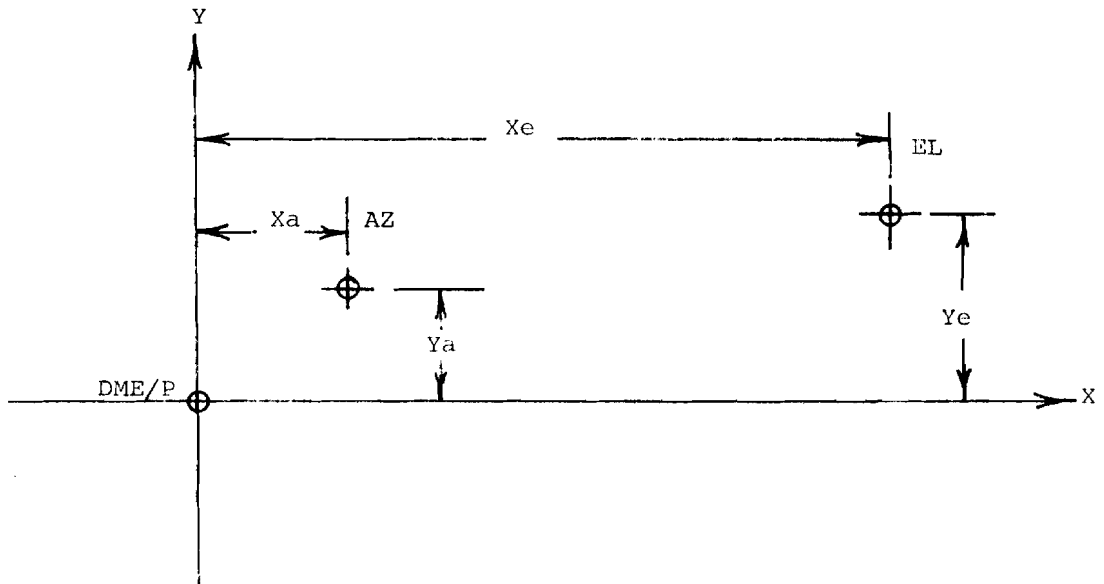
```

SUBROUTINE CASE XI (THET,PHI,RHOD,XA,YA,ZA,XE,YE,ZE,X,Y,Z,LIM)
C***** THIS ALGORITHM PROVIDES CARTESIAN X,Y,Z COORDINATE OUTPUT
C FOR MLS ANGLE AND DME/P INPUTS
C
C THET=RCVR AZ (RADIAN)
C PHI = RCVR EL (RADIAN)
C RHOD = DME/P (FEET)
C
C XA = AZ UNIT X COORDINATE
C YA = AZ UNIT Y COORDINATE
C ZA = AZ UNIT Z COORDINATE
C
C XE = EL UNIT X COORDINATE
C YE = EL UNIT Y COORDINATE
C ZE = EL UNIT Z COORDINATE
C
C LIM = ERROR TOLERANCE
C
C CALCULATE POWERS AND TRANSCENDENTAL FUNCTIONS
C
C RHOD2=RHOD*RHOD
C
C TANTH=SIN(THET)/COS(THET)
C TAN2TH=TANTH*TANTH
C XA2=XA*XA
C YA2=YA*YA
C CALCULATE FIRST VALUES OF X AND Y
C X=RHOD*COS(PHI)*COS(THET)
C
C Y=-1.0*RHOD*COS(PHI)*SIN(THET)
C
C CALCULATE Z STARTING POINT
C
C Z=RHOD*SIN(PHI)
C
C CALCULATE QUADRATIC FOR NEXT X VALUE,XN
C
10 A=1.0+TAN2TH
C B=-2.0*YA*TANTH-2.0*XA*TAN2TH
C C=Z*Z-RHOD2+XA2*TAN2TH+2.0*XA*YA*TANTH+YA2
C XN=(-B+SQR(B*B-4.0*A*C))/(2.0*A)
C
C CALCULATE YN, THE NEXT VALUE OF Y
C
C YN=YA-(X-XA)*TANTH
C
C CALCULATE NEXT Z VALUE,ZN
C
C ZN=ZE+SIN(PHI)*SQRT((XN-XE)**2+(YN-YE)**2+(Z-ZE)**2)
C
C COMPUTE ERROR BOX

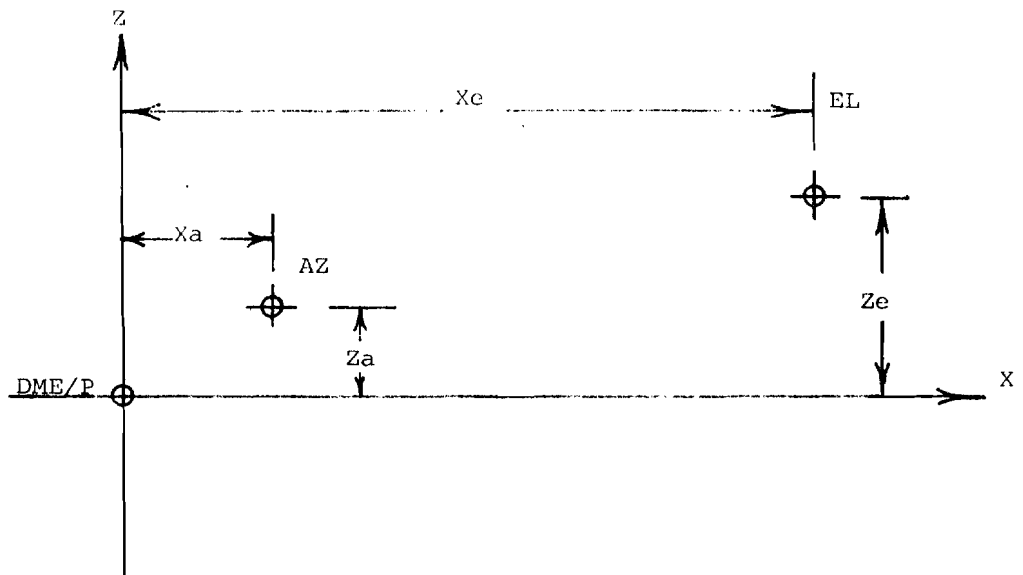
```

```
C      EPS=ABS(ZN-Z)+ABS(YN-Y)+ABS(XN-X)
      Z=ZN
      Y=YN
      X=XN
C
C      TEST FOR CONVERGENCE
C
      IF(EPS.GE.LIM) GO TO 10
      RETURN
      END
```

CASE XI



PLAN VIEW



ELEVATION VIEW

FIGURE 13. CASE XI, GEOMETRY

CASE XII:

This case illustrates a procedure used to effect the transformation from MLS angle and DME/P coordinates to a cartesian system for completely general ground station locations. The azimuth unit is located at (x_a, y_a, z_a) and is assumed to produce a conical beam. The elevation unit is located at (x_e, y_e, z_e) and also produces a conical beam. The DME/P unit is assumed to be located at position (x_d, y_d, z_d) . Three nonlinear equations result, precluding a useful closed form solution. Rather, a Newton-Raphson iterative technique in three dimensions is employed to find a solution. This algorithm is referred to as the "Shreeve Algorithm" after its originator. It is readily adaptable to implementation in matrix form. The illustrative FORTRAN program is adapted from FORTRAN IV Programming and Computing by James T. Golden.

The equations which result are as follows:

$$\text{From DME/P: } (x-x_d)^2+(y-y_d)^2+(z-z_d)^2= \rho^2 \quad (1)$$

$$\text{From conical azimuth: } (x-x_a)^2+(z-z_a)^2=(y-y_a)^2 \cot^2 \theta \quad (2)$$

$$\text{From conical elevation: } (x-x_e)^2+(y-y_e)^2=(z-z_e)^2 \cot^2 \phi \quad (3)$$

Equation (1) can be rewritten as:

$$f(x,y,z)=(x-x_d)^2+(y-y_d)^2+(z-z_d)^2-\rho^2 \quad (4)$$

Equation (2) can be rewritten as:

$$g(x,y,z)=-\cos^2 \theta (y-y_a)^2+\sin^2 \theta (x-x_a)^2+\sin^2 \theta (z-z_a)^2 \quad (5)$$

Similarly with equation (3):

$$h(x,y,z)=-\sin^2 \phi (x-x_e)^2-\sin^2 \phi (y-y_e)^2+\cos^2 \phi (z-z_e)^2 \quad (6)$$

The Newton-Raphson process is applied to equations (4), (5), and (6) as follows:

Construct a linear Taylor Series approximation in three variables, x , y , and z for each of equations (4), (5), and (6):

$$\text{For (4): } f(x+\Delta x, y+\Delta y, z+\Delta z)=f(x,y,z) + \frac{\partial f}{\partial x} \Delta x + \frac{\partial f}{\partial y} \Delta y + \frac{\partial f}{\partial z} \Delta z \quad (7)$$

$$\text{For (5): } g(x+\Delta x, y+\Delta y, z+\Delta z)=g(x,y,z) + \frac{\partial g}{\partial x} \Delta x + \frac{\partial g}{\partial y} \Delta y + \frac{\partial g}{\partial z} \Delta z \quad (8)$$

$$\text{For (6): } h(x+\Delta x, y+\Delta y, z+\Delta z)=h(x,y,z) + \frac{\partial h}{\partial x} \Delta x + \frac{\partial h}{\partial y} \Delta y + \frac{\partial h}{\partial z} \Delta z \quad (9)$$

In the Newton-Raphson process, the left hand sides of (7), (8), and (9) are linear approximations of the functions which we desire to solve. That is, we are trying to solve for the roots x , y , and z which make:

$$f(x+\Delta x, y+\Delta y, z+\Delta z)=0 \quad (10)$$

$$g(x+\Delta x, y+\Delta y, z+\Delta z)=0 \quad (11)$$

$$h(x+\Delta x, y+\Delta y, z+\Delta z)=0 \quad (12)$$

Adopting the notation that:

$$\frac{\partial f}{\partial x} = f_x, \quad \frac{\partial f}{\partial y} = f_y, \quad \frac{\partial f}{\partial z} = f_z \quad (13-15)$$

$$\frac{\partial g}{\partial x} = gx, \quad \frac{\partial g}{\partial y} = gy, \quad \frac{\partial g}{\partial z} = gz \quad (16-18)$$

$$\frac{\partial h}{\partial x} = hx, \quad \frac{\partial h}{\partial y} = hy, \quad \frac{\partial h}{\partial z} = hz \quad (19-21)$$

Combining equations (7) thru (21) in matrix notation for compactness:

$$-\begin{bmatrix} f(x,y,z) \\ g(x,y,z) \\ h(x,y,z) \end{bmatrix} = \begin{bmatrix} fx & fy & fg \\ gx & gy & gz \\ hx & hy & hz \end{bmatrix} \begin{bmatrix} \Delta x \\ \Delta y \\ \Delta z \end{bmatrix} \quad (22)$$

The desired quantities are x , y , and z . These are obtained by premultiplying both sides of (22) by the inverse of the partial derivative matrix:

$$-\begin{bmatrix} \Delta x \\ \Delta y \\ \Delta z \end{bmatrix} = \begin{bmatrix} fx & fy & fg \\ gx & gy & gz \\ hx & hy & hz \end{bmatrix}^{-1} \begin{bmatrix} f(x,y,z) \\ g(x,y,z) \\ h(x,y,z) \end{bmatrix} \quad (23)$$

Once the left hand side of (23) is obtained, the delta x , y , and z are added to the original values of x , y , and z , and a new point is obtained:

$$x_{i+1} = x_i + \Delta x \quad (24)$$

$$y_{i+1} = y_i + \Delta y \quad (25)$$

$$z_{i+1} = z_i + \Delta z \quad (26)$$

These new values are used to recompute the partial derivatives and function values, and the resulting quantities are used in recomputing the Δx , Δy , and Δz in equation (23).

The iteration is then continued until the delta x , y and z values have decreased to a size which is less than specified tolerance values.

Starting values for x , y , and z are of particular importance in insuring that the iteration converges to the proper point. Taking direction from the technique employed in the previous case let:

$$x_0 = \rho \cos \theta$$

$$y_0 = -\rho \sin \theta$$

$$z_0 = \rho \sin \phi$$

$$(29)$$

Note that we align the x -axis of our coordinate system in the direction of the azimuth centerline ($\theta=0$) which assures that the cross partial derivative terms of f , g , and h are zero. This helps to avoid the potential of improper convergence.

```

C*****
C*
C*          FORTRAN SUBROUTINE FOR MLS RECONSTRUCTION
C*          ALGORITHM CASE XII
C*
C*          THIS SUBROUTINE PROVIDES CARTESIAN X,Y,Z COORDINATE
C*          OUTPUT FOR MLS ANGLE AND DME/P INPUTS.
C*
C*  VARIABLES :
C*          THET = RCVR AZ (RADIAN)
C*          PHI  = RCVR EL (RADIAN)
C*          RHOD = DME/P (FEET)
C*
C*          XA = AZ UNIT X COORDINATE
C*          YA = AZ UNIT Y COORDINATE
C*          ZA = AZ UNIT Z COORDINATE
C*
C*          XE = EL UNIT X COORDINATE
C*          YE = EL UNIT Y COORDINATE
C*          ZE = EL UNIT Z COORDINATE
C*
C*          XD = DME/P UNIT X COORDINATE
C*          YD = DME/P UNIT Y COORDINATE
C*          ZD = DME/P UNIT Z COORDINATE
C*
C*          C = 3X3 MATRIX OF PARTIAL DERIVATIVES (JACOBIAN)
C*          X(1) = CARTESIAN X COORDINATE
C*          X(2) = CARTESIAN Y COORDINATE
C*          X(3) = CARTESIAN Z COORDINATE
C*
C*          F(1) = DME EQUATION = F(X,Y,Z)
C*          F(2) = AZIMUTH EQUATION = G(X,Y,Z)
C*          F(3) = ELEVATION EQUATION = H(X,Y,Z)
C*
C*          DELT(1) = DELTA X VALUE
C*          DELT(2) = DELTA Y VALUE
C*          DELT(3) = DELTA Z VALUE
C*
C*          TOL(1) = TEST VALUE FOR X CONVERGENCE
C*          TOL(2) = TEST VALUE FOR Y CONVERGENCE
C*          TOL(3) = TEST VALUE FOR Z CONVERGENCE
C*
C*          LIM = NUMBER OF ITERATIONS/INVERSION OF C MATRIX
C*          INDIC COUNTS NUMBER OF ITERATIONS
C*****
C
C
C
C          SUBROUTINE CASE12(THET, PHI, RHOD, XA, YA, ZA, XE, YE, ZE, XD, YD, ZD,
C*          F, X, DELT, LIM)
C
C
C          REAL * 4 THET, PHI, RHOD, XA, YA, ZA, XE, YE, ZE, XD, YD, ZD
C          REAL * 4 C(3,3), DELT(3), X(3), F(3), TOL(3), CIV(3,3)
C          DATA TOL /.1, .1, .1/
C
C
C          INDIC = 0
C          LIM = 20

```

```

C
X(1) = RHOD * COS(THET)
X(2) = -RHOD * SIN(THET)
X(3) = RHOD * SIN(PHI)
C
C***** FVECT COMPUTES THE DME, AZ AND EL EQUATIONS *****
C
1 CALL FVECT(F,X,THET,PHI,RHOD,XA,YA,ZA,XD,YD,ZD,XE,YE,ZE)
C
C***** PARTL COMPUTES THE C MATRIX OF PARTIAL DERIVATIVES *****
C
CALL PARTL( XA,YA,ZA,XE,YE,ZE,XD,YD,ZD,THET,PHI,X,C)
C
C***** INVERT IS A STANDARD MATRIX INVERSION ROUTINE *****
C
INVERT OPERATES ON MATRIX C
C
CALL INVERT(C,CIV,IFLAG)
C
C***** NDX IS A FLAG FOR ITERATION, =1 FOR QUIT, =2 FOR CONTINUE *****
C
IFLAG IS A FLAG=1 FOR INVERSION, =2 FOR NONE
C
IF (IFLAG .EQ. 2) THEN
WRITE(3, 1000) THET, PHI, RHOD,(X(I),I=1,3),(DELT(I),I=1,3)
GOTO 99
ENDIF
C
C***** MTXMP IS A STANDARD MATRIX MULTIPLICATION SUBROUTINE *****
C
CALL MTXMP (CIV,F,DELT)
C
NDX = 1
DO 13 I=1,3
X(I) = X(I)-DELT(I)
IF (ABS(DELT(I)) .GT. TOL(I)) NDX = 2
13 CONTINUE
IF (NDX .NE. 2 ) GOTO 99
C
C***** INCREMENT ITERATION COUNTER *****
C
INDIC = INDIC + 1
IF (INDIC .GT. LIM) THEN
WRITE(3, 1010) THET, PHI, RHOD,(X(I),I=1,3),(DELT(I),I=1,3)
NDX = 1
ENDIF
C
1000 FORMAT( 1X,'THE JACOBIAN = 0 AT (THET,PHI,RHOD) = ',3F11.4,
& /1X,'WHEN ( X , Y , Z ) = ',3F11.1,
& /1X,'AND DELTA IS (DX ,DY , DZ ) = ',3F11.4)
1010 FORMAT( 1X,'EXCEED 20 ITERATIONS(THET,PHI,RHOD) = ',3F11.4,
& /1X,'WHEN ( X , Y , Z ) = ',3F11.1,
& /1X,'AND DELTA IS (DX ,DY , DZ ) = ',3F11.4)
C
GOTO (99, 1) , NDX
99 RETURN
END
C*****
C*
C* SUBROUTINE FVECT COMPUTES THE AZ, EL, AND DME/P EQUATIONS.
C*
C*****

```

```

C
C
SUBROUTINE FVECT(F,X,THET,PHI,RHOD,XA,YA,ZA,XD,YD,ZD,XE,YE,ZE)
C
DIMENSION F(3),X(3)
C
F(1)=(X(1)-XD)**2+(X(2)-YD)**2+(X(3)-ZD)**2-RHOD**2
F(2)=-((COS(THET)*(X(2)-YA))**2+(SIN(THET)*(X(1)-XA))**2+
1 (SIN(THET)*(X(3)-ZA))**2
F(3)=(SIN(PHI)*(X(1)-XE))**2+(SIN(PHI)*(X(2)-YE))**2
2 - (COS(PHI)*(X(3)-ZE))**2
RETURN
END
C*****
C*
C* SUBROUTINE MTXMP IS A MATRIX MULTIPLICATION SUBROUTINE *
C* IT MULTIPLIES C AND F TO RETURN DELT *
C* *
C*****
C
C
SUBROUTINE MTXMP (CIV, F, DELT)
C
DIMENSION CIV(3, 3), F(3), DELT(3)
C
DO 20 I = 1,3
DELT(I) = 0.0
DO 10 J = 1,3
DELT(I) = CIV(I, J) * F(J) + DELT(I)
10 CONTINUE
20 CONTINUE
RETURN
END
C*****
C*
C* SUBROUTINE PARTL TO CALCULATE THE JACOBIAN OF f AT (x,y,z) *
C* AND TO TEST ITS INVERTIBILITY. *
C* *
C*****
C
C
SUBROUTINE PARTL(XA,YA,ZA,XE,YE,ZE,XD,YD,ZD,THET,PHI,X,C)
C
DIMENSION C(3,3), X(3)
C
C(1, 1) = 2.0 * (X(1) - XD)
C(1, 2) = 2.0 * (X(2) - YD)
C(1, 3) = 2.0 * (X(3) - ZD)
C
C(2, 1) = 2.0 * (SIN(THET) * SIN(THET)) * (X(1) - XA)
C(2, 2) = -2.0 * (COS(THET) * COS(THET)) * (X(2) - YA)
C(2, 3) = 2.0 * (SIN(THET) * SIN(THET)) * (X(3) - ZA)
C
C(3, 1) = 2.0 * (SIN(PHI) * SIN(PHI)) * (X(1) - XE)
C(3, 2) = 2.0 * (SIN(PHI) * SIN(PHI)) * (X(2) - YE)
C(3, 3) = -2.0 * (COS(PHI) * COS(PHI)) * (X(3) - ZE)
C
RETURN
END
C*****

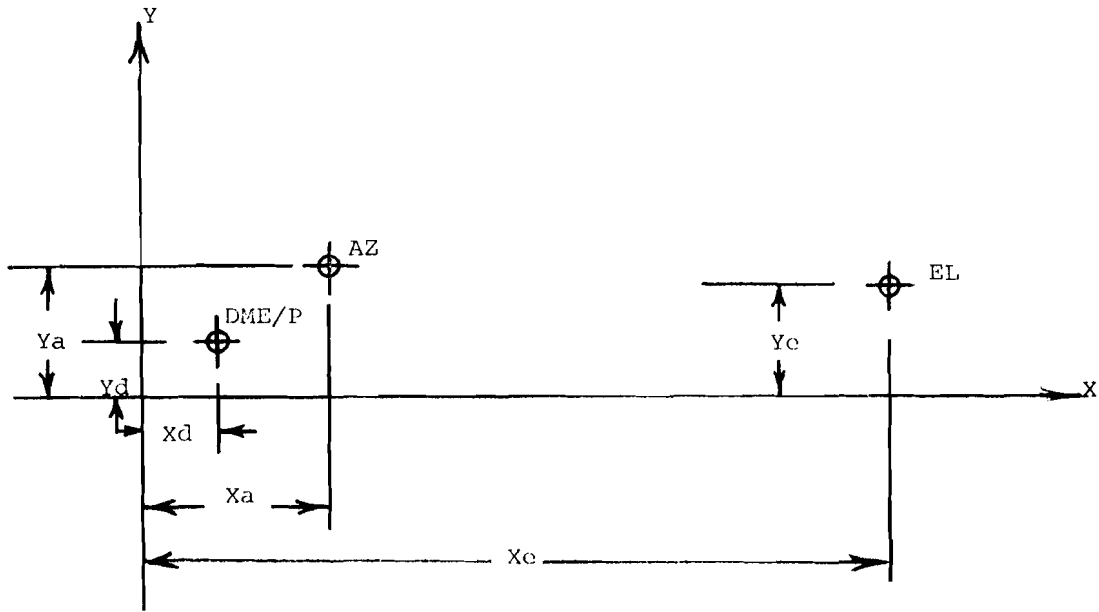
```

```

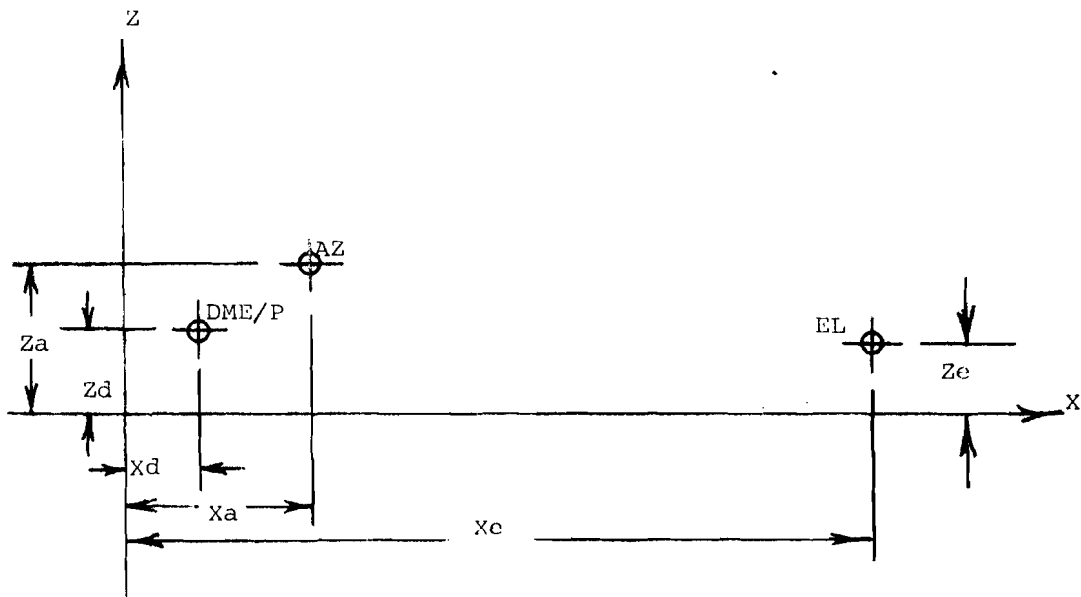
C*      SUBROUTINE TO CALCULATE INVERSE OF A 3 X 3 MATRIX.      *
C*****
C
C      SUBROUTINE INVERT(C,CIV,IFLAG)
C
C      DIMENSION  C(3,3),CI(3,3),CP(2,2),CIV(3,3)
C
C      VZ = .1E-26
C      IFLAG = 1
C
C***** TO GET THE CO-MATRIX *****
C
C      DO 80 I=1,3
C      DO 70 J=1,3
C      IF(I-1)900,55,40
40  DO 50 I1=1,I-1
C      IF(J-1)900,45,42
42  DO 44 J1=1,J-1
C      CP(I1,J1)=C(I1,J1)
44  CONTINUE
45  DO 46 J1=J+1,3
C      CP(I1,J1-1)=C(I1,J1)
46  CONTINUE
50  CONTINUE
55  DO 64 I1=I+1,3
C      IF(J-1)900,62,57
57  DO 60 J1=1,J-1
C      CP(I1-1,J1)=C(I1,J1)
60  CONTINUE
62  DO 63 J1=J+1,3
C      CP(I1-1,J1-1)=C(I1,J1)
63  CONTINUE
64  CONTINUE
C      CI(I,J)=(-1)**(I+J)*(CP(1,1)*CP(2,2)-CP(2,1)*CP(1,2))
70  CONTINUE
80  CONTINUE
C
C***** TO CALCULATE THE DETERMINANT *****
C
C      DET = 0.
C      DO 85 J=1,3
85  DET=DET+C(1,J)*CI(1,J)
C      IF(ABS(DET).LT.VZ) THEN
C      IFLAG = 2
C      GO TO 900
C      ENDIF
C
C***** TO GET THE INVERSE *****
C
C      DO 100 I =1,3
C      DO 95 J =1,3
C      CIV(I,J)=CI(J,I)/DET
95  CONTINUE
100 CONTINUE
900 RETURN
END

```

CASE XII



PLAN VIEW



ELEVATION VIEW

FIGURE 14. CASE XII, GEOMETRY

transformation algorithm undergoing testing. The MLS transformation algorithm was then used to regenerate the corresponding cartesian triple. This cartesian triple was compared to the starting value on a point by point basis. The algorithm was debugged and fine tuned until the two cartesian triples matched to a tolerance of at least 0.1 foot.

The equations used to generate the MLS triples from the cartesian grid are given in appendix A. A block diagram of the validation process employed is also shown in the appendix under the designation "Truth Model."

MLS RNAV FLIGHT SIMULATIONS (SYNTHESIZED INPUT DATA).

In addition to the aforementioned grid tests, certain algorithms, notably cases XI and XII (referred to as Thedford and Shreeves, respectively) were tested via simulation of single segment MLS RNAV route flights. These tests generated a series of MLS triples which corresponded to flying a given single linear segment route defined by an approach angle, a glide slope angle, and a terminal waypoint (given in cartesian coordinates). The MLS signal sources (azimuth, elevation, and DME/P) were specifically located at various siting geometries as defined by various cartesian triples in order to test the accuracy of the algorithms over as wide a range of conditions as possible. Errors were tabulated for height, along-track, and crosstrack components as a function of true slant range to the DME/P.

Figures 15, 16, and 17 illustrate the along-track, crosstrack, and height error plotted as a function of the slant range from the coordinate system origin for a simulation which uses a case XII (Shreeves) transformation algorithm. The route flown was biased at a 10° angle to the runway centerline at a glidepath angle of 6° . The terminal waypoint was located along the runway centerline, 3600 feet in front of the elevation antenna. The resulting errors were quite small in all dimensions. The sawtooth pattern of figure 16 reflects the granularity in the test procedure. Position determination was tested every 100 feet on the segment from 2.6 nmi into the terminal waypoint. Four sets of MLS RNAV computer generated simulations have been selected for presentation herein. They represent a small sampling of the multitude of simulations which were performed using computer generated flightpaths and MLS triples. The pertinent equipment siting geometry, terminal waypoint glidepath angle, and bearing angle are tabulated for these four simulations in table 2.

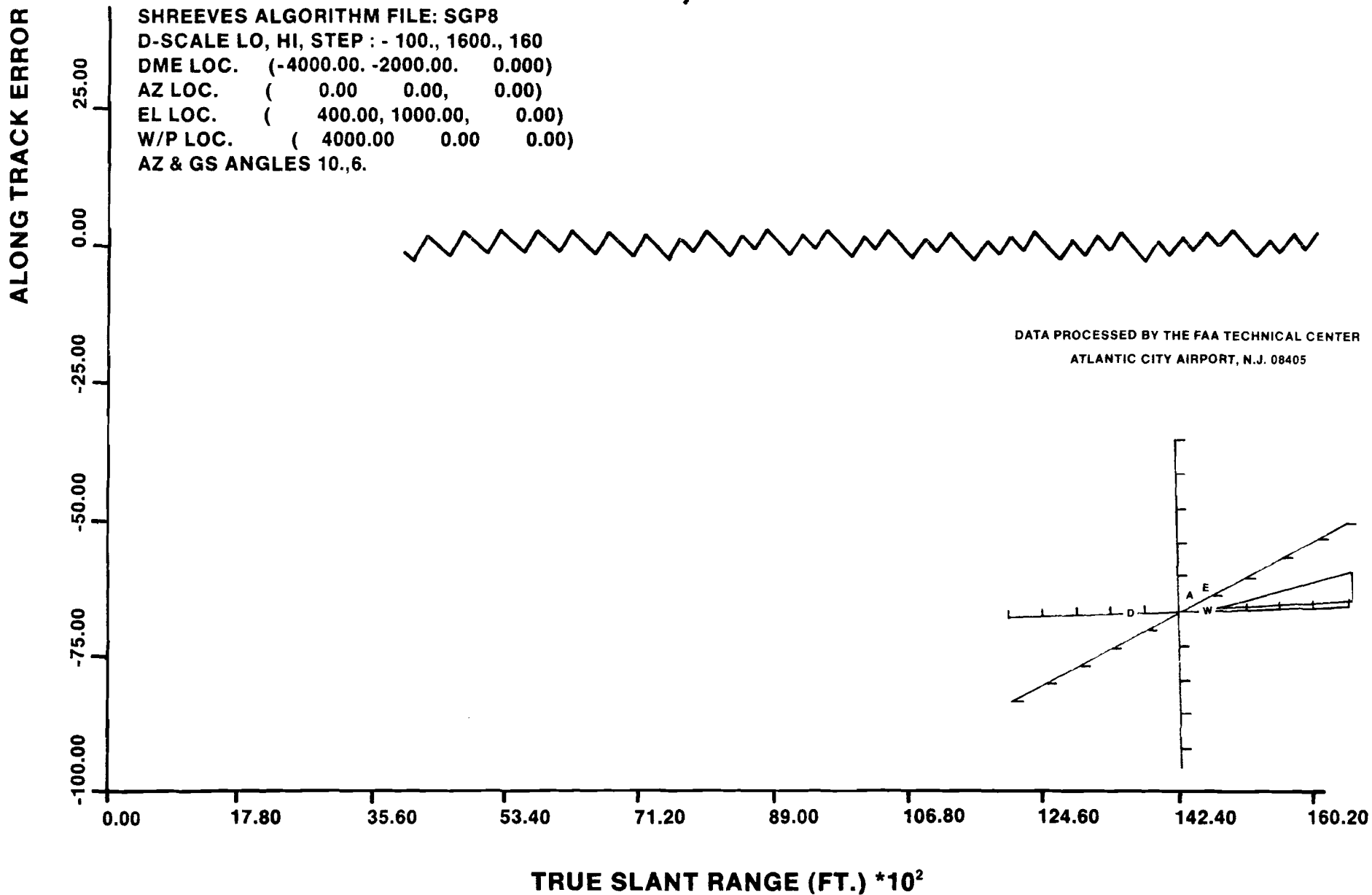


FIGURE 15. LAB SIMULATION 1, ALONG-TRACK ERROR, SHREEVES ALGORITHM, 10° AZIMUTH, 6° GLIDEPATH

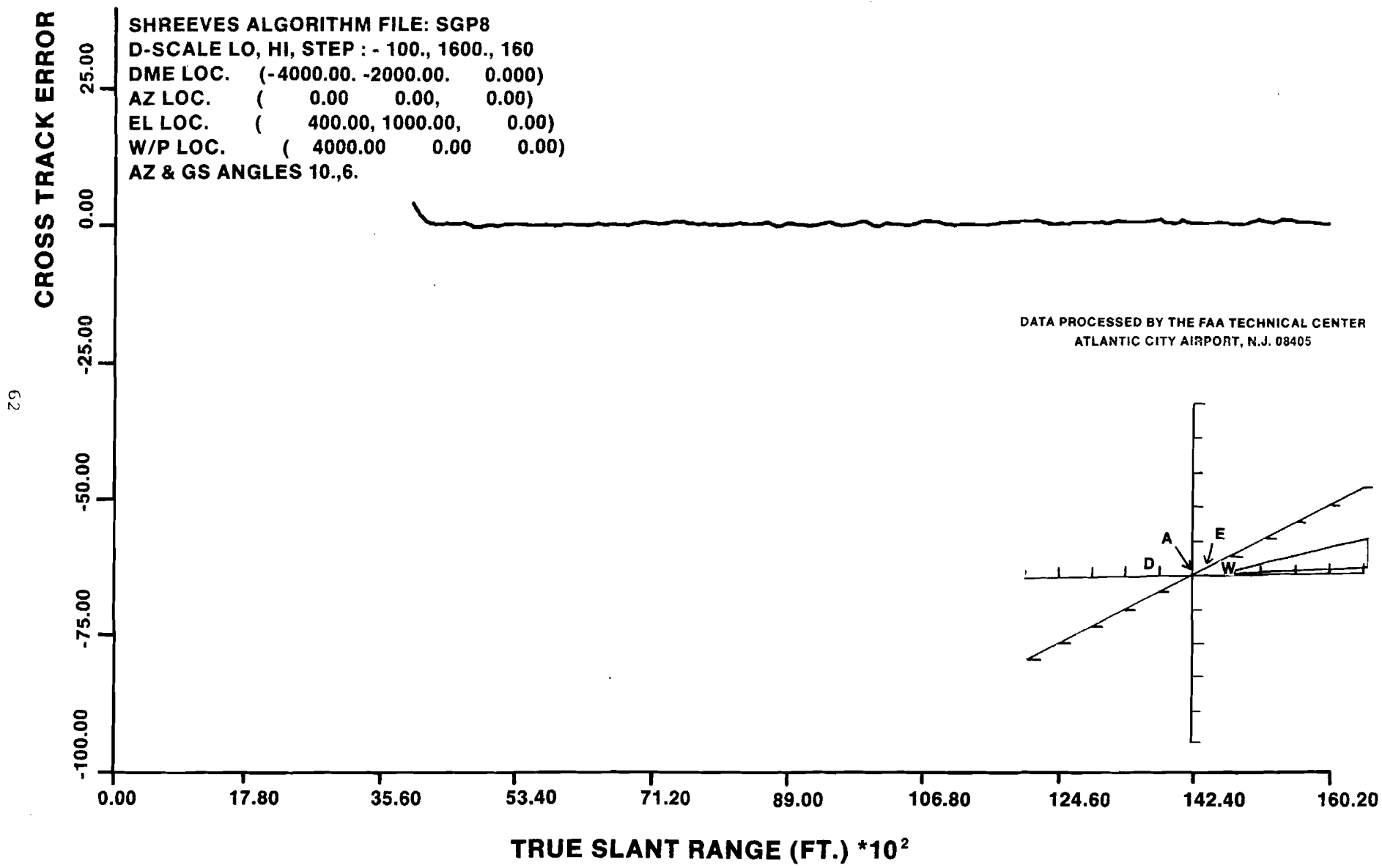


FIGURE 16. LAB SIMULATION 1, CROSSTRACK ERROR, SHREEVES ALGORITHM, 10° AZIMUTH, 6° GLIDEPATH

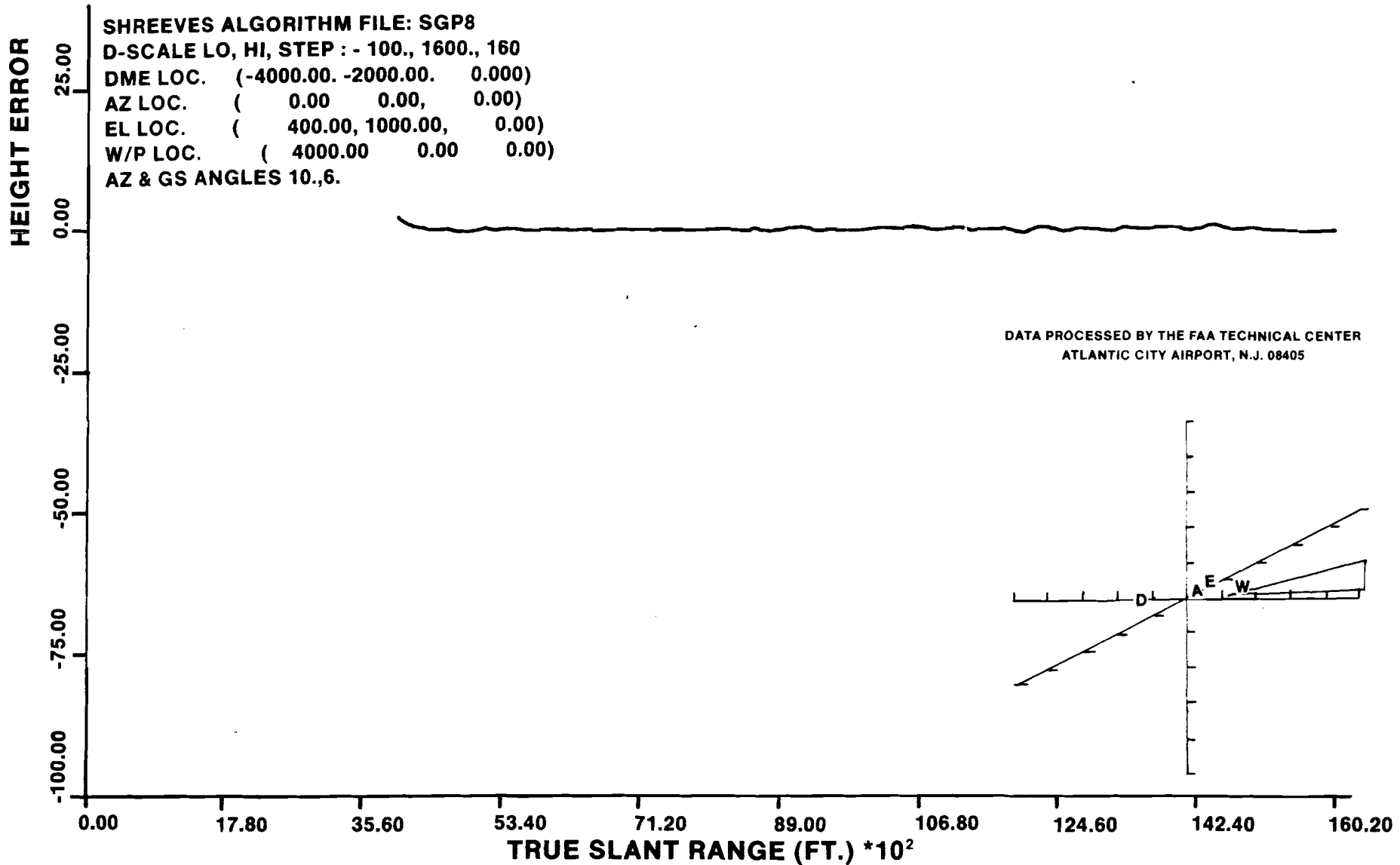


FIGURE 17. LAB SIMULATION 1, HEIGHT ERROR SHREEVES ALGORITHM, 10°, AZIMUTH, 6° GLIDEPATH

TABLE 2. TEST PARAMETERS FOR MLS RNAV LAB SIMULATIONS

Simulation Number	Parameter	Algorithm	Approach Angle (deg)	Glidepath Angle (deg)	X (ft)	Y (ft)	Z(ft)
1	Waypoint Loc.	Case 12			4000	0	0
	DME/P Loc.	(Shreeves)	10	6	-4000	-2000	0
	AZ Loc.				0	0	0
	EL Loc.				400	1000	0
2	Waypoint Loc.	Case 12			100	100	100
	DME/P Loc.	(Shreeves)	30	9	-4000	-2000	0
	AZ Loc.				0	0	0
	EL Loc.				1000	700	100
3	Waypoint Loc.	Case 11			016.16	0	0
	DME/P Loc.	(Thedford)	10	6	0	0	0
	AZ Loc.				0	-303.8	0
	EL Loc.				425.32	972.16	0
4	Waypoint Loc.	Case 11			121.52	121.52	121.52
	DME/P Loc.	(Thedford)	30	9	0	0	0
	AZ Loc.				0	-303.8	0
	EL Loc.				972.16	729.12	121.52

Figures 18, 19, and 20 illustrate a linear flightpath simulation biased at 30° to the runway centerline at a 9° glidepath angle. A case 12 (Shreeves) transformation algorithm has been used here along with a change in the ground equipment siting. The error plots (crosstrack, along-track, and height) are well behaved down to the terminal waypoint, which is offset from the runway centerline and coordinate system origin by 100 feet in the x, y, and z directions. A unique feature of this simulation is that it was flown "behind" the elevation station, which is situated 1000 feet down the runway centerline. This illustrates a crucial point in the design of MLS RNAV system software. That is, that logic must be inserted in a real-time system to discriminate between the multiple points of solution which result as well as monitor flag status for received MLS data.

The next set of simulations, figures 21, 22, and 23 for along-track, crosstrack, and height error, respectively, model a flightpath biased at 10° relative to the runway centerline and having a 6° glidepath angle. The final waypoint is located 3585 feet in front of the elevation unit, along the runway centerline. The principal difference between this and the previous simulations is the use of a

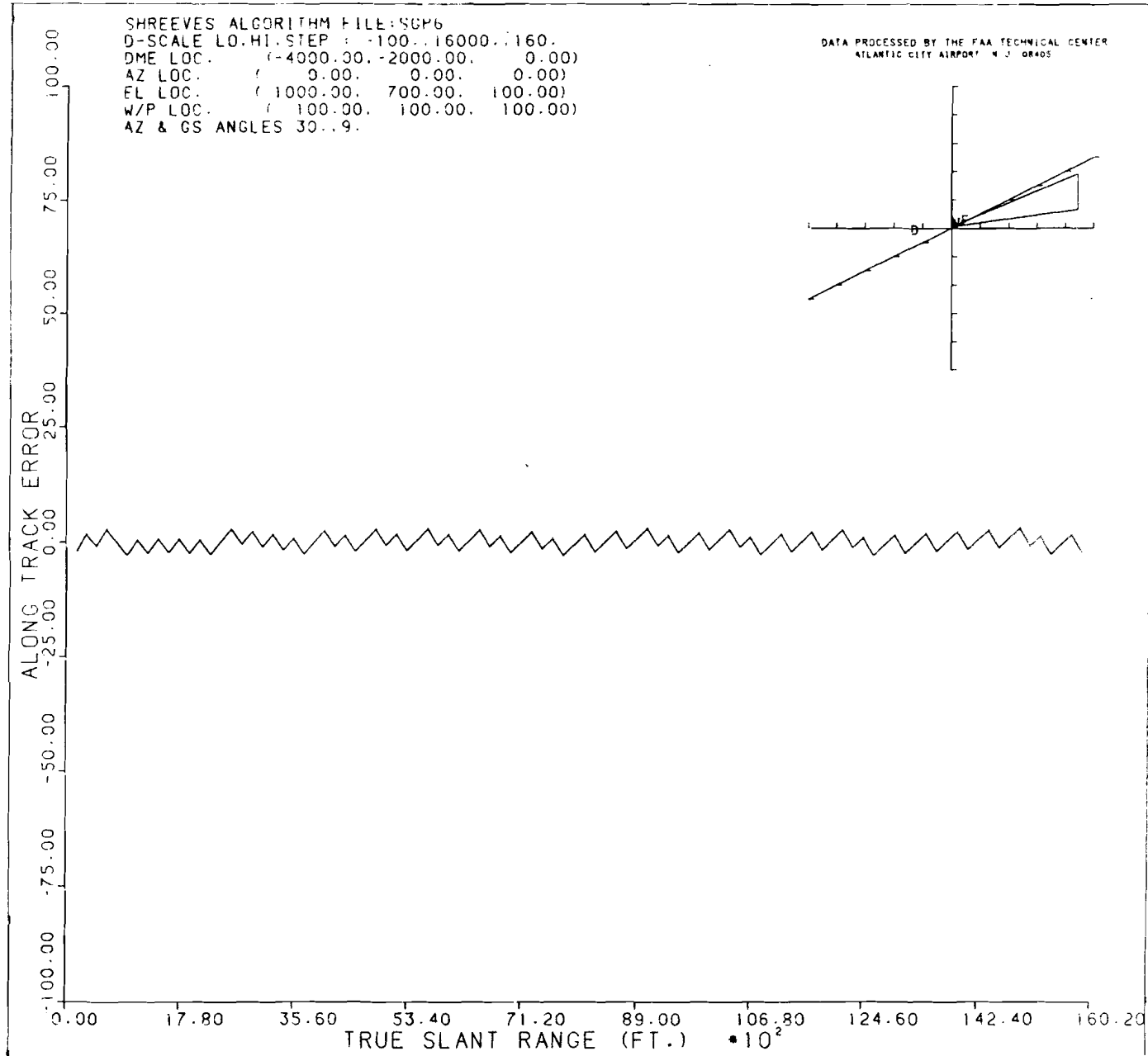


FIGURE 18. LAB SIMULATION 2, ALONG-TRACK ERROR, SHREEVES ALGORITHM, 30° AZIMUTH,
 9° GLIDEPATH

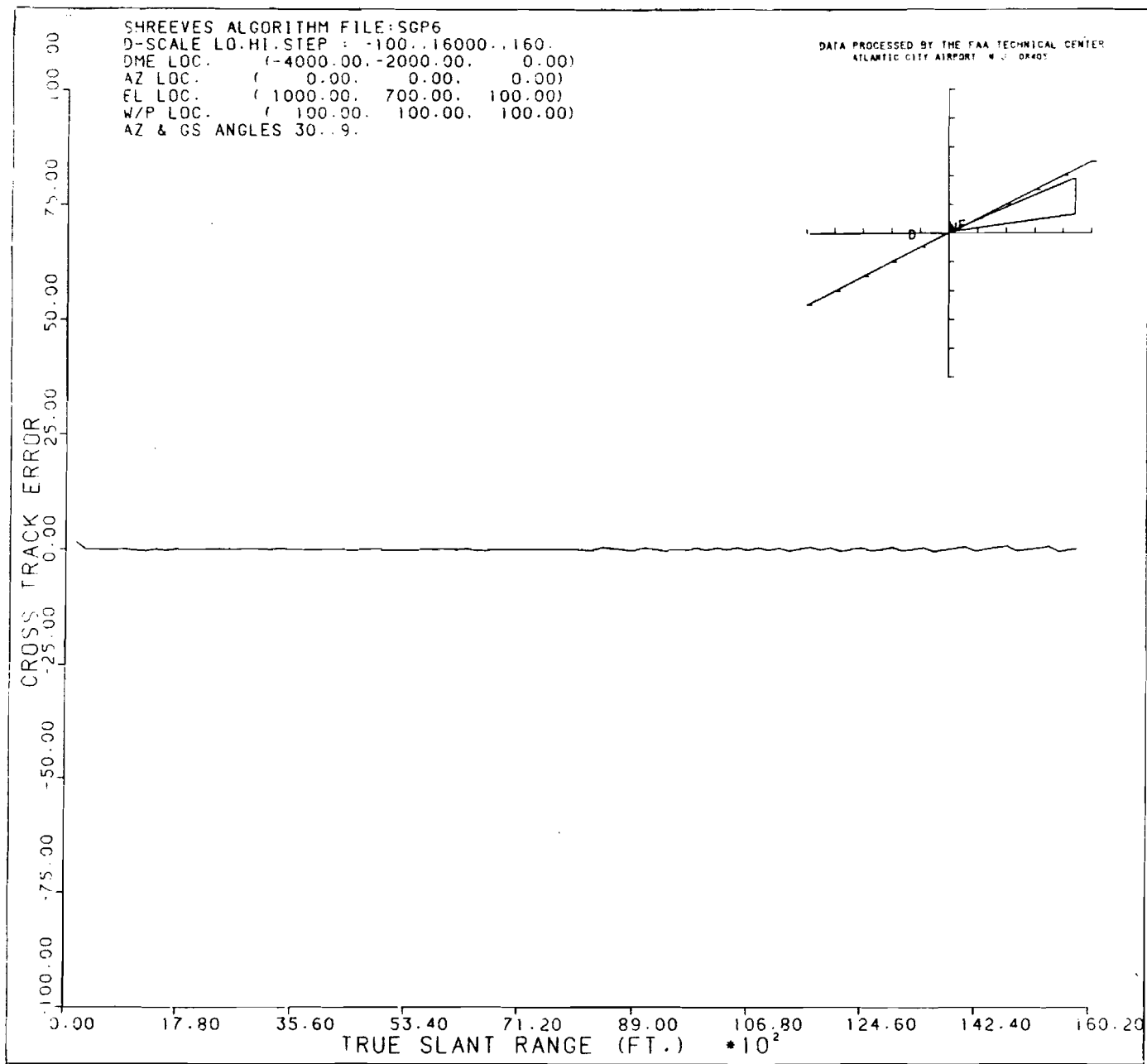


FIGURE 19. LAB SIMULATION 2, CROSSTRACK ERROR, SHREEVES ALGORITHM, 30°
 AZIMUTH, 9° GLIDEPATH

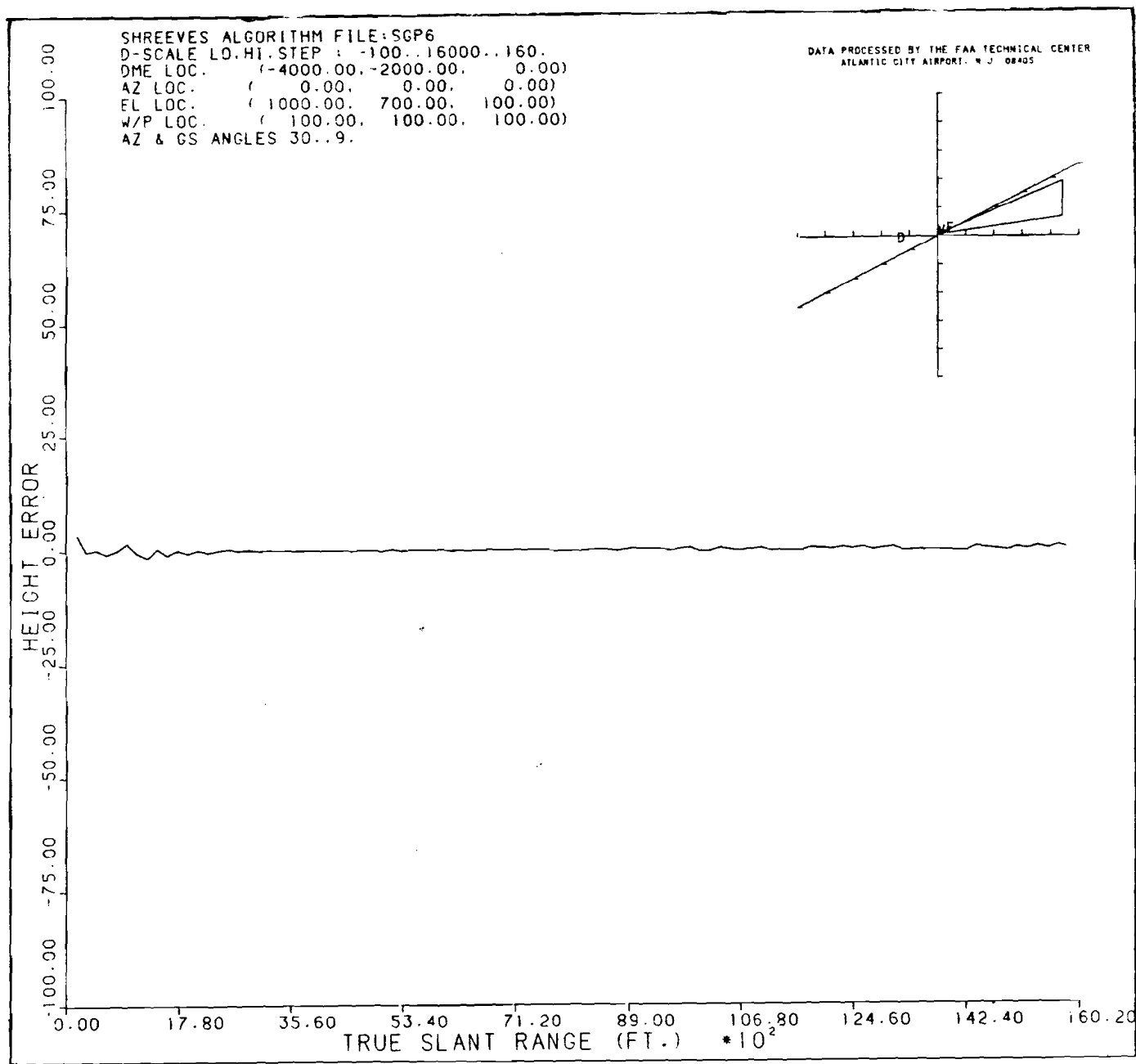


FIGURE 20. LAB SIMULATION 2, HEIGHT ERROR, SHREEVES ALGORITHM, 30° AZIMUTH,
 9° GLIDEPATH

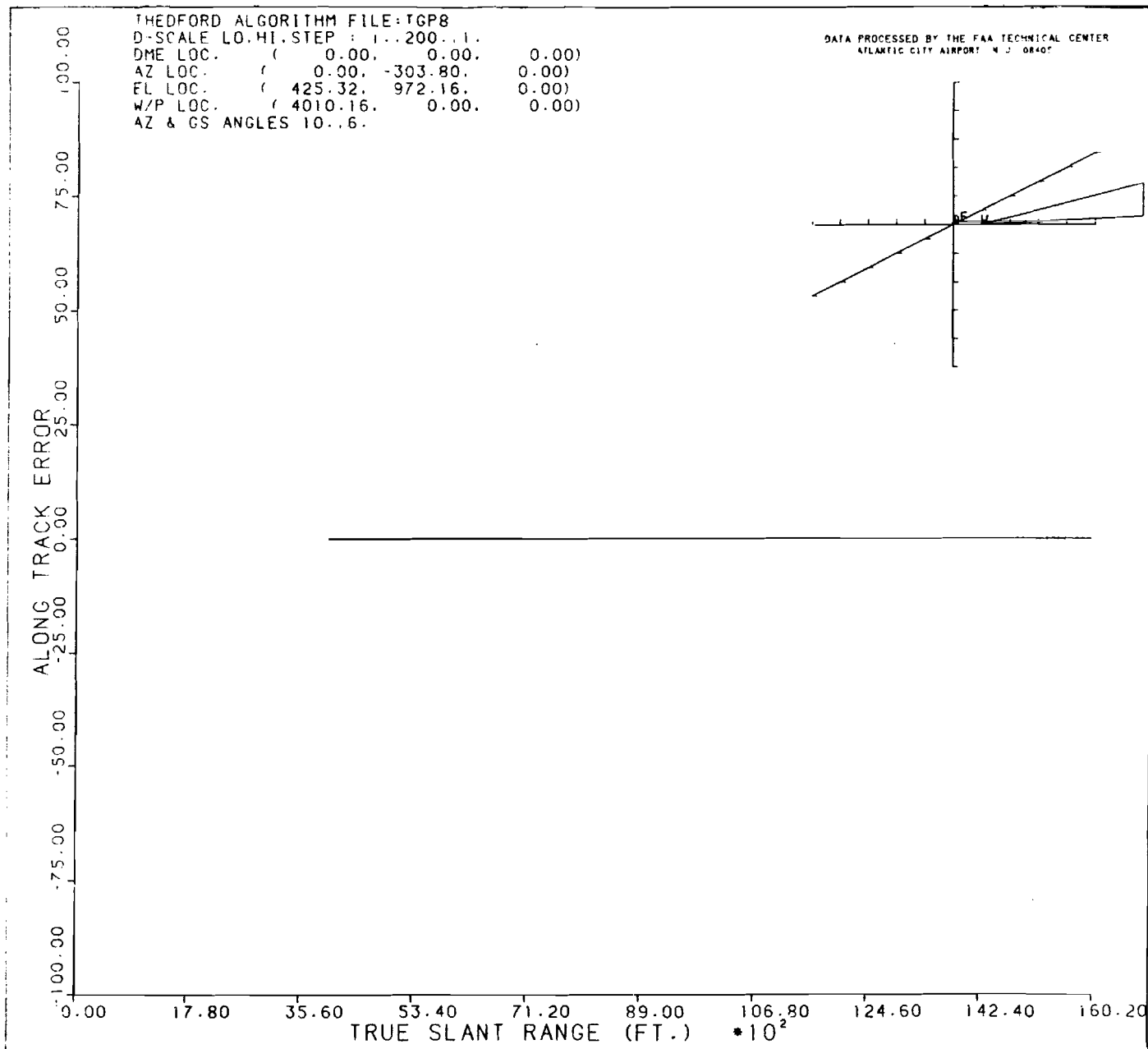


FIGURE 21. LAB SIMULATION 3, ALONG-TRACK ERROR, THEDFORD ALGORITHM, 10°
 AZIMUTH, 6° GLIDEPATH

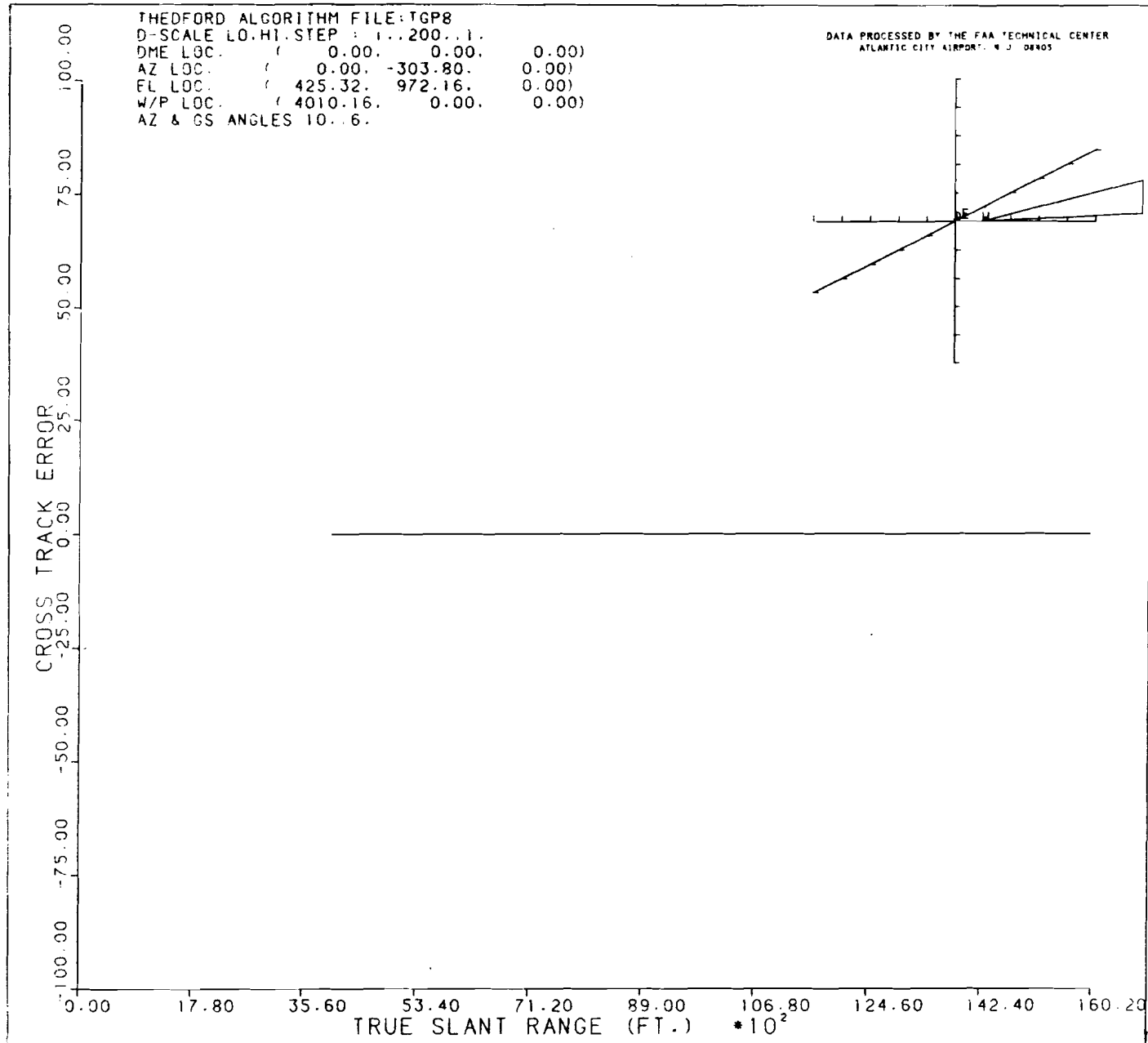


FIGURE 22. LAB SIMULATION 3, CROSSTRACK ERROR, THEDFORD ALGORITHM, 10°
 AZIMUTH, 6° GLIDEPATH

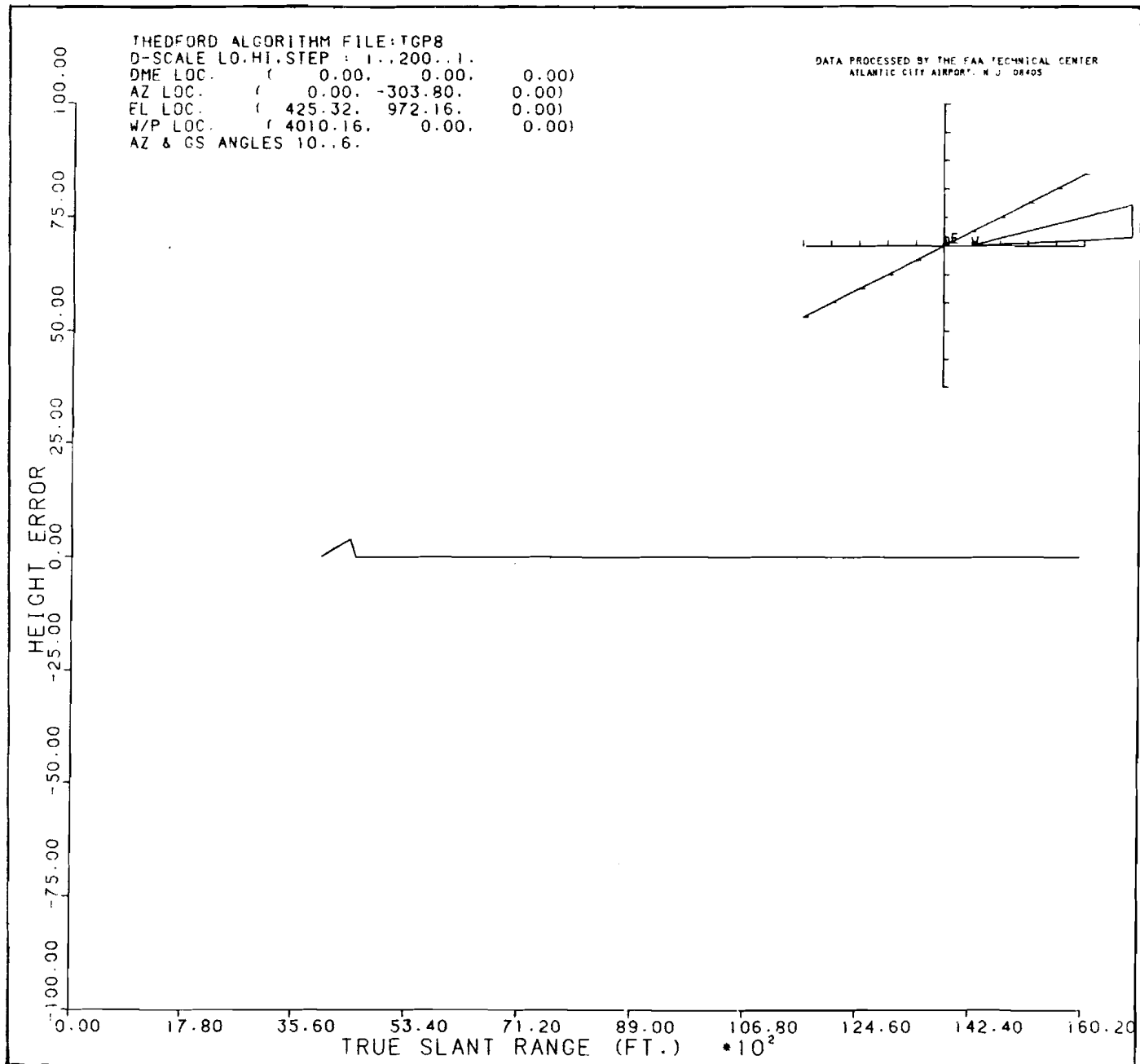


FIGURE 23. LAB SIMULATION 3, HEIGHT ERROR, THEDFORD ALGORITHM, 10° AZIMUTH
 6° GLIDEPATH

case XI (Thedford) coordinate transformation algorithm. This algorithm approximates the conical azimuth signal by a planar approximation. For small glidepath angles, the difference between conical and planar azimuth is very small. Examination of the almost negligible error shown on the error plots bears out this assumption. Advantages incurred by using this algorithm are simplicity of code and speed of execution compared to use of a case XII algorithm.

The final set of simulations, figures 24, 25, and 26 (along-track, crosstrack, and height error, respectively) are based upon a flightpath oriented at a 30° bearing relative to the 0° azimuth runway centerline (x axis). The glidepath angle used is 9° . The intent here is to simulate MLS RNAV performance at large azimuth and elevation angles. A Thedford algorithm (case XI) is used. The ground transmitters are widely dispersed (see table 2) in order to assess software performance with worst case inputs. Only the DME/P is located at the center of the coordinate system (necessitated by the algorithm used), but this can be changed if needed by a simple translation. The resulting error plots reveal negligible along-track and crosstrack, and slight height error down to the final waypoint, located 121.52 feet in three dimensions from the DME/P (coordinate system origin) ground transponder. It should be noted that in the course of executing this simulation the aircraft position traverses a path which takes it from ahead of to behind the elevation transmitter. Although no problems were encountered with the algorithm employed in the simulation, in the real world it would be impossible to determine aircraft position for the segment of the course out of elevation coverage.

MLS RNAV FLIGHT SIMULATIONS (ACTUAL FLIGHT DATA).

In the course of developing the system software for an MLS RNAV system, numerous flight critical issues need to be addressed. Among these issues are flight dynamic effects on algorithm performance and algorithm cycle timing. This was accomplished by testing the RNAV system software with live flight data. The RNAV system software is depicted in block diagram form in figure 27. One of the most complex forms of the MLS coordinate transformation algorithms (case XI, Thedford) was selected for testing with live flight data. These data consisted of time oriented triples recorded (ρ, θ, ϕ) on tape in the course of executing conventional MLS approaches and departures with the FAA Technical Center's Sikorsky S-76 helicopter. Independent tracking of the helicopter while executing these profiles was provided by the GTE laser tracker or Extended Area Instrumentation Radar (EAIR). The flight derived MLS triples were then input to the MLS software in the lab. This software generated crosstrack, along-track, and height deviation outputs when run on a PDP 11/34 minicomputer in the lab. The lab derived outputs were then compared to the independently obtained tracking data using a time oriented data merge procedure. It should be noted that the differences obtained in this comparison reflect more than algorithm error. Other errors include signal source error, receiver performance, and site alignment errors. Despite this, excellent results were obtained.

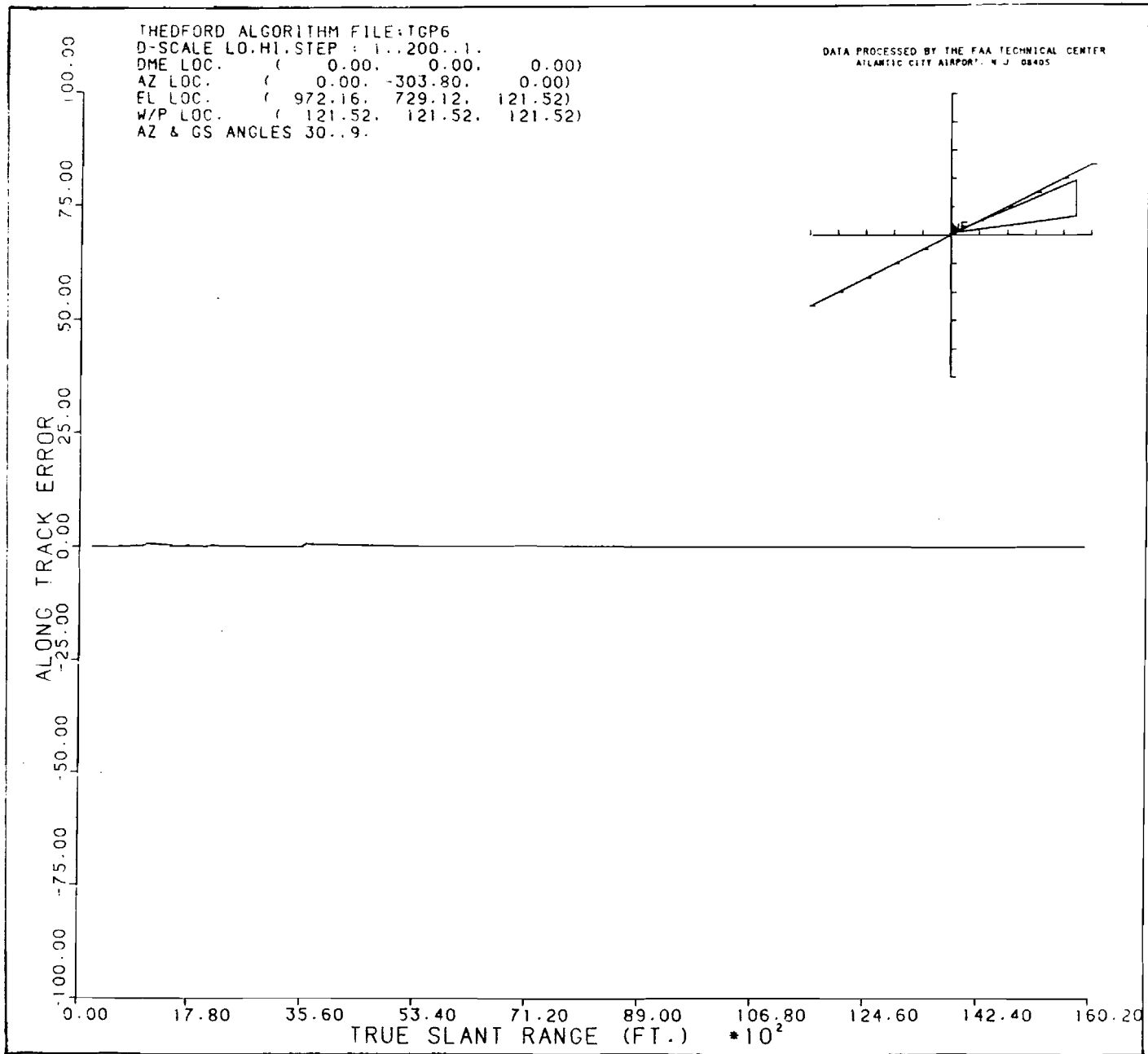


FIGURE 24. LAB SIMULATION 4, ALONG-TRACK ERROR, THEDFORD ALGORITHM, 30°
AZIMUTH, 9° GLIDEPATH

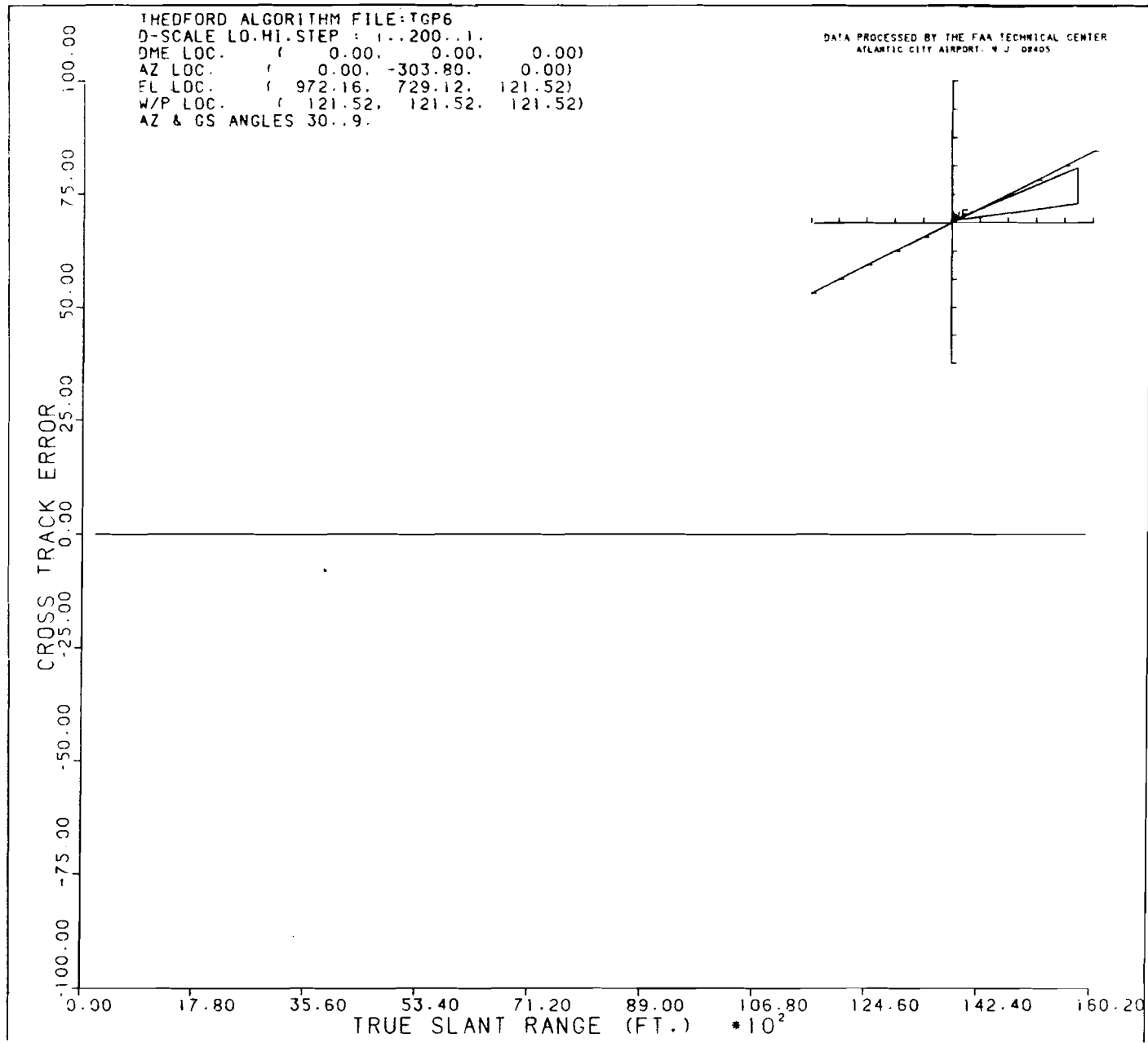


FIGURE 25. LAB SIMULATION 4, CROSSTRACK ERROR, THEDFORD ALGORITHM, 30° AZIMUTH,
 9° GLIDEPATH

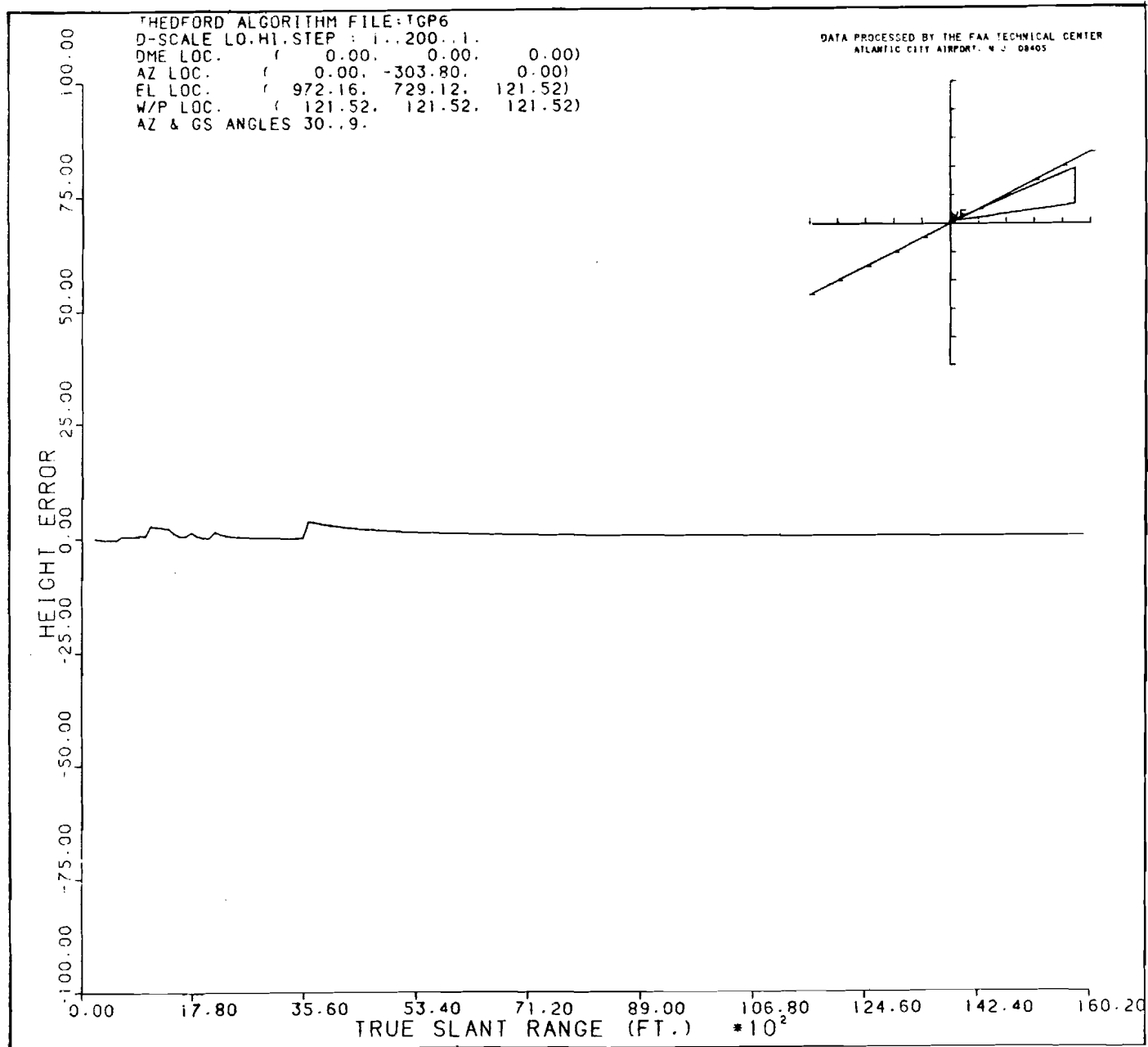


FIGURE 26. LAB SIMULATION 4, HEIGHT ERROR, THEDFORD ALGORITHM, 30° AZIMUTH,
 9° GLIDEPATH

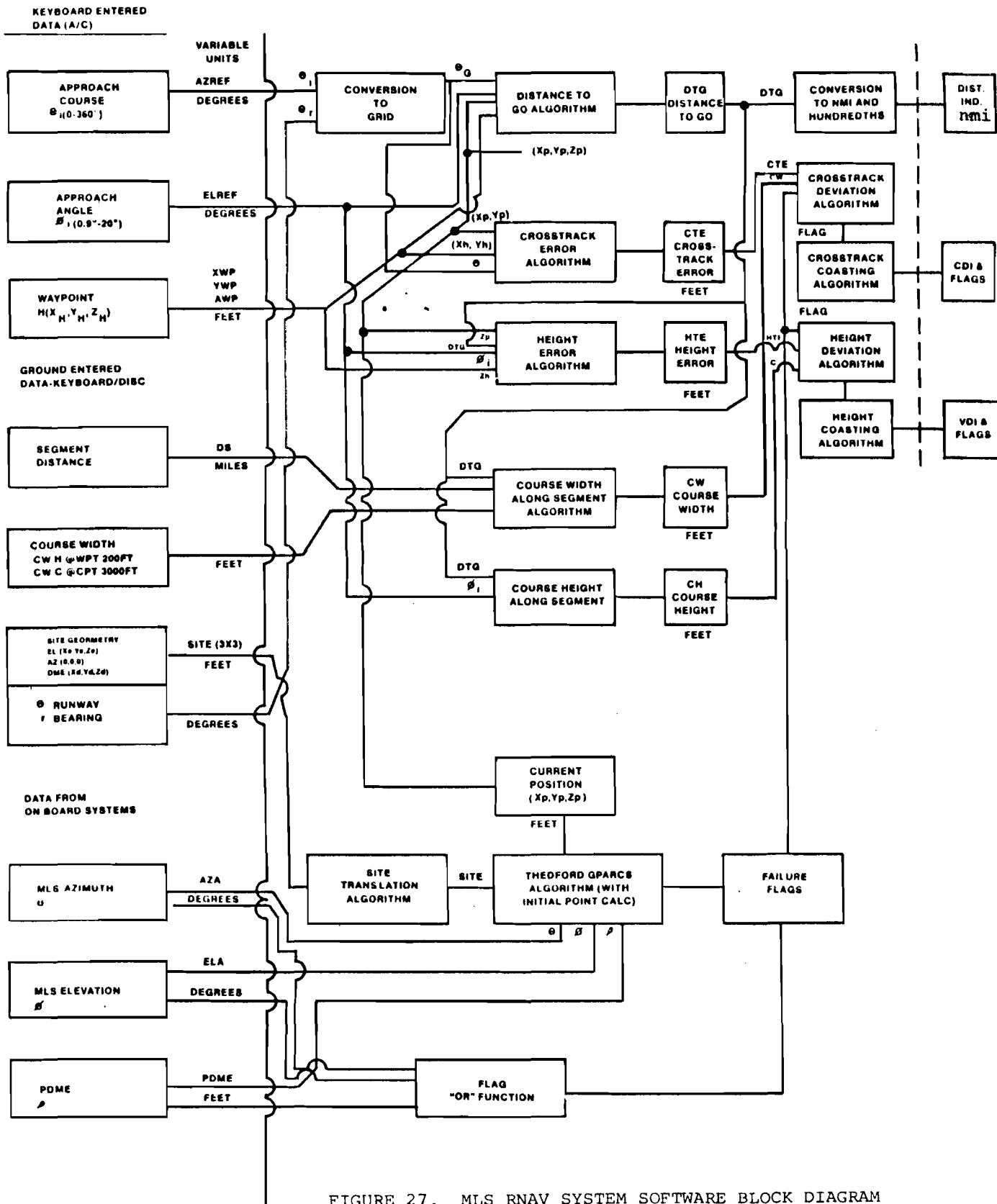


FIGURE 27. MLS RNAV SYSTEM SOFTWARE BLOCK DIAGRAM

Table 3 presents the means and twice the standard deviations of the differences between MLS RNAV position and the independently tracked position for each approach or departure profile flown by the helicopter. Approaches were flown from approximately 4 nmi (6.5 kilometer (km)) into a specified decision height (DH), on a specified glidepath angle, and the 0° azimuth. Departures were flown out to approximately 4 nmi and a specified altitude without a vertical guidance reference. Departures were flown on the 20° left and the 20° right azimuth as well as the 0° azimuth. The excellent results listed in table 3 actually represent the equivalent of navigation system error.

An additional level of system simulation was performed by playing the MLS and DME/P data through the MLS RNAV system software depicted in figure 27 and measuring the software execution cycle timing. The Thedford (case XI) coordinate transformation algorithm was used for this study. The entire software suite was found to consume less than 0.02 seconds per update cycle. Iterative solution convergence criteria of 0.1 foot were always satisfied. The maximum anticipated update rate (for coupling to the flight control system) is approximately 25 hertz (Hz). The timing analysis was accomplished on a PDP 11/34 minicomputer which is slower than the prototype (under development) system's Motorola 68020 VMEbus™ based computer.

SIGNAL SOURCE ERROR SIMULATIONS FOR COMPUTED CENTERLINE APPROACHES.

Regardless of how accurate the MLS reconstruction algorithms are, other systems limitations, such as within tolerance MLS signal source error, may limit the application of MLS RNAV techniques within the total volume of signal coverage. These limitations will influence the establishment of MLS RNAV TERPS procedures and approach minima. Analysis has been completed for two of the most useful applications of MLS RNAV, the parallel offset approach (computed centerline) and the parasite approach. The focus of this section is on the computed centerline approach.

Since the MLS (θ, ϕ, ρ) to cartesian (x, y, z) coordinate transformations are nonlinear, a direct computation of MLS signal source error impact on MLS RNAV position determination is prohibitively complex. To complicate matters further, the coordinate transformation must incorporate knowledge of the relative locations of the ground elements. However, by using Monte Carlo simulation techniques, the impact of signal source error on computed position can be determined with comparative ease. In the computed centerline case analyzed here, a case I MLS transformation algorithm was used. This algorithm provides cartesian (x, y, z) position output for a ground geometry in which the azimuth unit is offset from the runway centerline by a distance y_a (rather than being aligned with it in the normal siting). The DME/P unit is assumed to be collocated with the azimuth unit. The elevation unit is located along a line parallel to the centerline which passes through the azimuth unit and is separated by a distance x_e from this unit. All three MLS ground units are assumed to be located in the Z plane. This configuration is illustrated in figure 28.

The simulation proceeds by establishing a reference point at DH on which to base the simulation. In the computed centerline case, for a given lateral offset distance, azimuth transmitter to elevation transmitter distance, DH and approach elevation angle combination, there exists only one MLS coordinate triple to

TABLE 3. TOTAL MLS RNAV SYSTEM ERROR IN POSITION DETERMINATION

Run No.	Approach Angle (deg)	DH or Final Alt. (ft)	Along-Track Error (ft)		Crosstrack Error (ft)		Height Error (ft)	
			\bar{X}	2σ	\bar{X}	2σ	\bar{X}	2σ
1	Departure	800	-46.86	47.30	-8.92	25.26	-7.26	31.70
2	3.0	150	11.90	50.46	-4.60	18.64	-8.07	21.12
3	6.0	200	30.66	50.46	-1.02	11.84	-7.87	16.21
4	Departure	2000	-18.82	31.22	27.67	26.47	2.97	19.62
5	9.0	350	16.09	28.98	-0.22	14.28	-11.60	26.96
6	6.0	150	21.96	58.11	-2.34	27.62	-2.20	21.48
7	3.0	100	40.59	86.02	-15.81	48.30	-1.27	28.98
8	3.0	200	10.07	65.16	-6.09	15.82	4.36	31.16
9	3.0	200	0.56	50.32	16.17	25.88	6.70	29.98
10	Departure 20°L	1400	7.90	48.12	-7.01	21.66	-7.52	19.64
11	6.0	200	4.67	33.02	-10.72	22.08	-4.13	24.34
12	6.0	300	16.54	43.28	-5.69	24.62	-3.67	20.30
13	Departure	2000	-39.23	51.32	-5.05	25.00	10.73	18.16
14	9.0	350	26.47	65.84	-2.84	30.14	2.14	34.88
15	3.0	100	30.82	67.48	8.71	26.18	0.64	32.30
16	3.0	150	26.33	63.30	-8.92	22.44	-1.49	26.64
17	Departure	2000	-25.41	44.54	-8.08	34.36	2.77	27.10
18	9.0	350	21.30	72.14	-1.77	25.54	-2.85	24.14
19	Departure 20°R	1400	11.11	35.08	-5.30	42.06	1.82	44.54
20	6.0	300	23.92	62.34	-8.42	39.44	-1.21	18.47
21	6.0	200	26.70	69.18	-30.88	37.86	0.49	38.90
22	3.0	200	9.64	30.06	1.59	12.68	-5.52	21.42
23	3.0	150	23.41	58.72	-1.27	9.38	-3.73	20.24
24	3.0	100	25.57	50.42	-0.93	11.92	-6.06	19.54

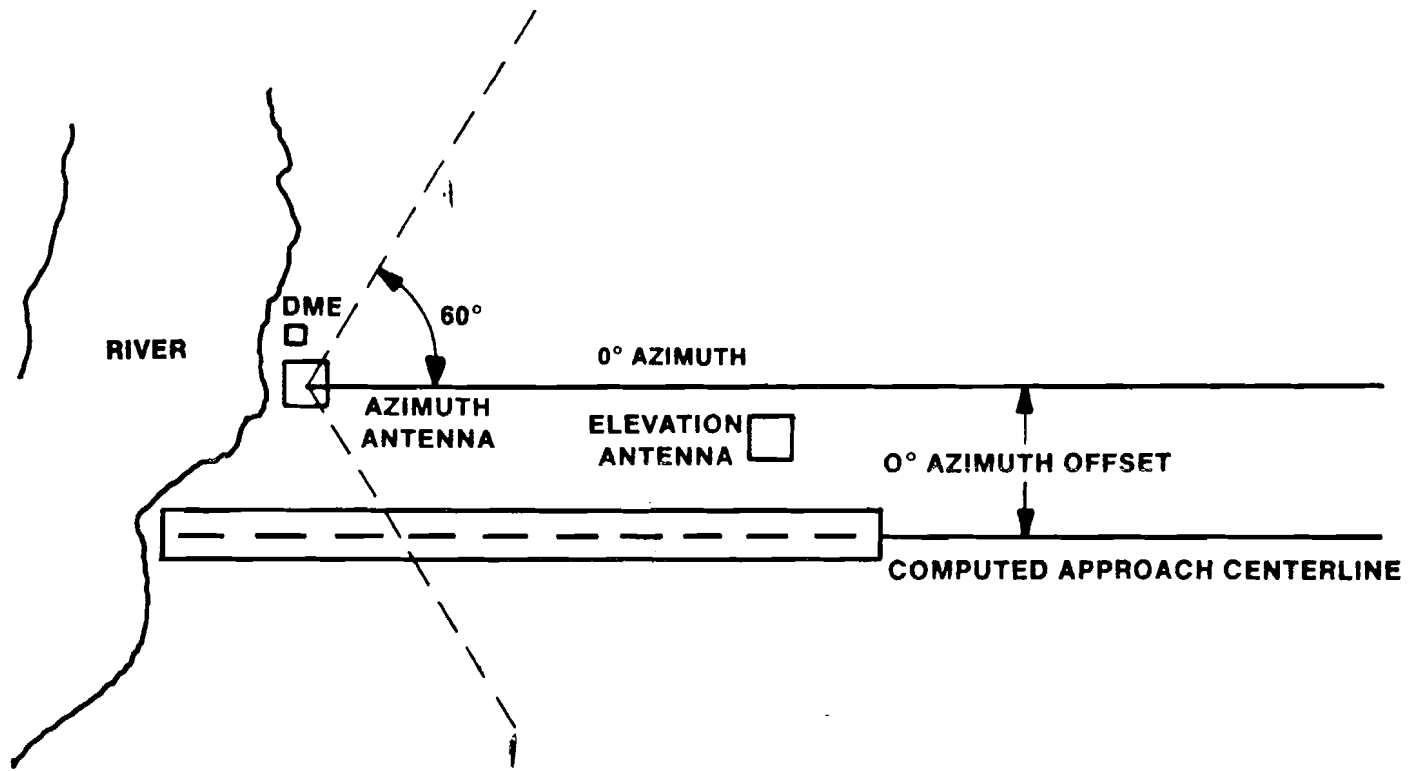


FIGURE 28. EXAMPLE OF MLS RNAV OFFSET AZIMUTH COMPUTER CENTERLINE APPROACH

represent that DH point. Assume the MLS triple is (θ, ϕ, ρ) . Through simulation this triple can be perturbed by a random error vector $(\theta_e, \phi_e, \rho_e)$, where θ_e , ϕ_e , and ρ_e are independent normally distributed random variables with standard deviation equal to 1/2 the error tolerances for azimuth, elevation, and DME/P, i.e., 0.115° , 0.120° , and 100 feet, respectively. The perturbed triple $(\theta + \theta_e, \phi + \phi_e, \rho + \rho_e)$ is then used as input to the MLS RNAV position computation algorithm. The resulting MLS RNAV position is compared to the exact DH location to obtain crosstrack and along-track errors.

The above procedure is repeated 1,000 times to obtain statistics on the along-track and crosstrack errors. This technique has been illustrated in the form of a flow chart, figure 29.

This technique has been applied to a variety of final approach conditions. The DH and glidepath angle combinations analyzed were $(3^\circ, 200 \text{ feet})$, $(4.5^\circ, 250 \text{ feet})$, $(6^\circ, 300 \text{ feet})$ and $(9^\circ, 350 \text{ feet})$. The offset from the 0° azimuth to the runway centerline ranged from 0 to 2500 feet in 100-foot increments. The azimuth to elevation transmitter distances ranged from 3000 to 10000 feet in 500-foot increments.

Tables present the crosstrack and along-track 95 percent (2 sigma) error limits. Table 4 presents the crosstrack error results for the $3^\circ, 200 \text{ feet}$ DH approach. Generally, the crosstrack error increases as the offset distance increases. However, it decreases as the azimuth to elevation transmitter distance increases. Table 4 can be used to obtain the maximum offset to which category 1 approach minima might be applied. For instance, if error budgets allow 20-foot crosstrack error for position determination, the maximum offset for a 6000-foot azimuth to elevation transmitter distance would be 1000 feet.

Table 5 presents the along-track error results for a $3^\circ, 200\text{-foot}$ DH. The figures obtained for crosstrack error indicate that for this parallel offset approach, the crosstrack error at DH is an increasing function of azimuth offset distance and a decreasing function of azimuth to elevation distance. By contrast, the numbers obtained for along-track error exhibit little variation with these parameters.

Additional tables are provided which tabulate the cross and along-track errors at other glidepath - DH combinations. These are tables 6 and 7 for a $4.5^\circ, 250\text{-foot}$ combination; tables 8 and 9 for the $6^\circ, 300\text{-foot}$ pair; and tables 10 and 11 for the 9° glidepath, 350-foot DH combination. The conclusions, which were drawn earlier regarding the behavior of crosstrack and along-track errors as functions of azimuth offset and distance to elevation unit, are also valid here. There also appears to be an overall slight increase in along-track error as glidepath angle and DH increases.

In order to graphically illustrate the functional dependency of the crosstrack error, these data were plotted as a function of azimuth offset distance with azimuth to elevation distance as a parameter. This was done for the 3° glide slope 200-foot DH pair. The curves which result (figures 30, 31, and 32) pass through the origin and reveal a nearly linear increase in crosstrack error with offset. It can also be inferred from the graphs that crosstrack error decreases as the azimuth to elevation unit distance increases for the computed centerline approach example analyzed.

MONTE CARLO DETERMINATION OF MLS RNAV POSITION DETERMINATION ACCURACY

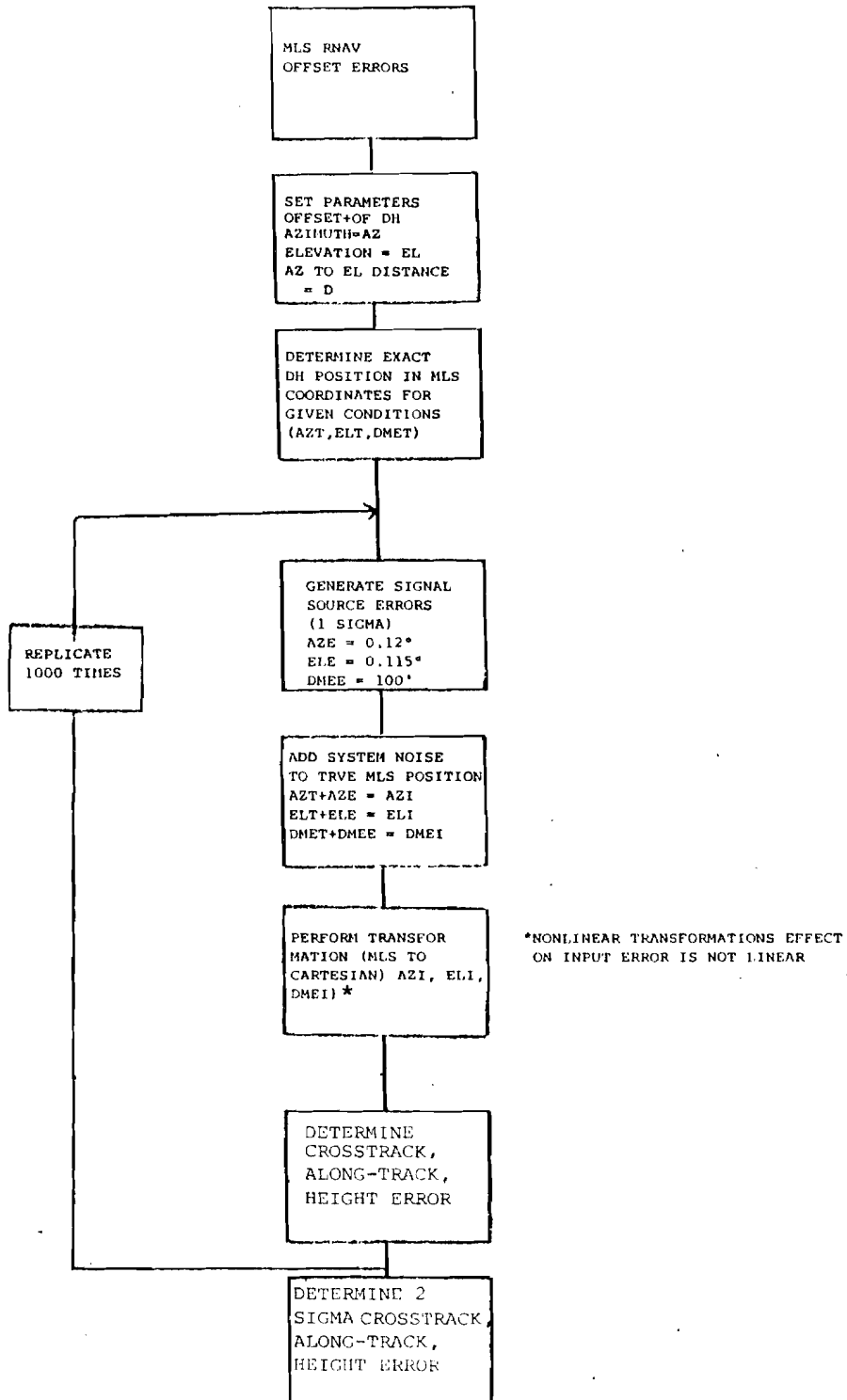


FIGURE 29. MONTE CARLO DETERMINATION OF MLS RNAV POSITION ERROR

TABLE 4. CROSSTRACK ERROR DUE TO AZIMUTH OFFSET, DH = 200 FT,
GLIDEPATH ANGLE = 3°

Offset (ft)	AZIMUTH TO ELEVATION DISTANCE (FT)														
	3000	3500	4000	4500	5000	5500	6000	6500	7000	7500	8000	8500	9000	9500	10000
0	0	0	0	0	0	0	0	0	0	0	0	0	0	0	0
100	3	3	2	2	2	2	2	2	2	2	2	2	2	2	1
200	6	5	5	5	4	4	4	4	4	3	3	3	3	3	3
300	9	8	8	7	7	6	6	6	6	5	5	5	5	4	4
400	12	11	10	10	9	9	8	8	7	7	7	7	6	6	6
500	14	14	12	12	12	10	10	9	10	8	8	8	8	7	7
600	18	16	15	14	14	13	12	12	11	10	10	10	9	9	8
700	20	20	17	17	15	15	14	14	13	12	12	11	11	11	10
800	24	22	20	18	18	17	16	16	14	14	14	13	12	12	11
900	26	23	22	21	19	19	18	18	17	16	15	14	14	13	13
1000	27	27	26	23	22	21	20	19	18	17	16	17	15	15	14
1100	32	29	27	26	25	23	22	21	20	19	18	17	17	16	15
1200	34	33	31	28	26	24	24	23	22	21	20	19	18	18	17
1300	36	33	33	30	29	27	26	25	23	22	21	20	20	19	17
1400	40	36	34	32	31	28	27	26	25	23	23	22	21	20	19
1500	42	41	37	35	33	29	28	28	26	26	25	24	23	22	21
1600	45	41	39	37	35	31	31	30	28	27	25	25	24	24	22
1700	46	44	40	38	38	35	31	31	29	29	28	27	25	25	24
1800	48	47	44	41	39	37	36	33	32	32	30	27	27	26	25
1900	52	49	47	43	41	39	37	35	33	33	31	30	28	28	27
2000	54	51	47	45	42	41	39	37	34	33	32	33	30	28	28
2100	57	55	48	48	45	41	39	38	34	34	35	33	32	29	28
2200	59	55	51	48	46	45	41	39	39	36	34	34	32	31	30
2300	61	57	53	50	47	46	43	41	41	38	37	37	33	33	31
2400	64	59	56	54	51	48	47	43	41	38	38	39	35	34	33
2500	64	62	58	55	51	50	47	46	43	43	39	38	37	35	34

TABLE 5. ALONG-TRACK ERROR DUE TO AZIMUTH OFFSET, DH = 200 FT,
GLIDEPATH ANGLE = 3°

Offset (ft)	AZIMUTH TO ELEVATION DISTANCE (FT)														
	3000	3500	4000	4500	5000	5500	6000	6500	7000	7500	8000	8500	9000	9500	10000
0	98	101	103	102	102	100	107	105	100	100	100	100	99	100	101
100	98	103	97	98	102	97	99	98	100	98	99	100	99	103	96
200	102	99	99	100	95	99	103	101	100	98	97	96	99	100	99
300	98	100	101	94	99	100	105	98	101	95	101	98	101	96	99
400	99	101	99	100	97	102	100	97	97	98	102	103	101	96	99
500	98	99	96	96	102	96	99	96	102	95	98	99	101	99	95
600	99	98	99	97	101	100	98	102	101	98	98	101	99	97	95
700	95	103	96	101	97	99	96	100	97	99	104	97	100	101	99
800	101	98	97	95	97	100	97	100	95	96	100	100	98	96	97
900	97	93	95	98	91	98	100	100	99	99	97	95	96	96	99
1000	92	97	100	95	98	98	99	99	96	99	96	101	97	101	99
1100	98	95	95	98	98	96	96	96	98	96	97	94	96	99	94
1200	95	100	100	96	95	94	96	100	98	98	97	98	96	99	99
1300	94	91	97	95	97	95	98	100	97	95	97	97	100	99	91
1400	96	94	95	94	98	93	93	95	94	92	98	95	97	95	95
1500	96	98	95	97	97	91	93	96	94	99	97	98	96	96	96
1600	95	93	95	96	95	91	93	97	96	95	93	95	95	99	95
1700	92	93	92	93	98	94	89	93	93	95	97	99	95	96	98
1800	90	94	94	94	94	95	98	95	95	100	98	93	94	96	95
1900	92	94	95	93	94	94	96	94	93	97	96	96	94	99	97
2000	91	92	92	93	92	95	96	96	92	92	95	101	97	93	97
2100	92	95	89	94	94	91	91	93	88	91	97	95	96	93	93
2200	91	91	91	91	91	94	91	92	95	93	91	94	94	94	94
2300	90	90	89	90	90	93	92	91	96	92	93	98	93	95	93
2400	90	89	81	93	92	93	95	92	93	90	93	99	93	94	95
2500	87	90	89	91	90	92	91	94	93	96	91	93	96	94	95

TABLE 6. CROSSTRACK ERROR DUE TO AZIMUTH OFFSET, DH = 250 FT,
GLIDEPATH ANGLE = 4.5°

Offset (ft)	AZIMUTH TO ELEVATION DISTANCE (FT)														
	3000	3500	4000	4500	5000	5500	6000	6500	7000	7500	8000	8500	9000	9500	10000
0	0	0	0	0	0	0	0	0	0	0	0	0	0	0	0
100	3	3	3	3	2	2	2	2	2	2	2	2	2	2	1
200	7	6	6	5	5	5	4	4	4	4	3	3	3	3	3
300	10	9	8	7	7	7	7	6	6	5	5	5	5	5	5
400	13	12	11	10	10	9	9	8	8	7	7	7	7	6	6
500	16	15	13	13	12	11	11	10	10	9	9	8	8	8	7
600	19	18	17	15	15	14	13	13	12	11	11	10	10	9	9
700	22	22	19	18	17	16	15	15	13	13	13	12	12	11	11
800	26	24	22	20	19	18	17	17	15	14	14	14	13	12	12
900	29	25	24	23	20	20	20	19	18	17	16	15	14	14	14
1000	30	29	28	25	24	23	22	20	19	19	17	17	16	16	15
1100	35	31	29	28	27	24	23	22	21	20	19	18	17	17	16
1200	37	36	33	30	28	26	25	25	23	22	21	20	19	19	18
1300	40	36	35	32	31	29	28	27	25	23	23	22	21	20	18
1400	44	39	37	34	34	30	28	28	26	24	25	23	22	21	20
1500	47	44	40	38	36	32	30	30	28	28	26	25	24	23	22
1600	49	45	42	40	37	34	33	32	30	29	27	26	25	25	23
1700	50	48	44	41	41	37	33	33	31	30	30	29	26	26	25
1800	53	51	47	44	42	39	39	35	34	34	32	29	28	27	26
1900	57	54	50	46	44	41	40	37	35	35	33	31	29	30	28
2000	59	55	51	48	45	44	42	40	36	35	34	35	32	29	30
2100	62	60	52	51	48	44	42	41	36	36	36	34	33	31	30
2200	65	60	56	52	49	48	44	42	41	38	36	35	34	33	31
2300	67	62	57	54	51	49	46	43	43	40	38	39	35	35	33
2400	70	64	61	58	54	51	50	46	44	41	40	41	37	36	35
2500	70	67	62	59	55	53	50	49	45	45	41	40	39	37	36

TABLE 7. ALONG-TRACK ERROR DUE TO AZIMUTH OFFSET, DH = 250 FT,
GLIDEPATH ANGLE = 4.5°

Offset (ft)	AZIMUTH TO ELEVATION DISTANCE (FT)														
	3000	3500	4000	4500	5000	5500	6000	6500	7000	7500	8000	8500	9000	9500	10000
0	98	101	103	102	102	99	107	105	100	100	100	100	99	100	101
100	98	103	96	98	102	97	99	98	99	98	99	100	99	103	96
200	102	99	99	100	95	99	102	101	99	98	97	96	99	100	99
300	98	100	101	94	99	100	105	98	101	95	101	98	101	96	99
400	98	101	99	100	97	102	100	97	97	98	102	103	101	96	99
500	97	99	96	96	102	96	99	96	102	95	98	99	101	99	95
600	99	98	99	97	101	100	98	102	101	98	98	101	99	97	95
700	94	103	96	100	97	99	96	100	97	99	104	97	100	101	99
800	101	98	96	95	97	100	97	100	95	96	100	100	97	96	97
900	97	93	95	97	91	98	100	100	99	99	97	95	96	96	99
1000	92	96	100	94	97	97	99	98	96	98	96	101	97	101	99
1100	97	94	95	97	98	96	96	96	98	96	97	94	96	98	94
1200	94	99	99	95	95	94	96	100	98	98	96	97	96	99	99
1300	94	91	97	95	97	95	98	99	97	94	97	97	100	98	91
1400	96	93	95	94	98	93	93	95	94	92	98	95	97	95	95
1500	95	98	94	97	96	91	93	96	94	99	97	97	96	96	96
1600	95	93	94	95	94	91	93	97	95	95	92	95	94	98	95
1700	91	93	92	92	97	94	88	92	92	95	97	99	95	96	98
1800	89	94	94	94	94	94	98	94	95	99	98	93	94	96	94
1900	91	93	95	92	93	94	96	94	93	97	96	96	94	99	96
2000	90	92	91	92	91	94	95	96	91	92	95	101	96	93	97
2100	91	94	88	93	93	91	90	93	87	91	96	95	96	92	93
2200	90	90	90	90	90	93	91	91	94	92	91	94	94	94	93
2300	89	89	88	89	89	93	91	90	95	92	93	97	92	95	93
2400	89	88	90	93	92	92	94	92	93	90	93	99	93	94	95
2500	85	89	88	90	89	92	91	94	92	96	90	92	95	94	94

TABLE 8. CROSSTRACK ERROR DUE TO AZIMUTH OFFSET, DH = 300 FT,
GLIDEPATH ANGLE = 6.0°

Offset (ft)	AZIMUTH TO ELEVATION DISTANCE (FT)														
	3000	3500	4000	4500	5000	5500	6000	6500	7000	7500	8000	8500	9000	9500	10000
0	0	0	0	0	0	0	0	0	0	0	0	0	0	0	0
100	3	3	3	3	3	2	2	2	2	2	2	2	2	2	1
200	7	6	6	5	5	5	5	4	4	4	4	3	3	3	3
300	10	9	9	8	8	7	7	6	6	6	6	5	5	5	5
400	14	13	12	11	10	10	9	8	8	8	8	7	7	6	6
500	17	16	14	13	13	12	11	10	10	9	9	9	9	8	7
600	20	19	17	16	15	14	13	13	12	11	11	11	10	9	9
700	23	23	20	19	17	17	15	15	14	13	13	12	12	11	11
800	28	25	23	21	20	19	18	17	16	15	15	14	13	12	12
900	30	26	25	24	21	21	20	19	18	17	16	15	15	14	14
1000	32	30	29	26	25	23	22	21	20	19	18	18	16	16	16
1100	37	33	31	29	28	25	24	33	22	20	20	18	18	18	16
1200	39	38	35	31	29	27	26	26	24	23	21	21	20	19	18
1300	42	37	37	34	32	30	29	28	26	24	23	22	22	21	18
1400	46	41	39	36	35	31	29	28	27	25	25	23	23	22	21
1500	49	46	41	40	37	33	31	31	29	29	27	26	24	23	22
1600	52	47	44	42	39	35	34	33	31	29	27	27	26	26	24
1700	53	50	46	43	42	38	34	34	32	31	30	30	27	27	26
1800	55	53	49	46	43	41	40	36	35	35	32	30	29	28	27
1900	59	56	53	48	45	43	41	38	36	36	34	32	30	30	29
2000	61	58	53	50	47	45	43	41	37	36	35	36	33	30	30
2100	65	63	54	53	50	46	43	42	37	37	37	35	34	31	30
2200	68	62	58	54	51	49	45	43	42	39	37	36	35	34	32
2300	70	65	59	56	52	51	48	45	45	41	40	40	36	35	33
2400	73	67	63	61	56	53	51	47	45	42	41	42	38	36	35
2500	73	70	65	61	57	55	51	50	47	46	42	41	40	38	37

TABLE 9. ALONG-TRACK ERROR DUE TO AZIMUTH OFFSET, DH = 300 FT,
GLIDEPATH ANGLE = 6.0°

Offset (ft)	AZIMUTH TO ELEVATION DISTANCE (FT)														
	3000	3500	4000	4500	5000	5500	6000	6500	7000	7500	8000	8500	9000	9500	10000
0	98	101	103	102	102	99	107	105	100	100	100	100	99	100	101
100	98	103	96	98	101	97	99	97	99	98	99	99	99	103	96
200	101	99	99	100	95	99	102	101	99	98	97	96	99	99	99
300	98	100	101	94	99	100	105	98	101	95	101	98	101	96	99
400	98	100	99	100	97	102	99	97	97	98	102	103	101	95	99
500	97	99	95	96	101	96	99	96	102	95	98	98	101	99	95
600	99	98	99	97	101	100	98	101	101	98	98	101	99	97	95
700	94	102	96	100	97	99	96	100	97	99	104	97	100	101	99
800	101	98	96	95	96	99	96	100	95	96	99	100	97	96	97
900	97	93	95	97	91	97	100	100	99	99	97	95	96	96	99
1000	92	96	99	94	97	97	99	98	96	98	96	101	96	101	99
1100	97	94	95	97	98	96	96	96	98	96	97	94	96	98	94
1200	94	99	99	95	95	94	96	99	98	97	96	97	96	99	98
1300	93	91	96	95	97	95	98	99	97	94	97	96	100	98	91
1400	95	93	94	93	97	92	93	95	94	92	98	95	96	95	94
1500	94	97	94	97	96	91	92	96	94	98	96	97	96	96	95
1600	94	92	94	95	94	90	93	97	95	95	92	95	94	98	95
1700	90	92	91	92	97	94	88	92	92	95	97	99	94	96	98
1800	89	93	93	93	93	94	98	94	94	99	97	93	94	95	94
1900	91	93	94	92	93	94	96	93	93	96	95	95	94	98	96
2000	89	91	91	92	91	94	95	95	91	92	95	101	96	93	97
2100	90	94	88	93	93	91	90	93	87	91	96	95	96	92	92
2200	89	89	90	90	90	93	90	91	94	92	91	94	94	94	93
2300	88	88	87	89	89	92	91	90	95	92	93	97	92	95	93
2400	88	87	89	92	91	92	94	92	92	90	93	98	92	93	95
2500	85	88	88	89	88	91	90	93	92	95	90	92	95	93	94

TABLE 10. CROSSTRACK ERROR DUE TO AZIMUTH OFFSET, DH = 350 FT,
GLIDEPATH ANGLE = 9.0°

Offset (ft)	AZIMUTH TO ELEVATION DISTANCE (FT)														
	3000	3500	4000	4500	5000	5500	6000	6500	7000	7500	8000	8500	9000	9500	10000
0	0	0	0	0	0	0	0	0	0	0	0	0	0	0	0
100	4	4	3	3	3	3	2	2	2	2	2	2	2	2	2
200	8	7	6	6	5	5	5	5	4	4	4	4	4	3	3
300	11	11	10	8	8	8	8	7	7	6	6	5	5	5	5
400	15	14	13	12	11	11	10	9	8	8	8	8	7	7	6
500	19	17	15	14	14	13	12	11	11	10	10	9	9	8	8
600	23	21	19	17	17	16	14	14	13	12	12	11	11	10	9
700	25	25	22	21	19	18	16	16	15	14	14	13	13	12	11
800	31	27	25	23	21	21	19	18	17	16	16	15	14	13	13
900	34	29	27	26	23	23	22	21	19	18	17	16	15	15	15
1000	35	34	32	28	27	25	24	23	21	20	19	19	17	17	16
1100	41	36	34	32	30	27	26	24	23	22	21	19	19	19	17
1200	43	42	38	34	32	29	28	27	25	24	22	22	21	20	19
1300	47	41	40	37	35	32	31	30	27	25	25	23	23	22	19
1400	51	46	43	39	38	34	32	30	29	26	27	25	24	23	22
1500	54	51	45	43	40	35	34	33	31	30	28	27	26	25	23
1600	58	52	48	45	42	38	36	36	33	31	29	28	27	27	25
1700	59	55	50	47	46	41	37	36	34	33	32	31	29	28	27
1800	61	59	54	50	47	44	43	39	37	37	34	31	30	29	28
1900	66	61	57	52	49	46	44	41	38	38	36	34	32	32	30
2000	68	63	58	54	50	49	46	44	40	38	37	38	34	32	32
2100	72	69	59	58	54	49	46	45	40	39	40	37	36	33	32
2200	75	68	63	59	55	53	48	46	45	42	39	38	37	35	34
2300	77	71	64	60	56	55	51	48	47	44	42	42	38	37	35
2400	80	73	69	66	61	57	55	51	48	44	44	44	40	38	37
2500	80	76	70	66	61	59	55	53	50	49	44	43	42	40	39

TABLE 11. ALONG-TRACK ERROR DUE TO AZIMUTH OFFSET, DH = 350 FT,
GLIDEPATH ANGLE = 9.0°

Offset (ft)	AZIMUTH TO ELEVATION DISTANCE (FT)														
	3000	3500	4000	4500	5000	5500	6000	6500	7000	7500	8000	8500	9000	9500	10000
0	97	101	102	101	101	99	106	105	99	100	99	100	99	100	101
100	97	103	96	97	101	97	99	97	99	97	99	99	98	103	96
200	101	99	98	99	95	99	102	100	99	97	97	96	99	99	99
300	97	99	100	94	99	100	104	98	100	95	101	98	101	96	99
400	98	100	99	99	97	102	99	97	96	98	102	102	100	95	98
500	97	98	95	95	101	96	98	96	102	95	98	98	101	99	95
600	98	98	98	97	100	100	98	101	101	98	98	101	98	96	95
700	94	102	96	99	96	99	96	100	96	98	103	97	100	101	99
800	100	97	96	94	96	99	96	99	95	95	99	99	97	96	97
900	96	92	94	97	90	97	99	99	99	98	97	94	96	95	99
1000	91	95	99	94	97	97	98	98	96	98	96	101	96	101	99
1100	96	93	94	97	97	95	96	96	98	96	97	94	96	98	94
1200	93	98	98	94	94	93	95	99	97	97	96	97	96	99	98
1300	92	90	96	94	96	94	98	99	96	94	97	96	99	98	90
1400	94	92	93	93	97	92	92	94	94	91	98	95	96	94	94
1500	93	96	93	96	95	90	92	96	94	98	96	97	95	95	95
1600	93	91	93	94	93	90	92	96	95	94	92	94	94	98	95
1700	89	91	90	91	96	93	88	92	92	95	96	98	94	96	97
1800	88	92	92	92	93	93	97	94	94	99	97	93	94	95	94
1900	89	92	93	91	92	93	95	93	92	96	95	95	93	98	96
2000	87	90	90	91	90	93	94	95	91	92	94	100	96	92	97
2100	89	92	87	92	92	90	89	92	87	90	96	94	95	92	92
2200	87	88	88	89	89	92	90	90	94	92	90	93	93	94	93
2300	86	87	86	87	88	91	90	89	94	91	92	97	92	94	93
2400	86	86	88	91	90	91	93	91	92	89	92	98	92	93	94
2500	83	86	86	88	87	91	90	93	91	95	90	92	95	93	94

T07: HELICOPTER MLS RNAV - CROSS TRACK ERROR SIMULATION
 AZ/DMEP & EL COLLINEAR CENTER LINE APPROACH: DR= 200 FT, PHI= 3.0 DEG.
 PREPARED BY ACT140/FAA ATLANTIC CITY AIRPORT N.W. 1 DEC 85

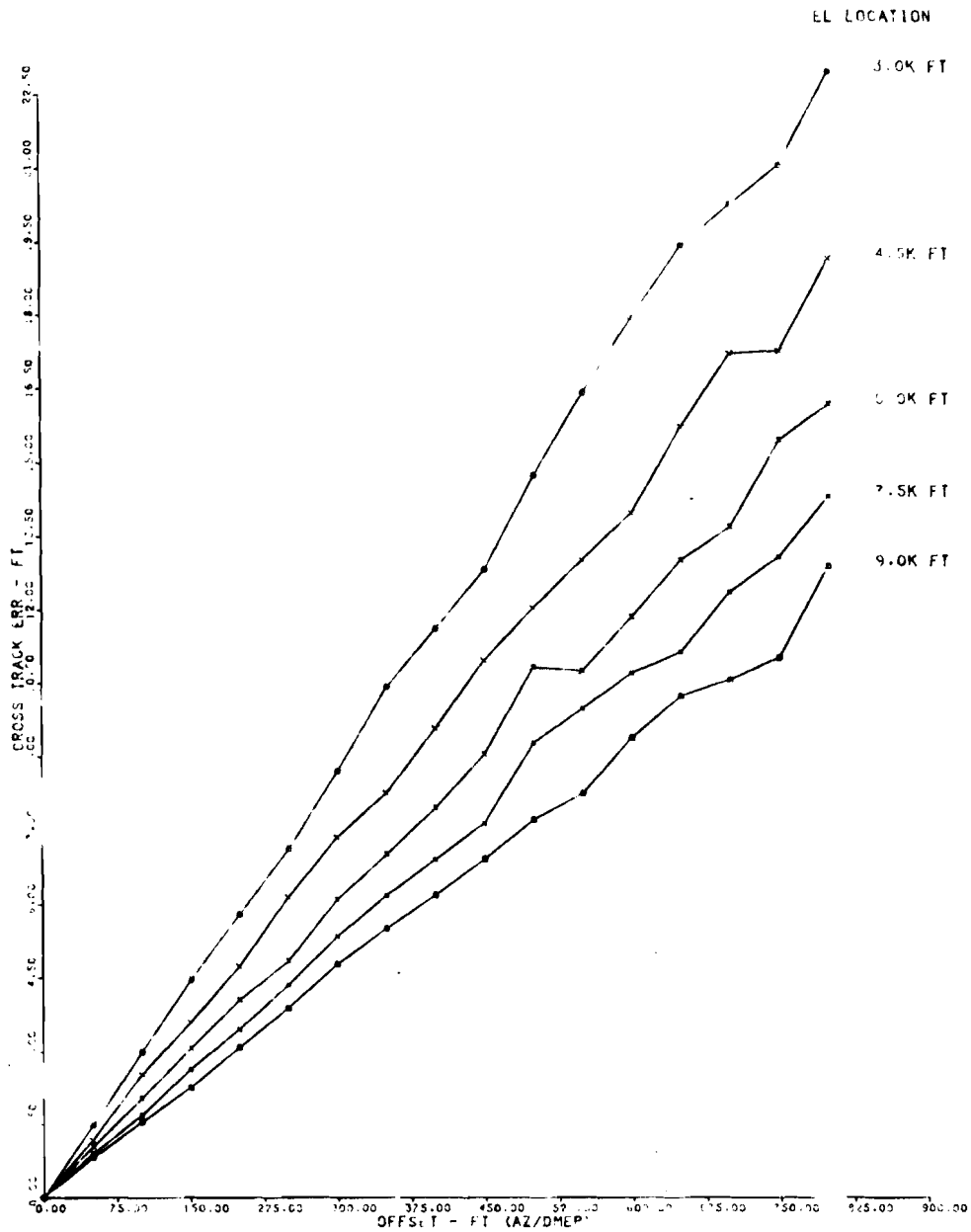


FIGURE 30. SIGNAL SOURCE ERROR SIMULATION RESULTS, CROSSTRACK ERROR, ELEVATION TRANSMITTER TO AZIMUTH TRANSMITTER DISTANCE, 3,000 to 9,000 FT

TO/HELICOPTER MLS RNAV - CROSS TRACK ERROR SIMULATION
 AZ/DMEP & EL COLINEAR CENTER LINE APPROACH DH= 200 FT. PHI= 3.0 DEG.
 *PREPARED BY ACT140/FAA ATLANTIC CITY AIRPORT N.J. - DEC. 1975

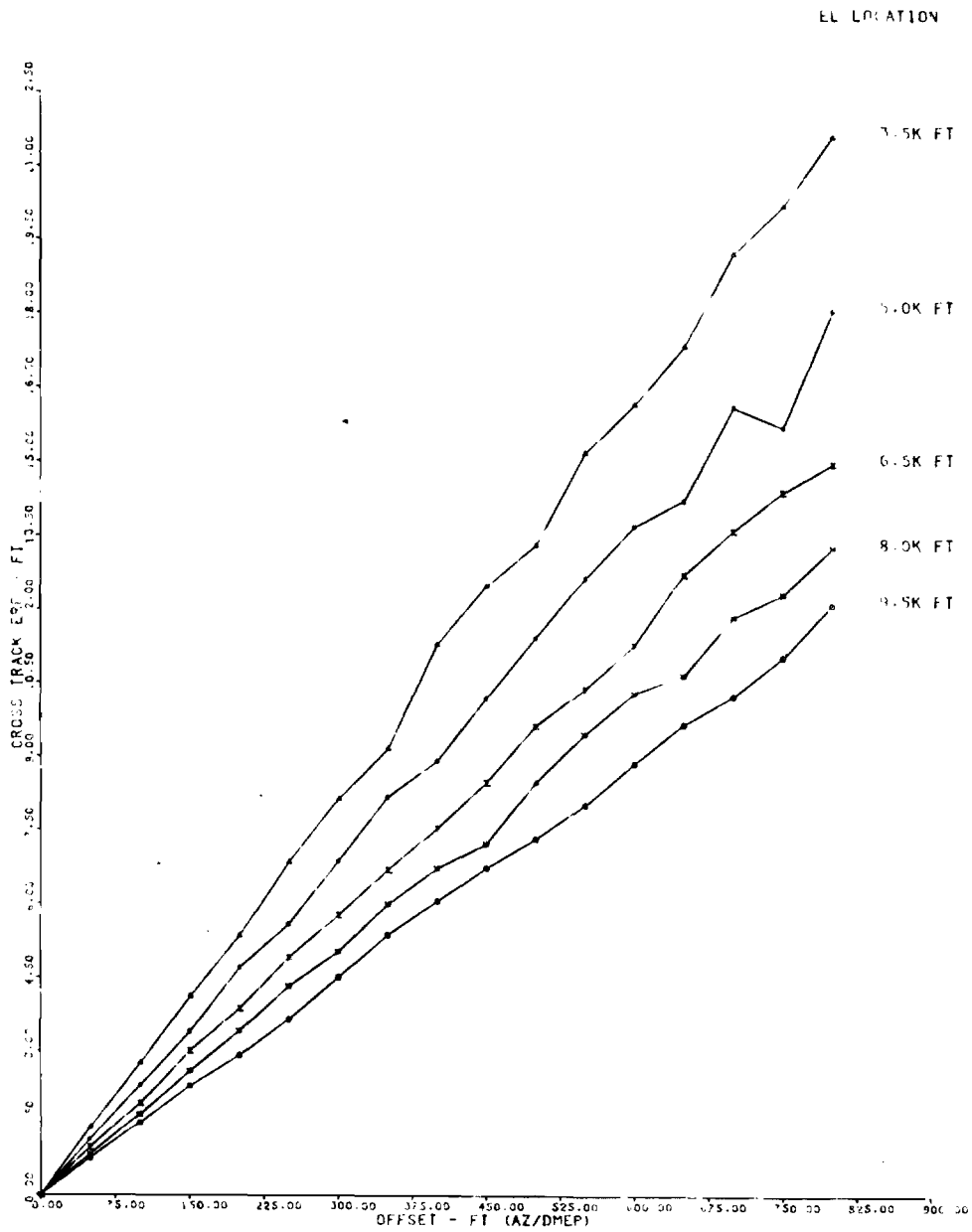


FIGURE 31. SIGNAL SOURCE ERROR SIMULATION RESULTS, CROSSTRACK ERROR, ELEVATION TRANSMITTER TO AZIMUTH TRANSMITTER DISTANCE, 3,500 TO 9,000 FT

T07: HELICOPTER MLS RNAV - CROSS TRACK ERROR SIMULATION
 AZ/DMEP & EL COLINEAR CENTER LINE APPROX: DM= 200.FT. PHI= 3.DEG.
 *PREPARED BY ACT140/FAA ATLANTIC CITY AIRPORT N.J. - DEC/85

ELLIGATION

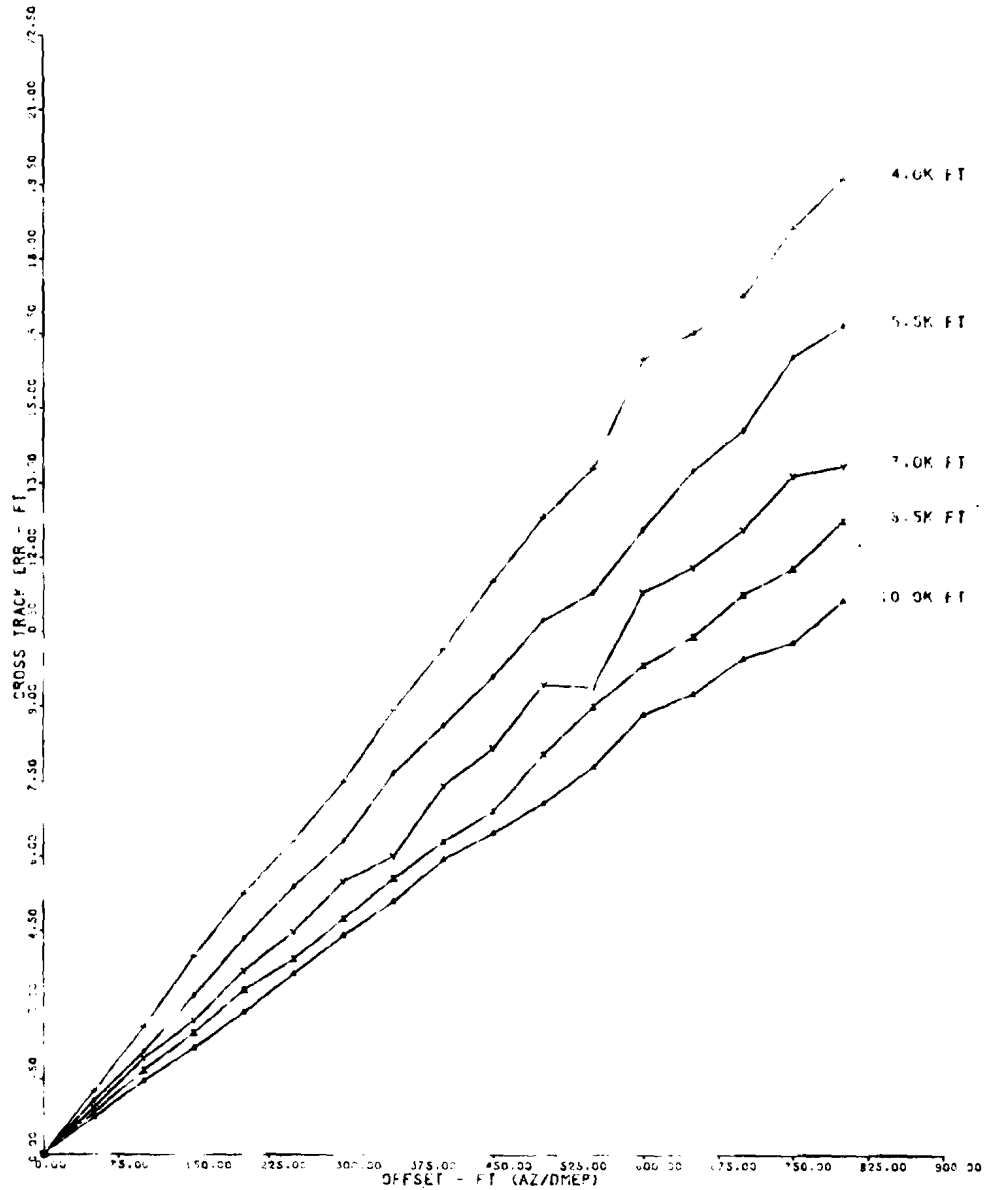


FIGURE 32. SIGNAL SOURCE ERROR SIMULATION RESULTS, CROSSTRACK ERROR,
 ELEVATION TRANSMITTER TO AZIMUTH TRANSMITTER DISTANCE,
 4,000 TO 10,000 FT

Along-track error was also plotted in a fashion similar to crosstrack error. That is, for a 3° glide slope, 200-foot DH, the 2 sigma along-track error values obtained for each azimuth to elevation distance were plotted as a function of elevation unit offset from the runway centerline. The resulting curves (figures 33, 34, and 35) do not pass through the origin, but rather are approximately horizontal and clustered about the 100-foot along track error value. There is a slight downward slope which results as centerline offset increases. Lower errors also appear to result from shorter elevation to azimuth separation distances. One possible explanation for these effects is the fact that larger offsets and smaller elevation separation results in larger off axis bearings to the MLS signal sources, thereby transferring more of the relatively large DME/P error out of the along-track axis and into the crosstrack axis.

SIGNAL SOURCE ERROR SIMULATIONS FOR PARASITE APPROACHES.

An analysis of MLS RNAV system accuracy for computed centerline approaches via simulation has already been described. Herein, an accuracy analysis of another MLS RNAV application, the parasite approach, is described. The parasite approach is similar to the computed centerline approach in that the flightpaths of both are defined by a linear segment. However, the parasite approach is much more general insofar as both the terminal waypoint and the angle formed with the runway centerline may assume any feasible value within the volume of MLS signal coverage. An example of this would include precision guidance to an intersecting but noninstrumented runway within MLS coverage (figure 36). An additional application of the parasite approach technique to helicopters is shown in figure 37. As the number of helicopter IFR operations continues to increase, mixing the helicopter with its slower approach speed with the traffic flow to the primary instrument runway tends to slow the entire traffic flow. However, using the parasite approach technique, a precision approach to an on-airfield heliport in MLS coverage could be used to separate the helicopter from the primary instrument runway traffic flow. Based on the results of the present analysis, a decision on where to retain category 1 approach minima could be made.

The system accuracy analysis of the parasite approach proceeds in a manner similar to that of the computed centerline approach in that both are simulations written in Fortran 77 and run on the VAX 11/750 computer. The simulation uses a Monte Carlo technique to generate a random variable triple in MLS coordinates (θ , ϕ , ρ). This normally distributed random variable has 2σ component values which are a function of their position in the volume of MLS coverage. In general, these 2σ values, which are given in appendix B, increase in magnitude as the angle off centerline and range increase. Appendix B is our interpretation of tolerance limits identified in reference 4. For each point at which system accuracy is to be assessed, 1000 random MLS triples are generated. These triples are individually fed to a case XII MLS transformation algorithm which produces an output cartesian triple (x,y,z). Also input to the case XII algorithm are the siting parameters of the signal source transmitters. These siting parameters conform to the Radio Technical Commission for Aeronautics Special Committee 151 (MLS RNAV) recommendations for a general test siting.

T07: HELICOPTER MLS RNAV - ALONG TRACK ERROR SIMULATION
AZ/DMEP & EL COLINEAR CENTER LINE APPCH : DH= 200.FT.PHI= 3.DEG.

PREPARED BY ACT1140/FAA ATLANTIC CITY AIRPORT N.J. - DEC. 85

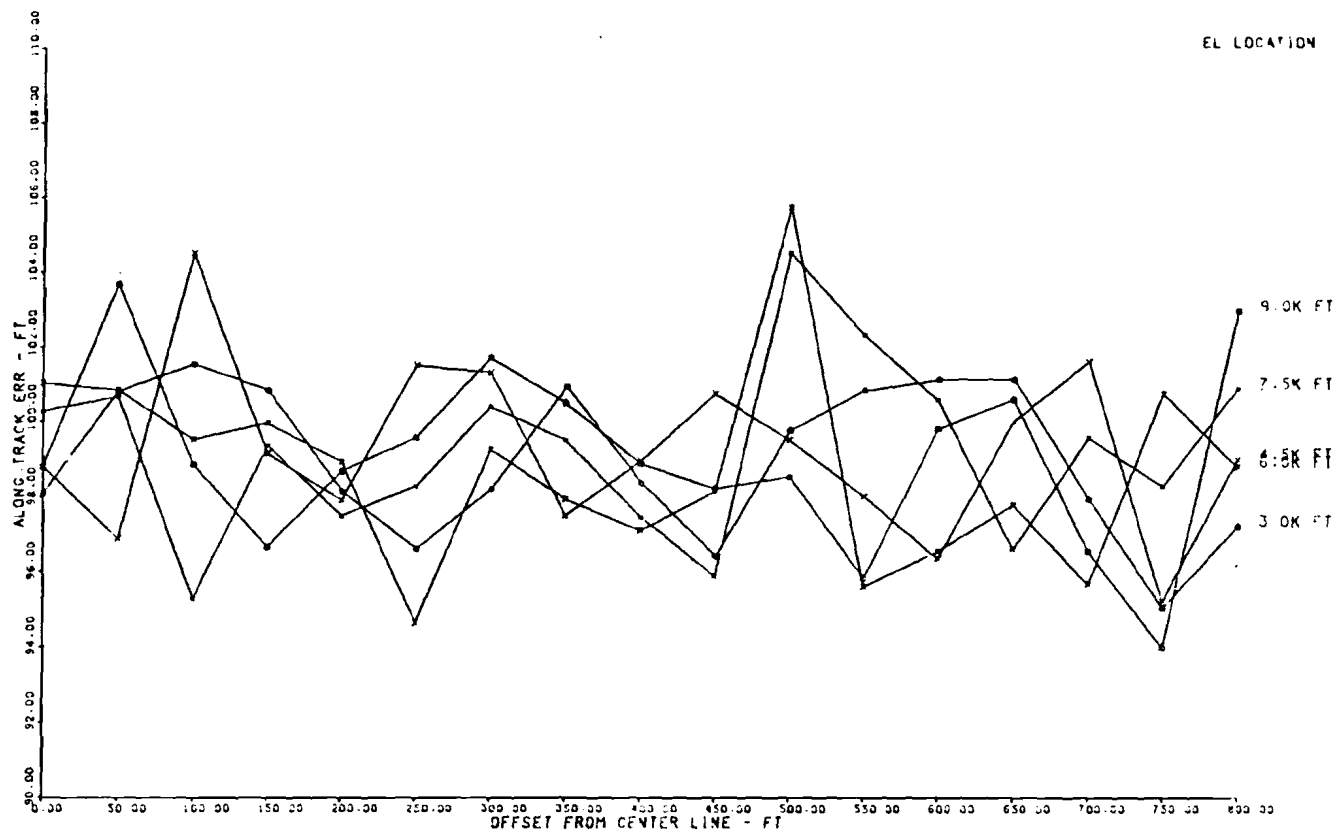


FIGURE 33. SIGNAL SOURCE ERROR SIMULATION RESULTS, ALONG-TRACK ERROR, ELEVATION TRANSMITTER TO AZIMUTH TRANSMITTER DISTANCE, 3,000 TO 9,000 FT

T07: HELICOPTER MLS RNAV - ALONG TRACK ERROR SIMULATION
AZ/DMEP & EL COLINEAR CENTER LINE APPCH :DH= 200.FT.PHI= 3.DEG.

PREPARED BY ACT140/FAA ATLANTIC CITY AIRPORT N.J. - DEC. 85

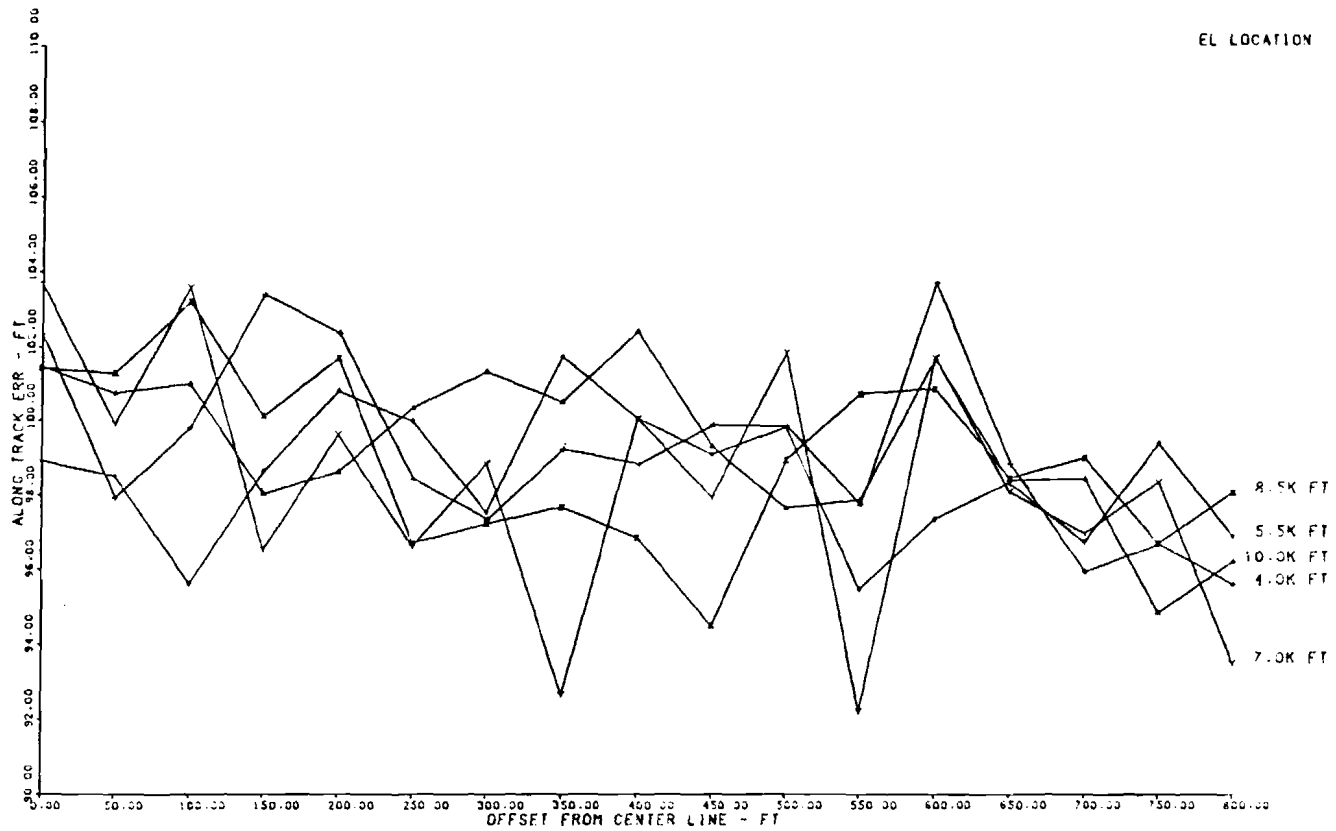


FIGURE 34. SIGNAL SOURCE ERROR SIMULATION RESULTS, ALONG-TRACK ERROR, ELEVATION TRANSMITTER TO AZIMUTH TRANSMITTER DISTANCE, 4,000 TO 10,000 FT

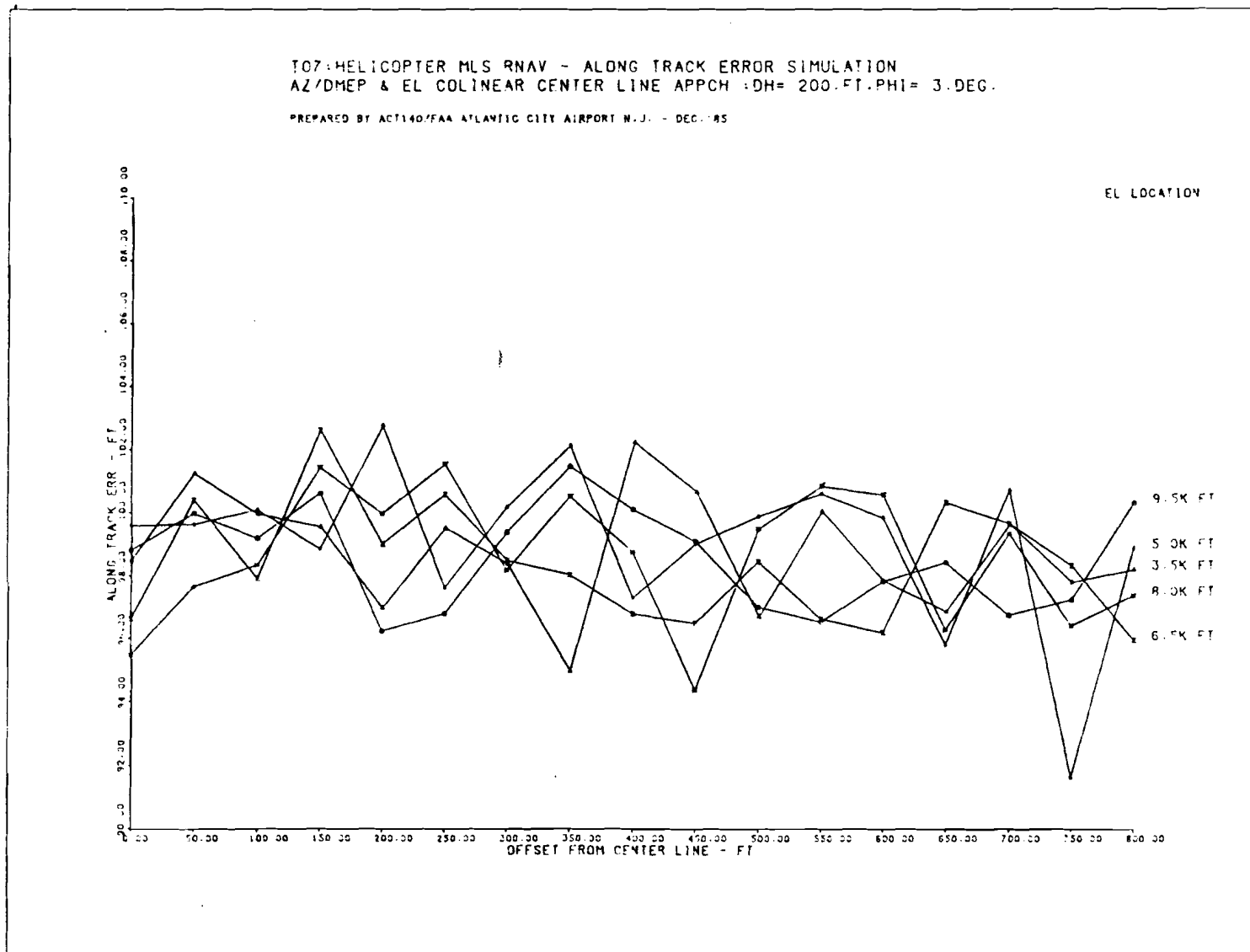


FIGURE 35. SIGNAL SOURCE ERROR SIMULATION RESULTS, ALONG-TRACK ERROR, ELEVATION TRANSMITTER TO AZIMUTH TRANSMITTER DISTANCE, 3,500 TO 9,500 FT

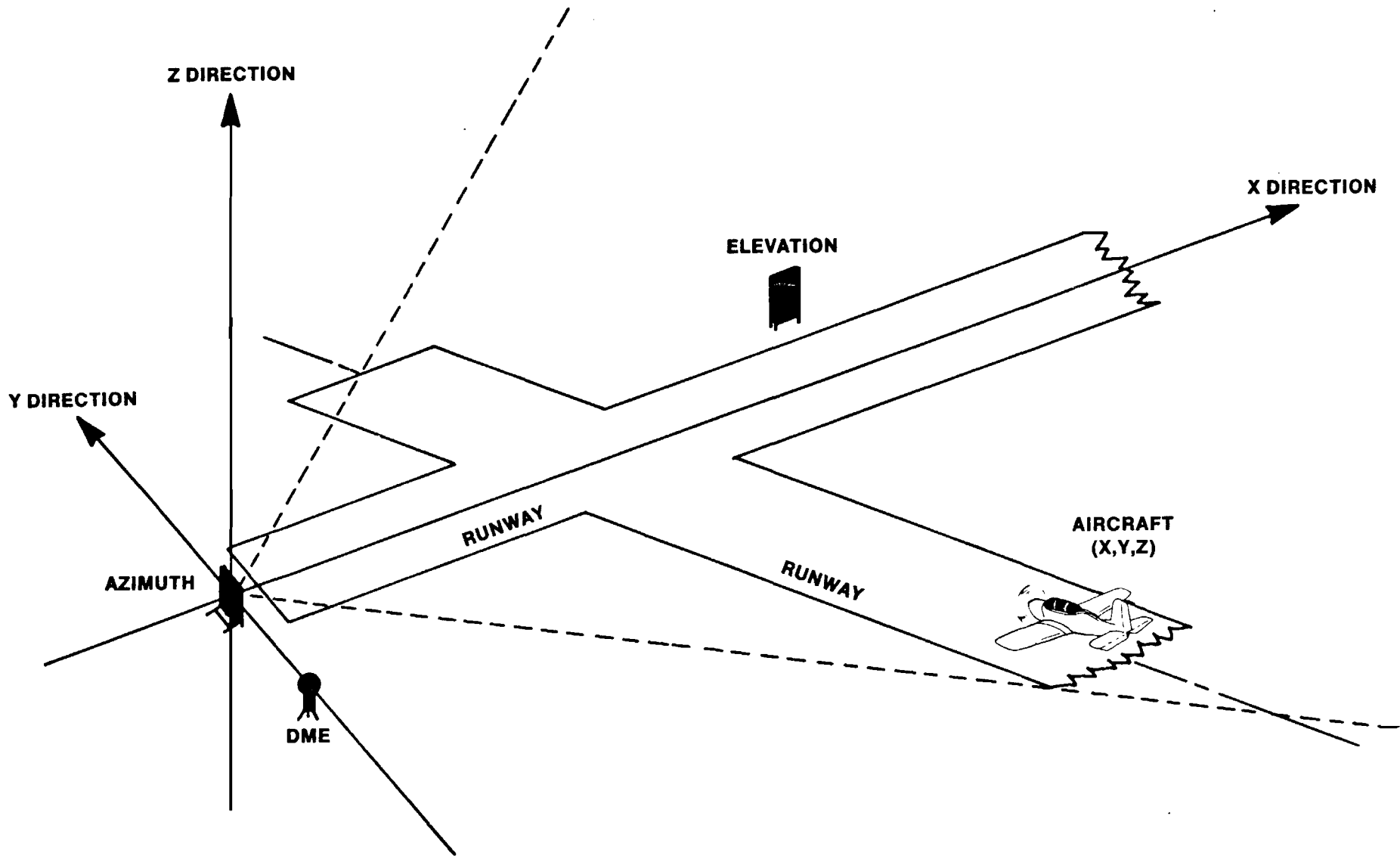


FIGURE 36. MLS RNAV APPROACH TO NONINSTRUMENTED RUNWAY

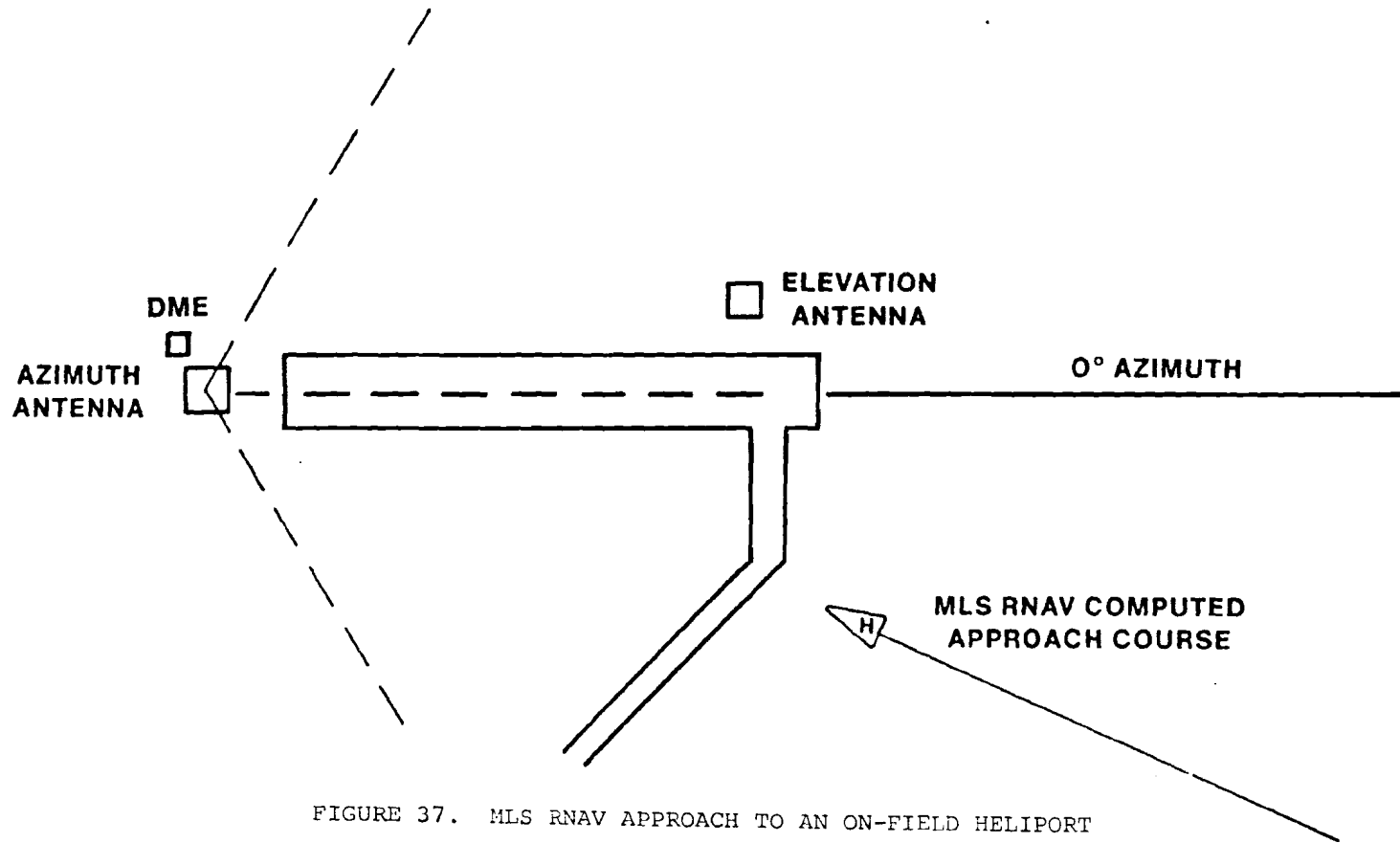


FIGURE 37. MLS RNAV APPROACH TO AN ON-FIELD HELIPORT

They are as follows (in meters) referenced to the MLS Datum Point:

	<u>x</u>	<u>y</u>	<u>z</u>
Azimuth	-4000	0	30
Elevation	0	120	2
DME/P	-3900	-137	30

The principal difference between the computed centerline and the parasite approach simulations is that in the former case, the ground transmitter locations are varied in order to assess the effect of offset azimuth. In the parasite case, they are fixed. However, since a parasite approach may terminate anywhere in the region of MLS coverage, accuracy is evaluated at a multitude of points over a 3000 by 4000-foot grid off the threshold of the runway. For each point, crosstrack, along-track, and vertical error values are computed. These error values correspond to the 2σ statistic computed from the 1000 cartesian triple values output by the case XII transformation algorithm for each test grid point evaluated. Error values were computed for assumed headings of 45° and 315° referenced to the runway centerline. DH values were also varied (200, 250, and 300 feet) at each grid evaluation point.

The results of the parasite approach accuracy simulation are listed in tables 12 and 13 for a 200-foot DH, tables 14 and 15 for a 250-foot DH, and tables 16 and 17 for a 300-foot DH. The results of the along-track and crosstrack error are plotted in figure 38 for all DH's and grid test points. The vertical track error curves for all DH's and grid test points are displayed in figure 39.

Some relevant conclusions are immediately apparent from the plots. First, the worst case errors for along-track and crosstrack components result at the largest distances from the datum point. In the case of along-track and crosstrack errors, the 2σ values encountered reach approximately 100 feet. For vertical track errors, these values are more randomly distributed and reach a maximum of approximately 40 feet at a DH of 200 feet at a point $x=4000$ feet, $y=3000$ feet from the datum point. Another fact evident from the plots is the similarity of the 45° crosstrack and 315° along-track error curves and the 45° along-track and 315° crosstrack error curves. Upon reflection, this seems plausible since the two headings evaluated, 45° and 315° , are 90° rotations of each other, resulting in the crosstrack axis becoming the along-track axis of the aircraft (and vice versa) when changing from one heading to the other. Finally, the slope of the curves in figure 38 may, at first glance, defy explanation. However, upon closer examination, the curves appear to slope upward or downward toward a 100-foot error in most cases. Further reflection indicates that this slope does not correlate with lateral grid point displacement, but rather with angular alignment to the DME/P interrogators. This fact becomes more apparent when one considers the fact that the 100-foot DME/P basic 2σ error closely approximates the maximum value of the plotted error curves. This leads one to conclude that the DME/P component appears to be the most significant contributor to parasite approach system accuracy.

PARASITE APPROACH MEASURES OF SKEWNESS AND KURTOSIS.

The overall MLS RNAV system accuracy was previously computed for parasite approach applications. These accuracy figures were the 2σ values calculated from output cartesian triples of the Monte Carlo process. One thousand cartesian

TABLE 12. PARASITE APPROACH SIMULATION, 45° COURSE ANGLE,
DECISION HEIGHT = 200 FT

DATE: 7/29/37

HELICOPTER-GROUP ACT140,
FAA/201, ATLANTIC CITY AIRPORT.

BACKGROUND:

* AZ ANTENNA OPERATION IS CONICAL;

WHEN REFERENCED TO THE DTM AND CENTER LINES, ANTENNA PHASE CENTERS ARE AT:

AZ = (-15123.20 0.00 98.42)
EL = (0.00 393.70 5.56)
DME = (-12795.12 -449.47 93.42);

* UNIT IS FT OR DEG.

PARASITE PATH ON 45. DEG

DEGRADATIONS AT DH = 200.FT

A-TRACK DIST FROM DTM	PATH-BASED DEGRADATION	GRID - OFFSET TO DTM ALONG LINE-X-DTM						
		-1500.00	-1000.00	-500.00	0.00	500.00	1000.00	1500.00
66 1000.00	ATE	56.61	24.77	34.39	84.36	73.94	72.08	75.09
	XTE	60.15	62.09	65.39	72.31	72.35	75.25	77.99
	VTE	17.44	22.43	24.17	19.35	13.71	11.32	10.50
2000.00	ATE	87.49	86.72	83.36	81.66	79.28	78.17	78.74
	XTE	69.23	73.51	75.08	78.06	80.32	83.84	89.45
	VTE	15.35	15.76	14.23	13.25	12.58	12.53	13.09
3000.00	ATE	91.32	89.61	86.23	85.18	83.24	78.94	77.71
	XTE	81.03	83.07	86.02	89.05	91.31	91.33	95.31
	VTE	14.79	14.44	14.32	16.40	19.10	21.50	24.93
4000.00	ATE	92.15	91.07	90.33	88.19	85.63	80.20	82.21
	XTE	89.49	93.04	97.09	99.71	101.71	100.13	107.82
	VTE	21.45	23.74	26.43	29.06	31.95	33.69	38.83

LEGEND

ATE = Along-Track Error
XTE = Crosstrack Error
VTE = Vertical Track Error

TABLE 13. PARASITE APPROACH SIMULATION, 315° COURSE
 ANGLE, DECISION HEIGHT = 200 FT

DATE: 7/29/37

HELICOPTER-GROUP ACT140,
 FAA/DOT, ATLANTIC CITY AIRPORT.

BACKGROUND:

* AZ ANTENNA OPERATION IS CONICAL;

WHEN REFERENCED TO THE DTM AND CENTER LINES, ANTENNA PHASE CENTERS ARE AT:

AZ = (-13123.20 0.00 93.42)
 EL = (0.00 393.70 6.56)
 DME = (-12795.12 -449.47 98.42);

* UNIT IS FT OR DEG.

PARASITE PATH ON 315. DEG

DEGRADATIONS AT DH = 200 FT

A-TRACK DIST FROM DTM	PATH-BASED DEGRADATION	GRID - OFFSET TO DTM ALONG LINE-X-DTM						
		-1500.00	-1000.00	-500.00	0.00	500.00	1000.00	1500.00
1000.00	ATE	59.91	62.33	65.04	69.33	69.36	78.51	78.06
	XTE	35.25	65.75	84.35	81.43	76.22	80.43	75.12
	VTE	17.32	22.71	23.91	18.58	13.23	11.33	10.46
2000.00	ATE	71.36	71.53	77.02	81.03	82.36	83.35	86.73
	XTE	90.03	84.47	85.49	84.73	81.81	77.67	76.33
	VTE	16.32	15.27	14.62	13.77	13.02	12.45	12.68
3000.00	ATE	73.73	33.53	86.31	83.23	90.79	93.13	97.00
	XTE	58.77	89.15	87.14	84.42	82.28	80.07	79.07
	VTE	14.45	14.51	14.32	16.23	18.82	21.32	25.34
4000.00	ATE	91.01	93.09	93.99	96.59	98.31	104.63	104.66
	XTE	93.77	91.15	87.41	85.43	82.77	83.37	79.32
	VTE	21.91	23.60	25.51	23.16	30.83	35.28	37.75

LEGEND

ATE = Along-Track Error
 XTE = Crosstrack Error
 VTE = Vertical Track Error

TABLE 14. PARASITE APPROACH SIMULATION, 45° COURSE ANGLE,
DECISION HEIGHT = 250 FT

DATE: 7/29/37

HELICOPTER-GROUP ACT140,
FAA/DOT, ATLANTIC CITY AIRPORT.

BACKGROUND:

* AZ ANTENNA OPERATION IS CONICAL;

WHEN REFERENCED TO THE DTM AND CENTER LINES, ANTENNA PHASE CENTERS ARE AT:

AZ = (-13133.20 0.00 98.42)
EL = (0.00 393.70 6.50)
DME = (-12795.12 -449.47 98.42);

* UNIT IS FT OR DEG.

PARASITE PATH ON 45. DEG

DEGRADATIONS AT DH = 250 FT

A-TRACK DIST FROM DTM PATH-BASED DEGRADATION

GRID - OFFSET TO DTM ALONG LINE-X-DTM

			-1500.00	-1000.00	-500.00	0.00	500.00	1000.00	1500.00
101	1000.00	ATE	91.09	91.47	94.51	84.25	77.45	78.62	78.63
		XTE	51.29	53.00	53.33	67.96	70.53	76.76	81.67
		VTE	22.35	29.58	32.22	22.33	16.25	13.62	12.69
	2000.00	ATE	87.67	88.47	87.44	86.03	73.66	77.37	76.20
		XTE	69.25	75.02	73.73	82.21	79.63	83.02	86.54
		VTE	19.74	19.27	17.80	16.37	14.39	14.07	14.13
	3000.00	ATE	90.67	86.21	84.90	84.34	82.14	79.22	77.99
		XTE	80.42	80.35	84.03	88.20	90.62	92.18	95.68
		VTE	17.05	16.03	15.37	15.92	15.90	16.24	19.56
	4000.00	ATE	90.55	86.24	83.76	87.33	81.04	83.03	79.25
		XTE	87.33	83.75	95.35	99.72	96.23	103.61	103.92
		VTE	16.93	17.54	20.69	25.34	24.95	29.37	31.96

LEGEND

ATE = Along-Track Error
XTE = Crosstrack Error
VTE = Vertical Track Error

TABLE 15. PARASITE APPROACH SIMULATION, 315° COURSE ANGLE
 DECISION HEIGHT = 250 FT

DATE: 7/29/87

HELICOPTER-GROUP ACT140,
 FAA/DOJ, ATLANTIC CITY AIRPORT.

BACKGROUNDS:

* AZ ANTENNA OPERATION IS CONICAL;

WHEN REFERENCED TO THE DTM AND CENTER LINES, ANTENNA PHASE CENTERS ARE AT:

AZ = (-13123.20 0.00 98.42)
 EL = (0.00 393.70 6.56)
 DME = (-12795.12 -449.47 98.42);

* UNIT IS FT OR DEG.

PARASITE PATH ON 315. DEG

DEGRADATIONS AT DH = 250.FT

A-TRACK DIST
 FROM DTM

PATH-BASED
 DEGRADATION

GRID - OFFSET TO DTM ALONG LINE-X-DTM

			-1500.00	-1000.00	-500.00	0.00	500.00	1000.00	1500.00
100	1000.00	ATE	59.32	52.17	63.27	66.77	73.57	77.33	77.91
		XTE	33.93	90.23	87.52	82.78	80.78	79.79	74.98
		VTE	21.39	29.13	29.36	22.43	16.90	13.90	12.06
200	2000.00	ATE	70.95	73.15	76.78	81.53	81.40	85.09	87.64
		XTE	33.39	36.21	65.21	85.38	80.34	79.28	77.13
		VTE	19.97	13.56	17.24	16.25	14.63	14.38	14.30
300	3000.00	ATE	80.94	85.33	84.15	86.23	91.53	94.17	97.50
		XTE	91.27	90.96	34.99	82.49	82.96	80.92	79.42
		VTE	17.13	13.97	15.91	13.61	18.06	16.57	19.85
400	4000.00	ATE	87.74	91.65	94.65	96.30	99.61	100.24	102.83
		XTE	70.37	29.69	86.07	85.65	83.81	30.29	78.44
		VTE	16.32	13.14	20.46	22.93	25.75	28.32	31.67

LEGEND

ATE = Along-Track Error

XTE = Crosstrack Error

VTE = Vertical Track Error

TABLE 16. PARASITE APPROACH SIMULATION 45° COURSE ANGLE
 DECISION HEIGHT = 300 FT

DATE: 7/29/87

HELICOPTER-GROUP ACT140,
 FAA/DOT, ATLANTIC CITY AIRPORT.

BACKGROUND:

* AZ ANTENNA OPERATION IS CONICAL;

WHEN REFERENCED TO THE DTM AND CENTER LINES, ANTENNA PHASE CENTERS ARE AT:

AZ = (-13123.20 0.00 93.42)

EL = (0.00 393.70 6.50)

DME = (-12795.12 -449.47 93.42)

* UNIT IS FT OR DEG.

PARASITE PATH ON 45. DEG

DEGRADATIONS AT DH = 300.FT

A-TRACK DIST FROM DTM	PATH-BASED DEGRADATION	GRID - OFFSET TO DTM ALONG LINE-X-DTM							
		-1500.00	-1000.00	-500.00	0.00	500.00	1000.00	1500.00	
100	1000.00	ATE	89.55			84.10	81.99	79.66	75.53
		XTE	57.30			64.30	71.55	77.75	78.49
		VTE	26.01			26.07	19.49	16.02	13.76
	2000.00	ATE	87.45	85.18	83.30	83.52	80.89	79.35	79.64
		XTE	59.30	72.24	75.02	79.76	81.93	85.14	90.49
		VTE	22.97	21.57	19.57	13.23	16.77	16.15	16.34
	3000.00	ATE	92.32	89.12	89.56	84.42	83.46	82.20	78.11
		XTE	32.33	33.54	83.73	88.25	92.13	95.62	95.83
		VTE	19.22	13.32	13.69	17.74	17.73	18.06	17.81
	4000.00	ATE	90.35	86.45	87.35	84.94	84.38	79.52	80.84
		XTE	87.73	83.35	93.88	96.05	100.32	99.69	105.97
		VTE	13.59	13.21	13.27	13.37	20.62	22.76	27.01

LEGEND

ATE = Along-Track Error

XTE = Crosstrack Error

VTE = Vertical Track Error

TABLE 17. PARASITE APPROACH SIMULATION, 315° COURSE ANGLE
 DECISION HEIGHT = 300 FT

DATE: 7/27/37

HELICOPTER-GROUP ACT140,
 FAA/DOT, ATLANTIC CITY AIRPORT.

BACKGROUND:

* AZ ANTENNA OPERATION IS CONICAL;
 WHEN REFERENCED TO THE DTM AND CENTER LINES, ANTENNA PHASE CENTERS ARE AT:

AZ = (-13113.20	0.00	93.42)
EL = (0.00	393.70	6.56)
DME = (-12725.12	-449.47	93.42)

* UNIT IS FT OR DEG.

PARASITE PATH ON 315. DEG

DEGRADATIONS AT DH = 300 FT

A-TRACK DIST FROM DTM
 PATH-BASED DEGRADATION

GRID - OFFSET TO DTM ALONG LINE-X-DTM

-1500.00 -1000.00 -500.00 0.00 500.00 1000.00 1500.00

104

A-TRACK DIST FROM DTM	PATH-BASED DEGRADATION	-1500.00	-1000.00	-500.00	0.00	500.00	1000.00	1500.00
1000.00	ATE	57.49			65.22	71.36	78.43	80.52
	XTE	39.95			85.37	81.73	80.37	77.43
	VTE	26.07			26.65	19.23	16.20	14.09
2000.00	ATE	59.31	74.33	75.43	80.00	82.91	86.59	87.80
	XTE	36.87	37.34	35.32	33.77	31.36	30.71	27.27
	VTE	22.87	22.20	19.73	18.34	16.93	16.44	15.85
3000.00	ATE	76.23	83.68	83.39	87.41	91.21	91.90	92.08
	XTE	35.95	39.26	35.20	33.50	32.53	28.97	25.02
	VTE	18.33	18.32	13.91	17.54	17.63	17.32	17.07
4000.00	ATE	86.05	92.27	92.11	92.90	101.49	104.42	105.39
	XTE	33.59	30.29	36.63	32.20	35.40	33.63	30.35
	VTE	13.44	19.05	13.75	16.32	20.70	23.37	26.73

LEGEND

ATE = Along-Track Error
 XTE = Crosstrack Error
 VTE = Vertical Track Error

REFERENCED TO DTM. ANTENNA STATIONS ARE:

AZ = (-13123, 0, 98°)
 EL = (0, 321, 7°)
 DMC = (-12795, -449, 98°)

X-AXIS STANDS FOR CROSS DISTANCE FROM DTM.
 EACH CURVE STANDS FOR ONE PARALLEL DISTANCE FROM DTM.
 UNIT IS FT.

PARASITE APPROACH - PATH DEGRADATIONS

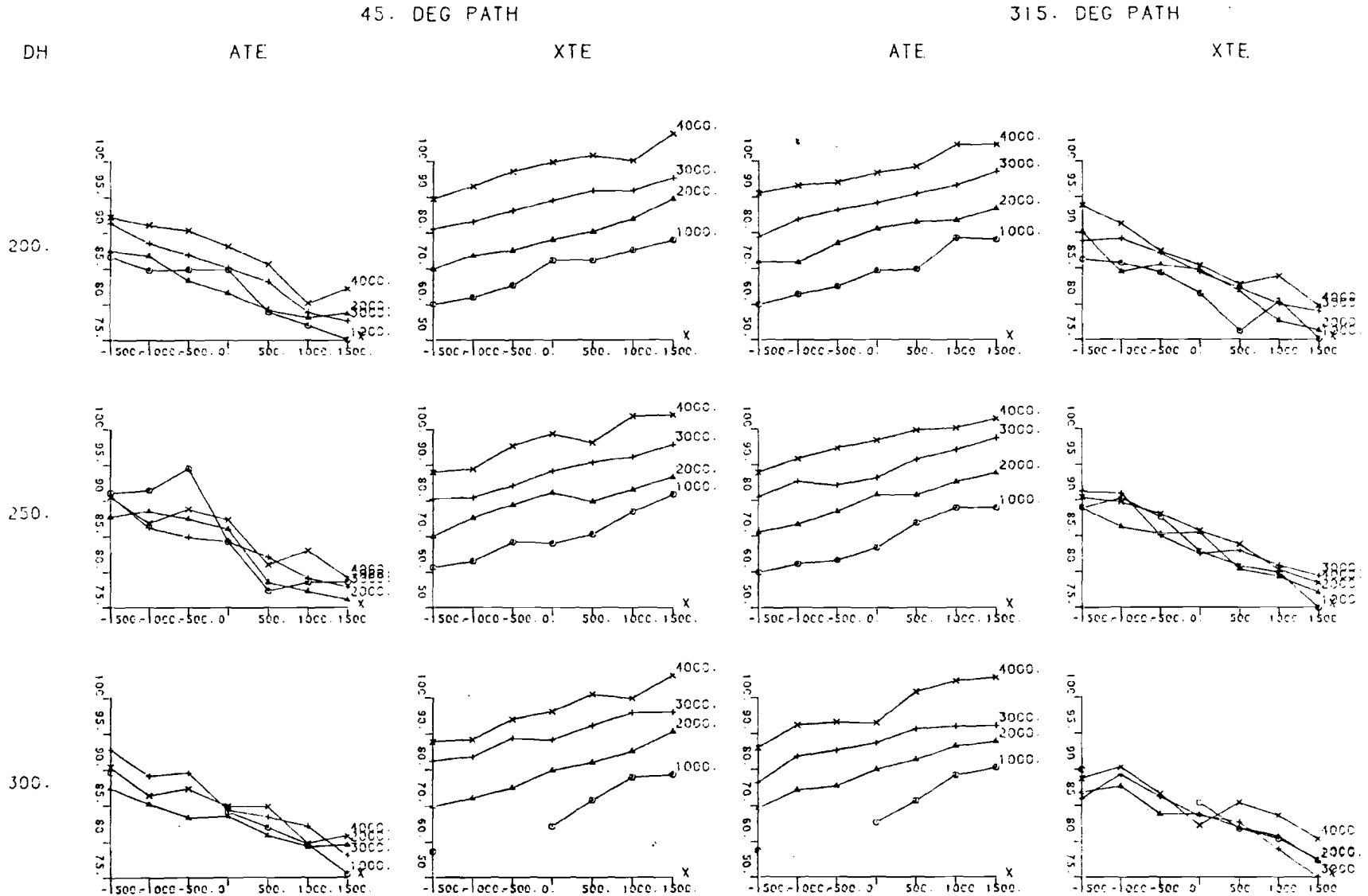


FIGURE 38. PARASITE APPROACH CROSS AND ALONG-TRACK ERROR PLOTS

DATA DATE: 7/20/87

FAA TECH. CENTER, POMONA, N. J. 08405.

REFERENCED TO DTM, ANTENNA STATIONS ARE:

AZ = (-13123, 0, 96),
EL = (0, 394, 7),
DME = (-12795, -449, 96).

X-AXIS STANDS FOR CROSS DISTANCE FROM DTM.
EACH CURVE STANDS FOR ONE PARALLEL DISTANCE FROM DTM.
UNIT IS FT.

PARASITE APPROACH - PATH DEGRADATIONS

45 DEG PATH & 315 DEG PATH

DH VTE

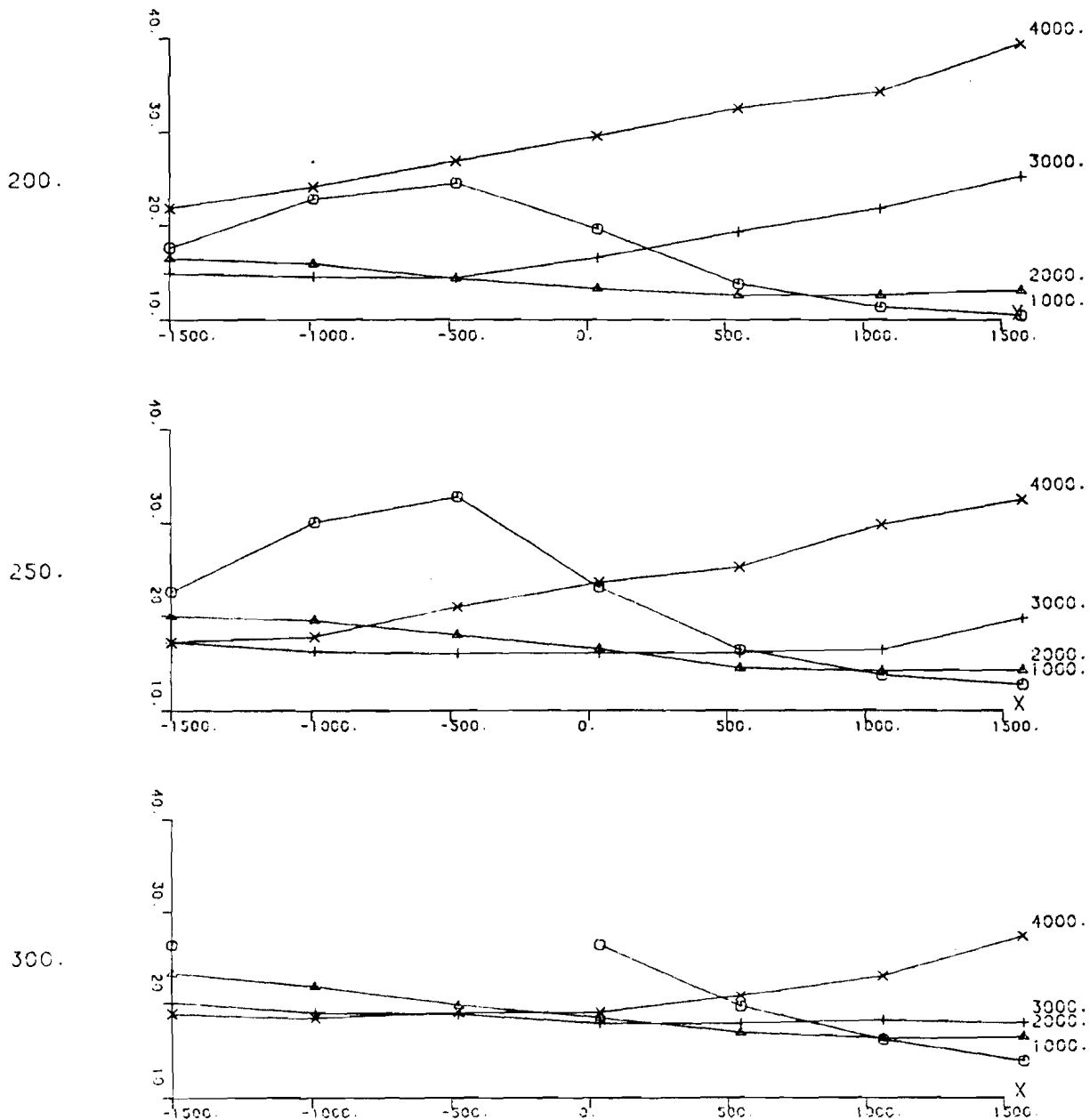


FIGURE 39. PARASITE APPROACH VERTICAL TRACK ERROR PLOTS

triples per grid evaluation point formed the basis of the 2σ accuracy calculation. Concern was expressed within the flight standards community over the normality of the distributions resulting from the Monte Carlo process. In order to address these concerns that the output data distribution was not Gaussian, a Fortran 77 program was developed. This program evaluates the skewness (asymmetry) and kurtosis (peakedness) of the 1000 cartesian triple output distribution for each test point. A skewness and kurtosis figure is then calculated for each point within the 3000 by 4000-foot test grid. Ideally, for perfectly symmetrical curves, such as the normal distribution, a skewness value equal to zero is desired. For kurtosis, a value equal to 3 is desired, since this is the value for the Gaussian distribution. An explanation of the methods used in computing the skewness and kurtosis is given as appendix C.

The results of this study are depicted in tables 18 through 23. Each table represents a different bearing (45° and 315°) and DH (200, 250, and 300-foot) combination. The values of skewness and kurtosis are tabulated over the $x=4000$ by $y=3000$ foot grid. A skewness and kurtosis pair is tabulated for along-track, crosstrack, and vertical track error at each point in the grid. Note that in all cases, the skewness, the first element of each pair (labeled S) is comparatively small, confirming the hypothesis of a symmetrical distribution. The second element of each pair (labeled K), is the kurtosis. Note that in all cases, these values are relatively close to a value of 3. This fact leads to the conclusion that the associated distribution of Monte Carlo cartesian triples obtained is a good approximation to a Gaussian distribution.

CONICAL ELEVATION INDUCED ERRORS.

Another limitation which must be considered in the assessment of MLS RNAV system accuracy is the error in vertical position which results from flying an unprocessed conical elevation signal. This error will probably be most serious in an RTCA SC-151 Level I system, such as a computed centerline type system in which the elevation unit is offset from the runway centerline and no processing of vertical deviation is performed prior to display. The net result of flying the path defined by this vertical guidance (flying a centered vertical deviation indicator (VDI)) is that the aircraft follows a hyperbolic path in space rather than the desired linear path. This hyperbolic path results in a constantly changing glide-path angle rather than a constant angle in the linear case. Another way of presenting this error is in terms of the linear vertical difference in feet between the hyperbolic and linear cases. These errors are listed in table 24 as a function of glidepath angle, DH, and offset of the elevation unit from centerline. Supplementing this tabulation are three graphical presentations of the vertical errors encountered for glidepath angles of 3° , 6° , and 9° and DH's of 200, 300, and 400 feet. These are figures 40, 41, and 42, respectively.

Some general conclusions can be reached regarding an interpretation of the forgoing data. Note that the vertical position error increases with increases in the elevation angle or magnitude of offset in the approach being simulated. Data shown on the graph can be used to identify the amount of offset which can be tolerated without causing an increase in the Category 1 approach minima when using raw elevation guidance. In theory, Category 1 approach minima could be applied across larger offset magnitudes if the vertical position error was eliminated through computed glidepath guidance.

TABLE 18. SKEWNESS AND KURTOSIS FOR PARASITE APPROACH
SIMULATION FOR 45° APPROACH AT DH = 200 FT

DATE: 3/20/87

HELICOPTER-GROUP ACT140,
FAA/DOT, ATLANTIC CITY AIRPORT.

BACKGROUNDS:

- * AZ ANTENNA OPERATION IS CONICAL;
WHEN REFERENCED TO THE DTM AND CENTER LINES, ANTENNA PHASE CENTERS ARE AT:
AZ = (-13123.20 0.00 98.42)
EL = (0.00 393.70 6.56)
DME = (-12795.12 -449.47 98.42);
- * UNIT IS FT OR DEG.

DATA NORMALITY STUDIES THROUGH SKEWNESS AND KURTOSIS

PARASITE ALONG 45. DEG AT DH = 200. FT

A-TRACK DIST FROM DTM	DATA OF	GRID - OFFSET TO DTM ALONG LINE-X-DTM													
		-1500.00		-1000.00		-500.00		0.00		500.00		1000.00		1500.00	
		S	K	S	K	S	K	S	K	S	K	S	K	S	K
1000.00	ATE	-0.04	2.38	0.00	2.72	0.13	2.74	-0.08	2.61	0.00	2.81	0.01	2.88	0.19	2.86
	XTE	-0.05	2.88	-0.01	2.72	0.11	2.73	-0.09	2.61	-0.01	2.81	-0.01	2.88	0.17	2.85
	VTE	0.11	2.92	0.10	2.73	0.22	2.81	0.08	2.60	0.20	2.83	0.19	2.91	0.33	3.02
2000.00	ATE	0.08	2.75	0.03	2.80	-0.01	2.90	-0.12	3.02	-0.08	2.97	0.00	3.07	-0.03	2.79
	XTE	0.07	2.74	0.02	2.80	-0.02	2.90	-0.13	3.03	-0.09	2.97	-0.01	3.06	-0.05	2.79
	VTE	0.18	2.73	0.14	2.81	0.12	2.92	0.01	2.97	0.04	2.96	0.12	3.13	0.06	2.80
3000.00	ATE	-0.07	2.93	-0.05	3.05	0.00	2.92	0.02	2.76	0.03	2.83	0.14	2.94	0.00	2.65
	XTE	-0.09	2.94	-0.07	3.06	-0.01	2.92	0.01	2.76	0.07	2.83	0.12	2.93	-0.02	2.65
	VTE	0.04	2.91	0.06	3.00	0.11	2.94	0.12	2.76	0.13	2.86	0.22	2.98	0.06	2.66
4000.00	ATE	0.06	2.66	0.08	2.73	0.08	2.92	-0.04	3.14	0.05	2.88	-0.02	2.88	-0.05	2.75
	XTE	0.05	2.66	0.06	2.72	0.06	2.91	-0.06	3.14	0.04	2.88	-0.03	2.88	-0.06	2.75
	VTE	0.15	2.60	0.17	2.76	0.16	2.98	0.07	3.17	0.14	2.91	0.06	2.88	0.02	2.75

LEGEND

ATE = Along-Track Error
XTE = Crosstrack Error
VTE = Vertical Track Error

TABLE 19. SKEWNESS AND KURTOSIS FOR PARASITE APPROACH SIMULATION
FOR 315° APPROACH AT DH = 200 FT

DATE: 6/20/87

HELICOPTER-GROUP ACT140,
FAA/DOT, ATLANTIC CITY AIRPORT.

BACKGROUNDS:

- * AZ ANTENNA OPERATION IS CONICAL;
WHEN REFERENCED TO THE DTM AND CENTER LINES, ANTENNA PHASE CENTERS ARE AT:
AZ = (-13123.20 0.00 98.42)
EL = (0.00 393.70 6.56)
DME = (-12795.12 -449.47 98.42);
- * UNIT IS FT OR DEG.

DATA NORMALITY STUDIES THROUGH SKEWNESS AND KURTOSIS

PARASITE ALONG 315. DEG AT DH = 200. FT

A-TRACK DIST FROM DTM	DATA OF	GRID - OFFSET TO DTM ALONG LINE-X-DTM													
		-1500.00		-1000.00		-500.00		0.00		500.00		1000.00		1500.00	
		S	K	S	K	S	K	S	K	S	K	S	K	S	K
1000.00	ATE	-0.11	2.87	-0.10	2.95	0.02	3.01	-0.03	2.97	-0.09	2.97	-0.06	2.92	-0.04	3.13
	XTE	0.09	2.87	0.09	2.95	-0.04	3.01	0.02	2.97	0.07	2.97	0.05	2.92	0.02	3.13
	VTE	0.06	2.87	0.02	2.96	0.15	3.03	0.16	3.00	0.13	3.00	0.15	2.91	0.15	3.14
2000.00	ATE	0.06	2.81	-0.04	2.79	-0.07	2.61	-0.09	2.94	0.09	2.92	-0.06	2.78	-0.10	3.07
	XTE	-0.07	2.81	0.03	2.79	0.06	2.61	0.07	2.94	-0.11	2.92	0.04	2.78	0.03	3.06
	VTE	0.18	2.85	0.08	2.78	0.05	2.62	0.06	2.95	0.23	2.98	0.05	2.75	0.02	3.03
3000.00	ATE	0.04	2.87	0.01	2.94	-0.03	2.46	0.01	2.94	-0.11	3.02	0.07	2.86	-0.01	2.81
	XTE	-0.05	2.87	-0.02	2.94	0.02	2.46	-0.02	2.94	0.10	3.01	-0.03	2.86	0.00	2.81
	VTE	0.16	2.89	0.13	2.95	0.06	2.46	0.12	2.99	0.00	2.97	0.17	2.89	0.08	2.83
4000.00	ATE	0.01	2.95	0.09	2.77	-0.08	2.90	-0.12	2.90	-0.02	2.92	-0.03	2.94	0.02	2.90
	XTE	-0.02	2.94	-0.10	2.77	0.07	2.89	0.11	2.90	0.01	2.93	0.01	2.94	-0.03	2.90
	VTE	0.13	2.95	0.20	2.31	0.03	2.89	-0.02	2.89	0.08	2.95	0.07	2.94	0.10	2.90

LEGEND

ATE = Along-Track Error
XTE = Crosstrack Error
VTE = Vertical Track Error

TABLE 20. SKEWNESS AND KURTOSIS FOR PARASITE APPROACH SIMULATION
FOR 45° APPROACH AT DH = 250 FT

DATE: 3/20/87

HELICOPTER-GROUP ACT140,
FAA/DOT, ATLANTIC CITY AIRPORT.

BACKGROUNDS:

- * AZ ANTENNA OPERATION IS CONICAL;
WHEN REFERENCED TO THE DTM AND CENTER LINES, ANTENNA PHASE CENTERS ARE AT:
AZ = (-13123.20 0.00 98.42)
EL = (0.00 393.79 6.56)
DME = (-12795.12 -449.47 98.42);
- * UNIT IS FT OR DEG.

DATA NORMALITY STUDIES THROUGH SKEWNESS AND KURTOSIS

PARASITE ALONG 45. DEG AT DH = 250. FT

A-TRACK DIST FROM DTM	DATA OF	GRID - OFFSET TO DTM ALONG LINE-X-DTM													
		-1500.00		-1000.00		-500.00		0.00		500.00		1000.00		1500.00	
		S	K	S	K	S	K	S	K	S	K	S	K	S	K
1000.00	ATE	-0.05	2.87	0.04	3.09	0.04	2.95	-0.06	2.88	0.09	2.73	0.01	2.83	0.05	2.86
	XTE	-0.06	2.87	0.02	3.03	0.02	2.95	-0.03	2.89	0.08	2.73	0.00	2.83	0.04	2.86
	VTE	0.10	2.85	0.15	3.17	0.16	2.99	0.12	2.85	0.27	2.82	0.19	2.89	0.21	2.93
2000.00	ATE	0.10	2.90	0.14	3.09	0.10	2.98	0.01	2.74	-0.10	2.95	0.06	3.10	0.13	2.84
	XTE	0.08	2.89	0.13	3.03	0.03	2.97	0.00	2.74	-0.11	2.95	0.04	3.10	0.12	2.83
	VTE	0.19	2.93	0.26	3.17	0.22	3.05	0.12	2.76	0.02	2.94	0.17	3.17	0.22	2.87
3000.00	ATE	-0.16	2.82	-0.02	2.87	0.02	2.93	-0.08	3.08	-0.03	3.27	-0.05	2.73	-0.03	2.79
	XTE	-0.17	2.82	-0.03	2.86	0.00	2.93	-0.10	3.03	-0.05	3.27	-0.06	2.73	-0.04	2.80
	VTE	-0.06	2.79	0.08	2.91	0.12	2.95	0.02	3.06	0.07	3.29	0.02	2.71	0.04	2.79
4000.00	ATE	0.03	2.75	-0.09	2.85	0.03	2.81	-0.06	2.79	0.02	2.81	0.02	2.78	0.06	2.90
	XTE	0.06	2.75	-0.10	2.86	0.06	2.81	-0.07	2.79	0.01	2.81	0.01	2.78	0.05	2.90
	VTE	0.15	2.79	-0.01	2.81	0.16	2.83	0.02	2.79	0.09	2.83	0.09	2.80	0.13	2.92

LEGEND

ATE = Along-Track Error
XTE = Crosstrack Error
VTE = Vertical Track Error

TABLE 21. SKEWNESS AND KURTOSIS FOR PARASITE APPROACH SIMULATION
FOR 315° APPROACH AT DH = 250 FT

DATE: 8/20/37

HELICOPTER-GROUP ACT140,
FAA/DOT, ATLANTIC CITY AIRPORT.

BACKGROUNDS:

- * AZ ANTENNA OPERATION IS CONICAL;
WHEN REFERENCED TO THE DTM AND CENTER LINES, ANTENNA PHASE CENTERS ARE AT:
AZ = (-13123.20 0.00 98.42)
EL = (0.00 393.70 6.56)
DME = (-12795.12 -449.47 98.42);
- * UNIT IS FT OR DEG.

DATA NORMALITY STUDIES THROUGH SKEWNESS AND KURTOSIS

PARASITE ALONG 315. DEG AT DH = 250. FT

A-TRACK DIST FROM DTM	DATA OF	GRID - OFFSET TO DTM ALONG LINE-X-DTM													
		-1500.00		-1000.00		-500.00		0.00		500.00		1000.00		1500.00	
		S	K	S	K	S	K	S	K	S	K	S	K	S	K
1000.00	ATE	-0.09	2.62	-0.08	2.90	0.02	2.88	-0.01	3.12	0.06	2.75	0.04	2.91	0.02	2.79
	XTE	0.03	2.62	0.06	2.90	-0.04	2.89	-0.01	3.12	-0.07	2.75	-0.06	2.91	-0.03	2.79
	VTE	0.05	2.61	0.04	2.33	0.14	2.93	0.20	3.16	0.26	2.79	0.25	2.94	0.13	2.82
2000.00	ATE	0.05	2.90	-0.12	3.08	-0.19	3.02	-0.06	3.28	-0.17	2.97	-0.03	2.86	-0.03	2.84
	XTE	-0.06	2.90	0.11	3.08	0.17	3.01	0.04	3.28	0.16	2.96	0.07	2.85	0.02	2.83
	VTE	0.16	2.95	0.01	3.02	-0.05	2.93	0.11	3.32	-0.04	2.91	0.03	2.85	0.07	2.83
3000.00	ATE	-0.06	2.95	-0.12	2.72	0.05	2.84	-0.02	2.86	0.00	2.86	0.02	3.08	-0.23	2.90
	XTE	0.05	2.95	0.11	2.71	-0.06	2.84	0.01	2.85	-0.01	2.86	-0.03	3.07	0.21	2.89
	VTE	0.06	2.94	-0.02	2.63	0.16	2.67	0.03	2.85	0.10	2.85	0.12	3.07	-0.14	2.83
4000.00	ATE	-0.07	2.64	-0.07	2.85	0.01	2.76	0.02	2.86	-0.06	3.12	0.00	2.86	0.09	2.73
	XTE	0.06	2.64	0.06	2.85	-0.03	2.76	-0.04	2.87	0.04	3.12	-0.01	2.86	-0.11	2.74
	VTE	0.02	2.63	0.03	2.33	0.11	2.78	0.12	2.90	0.04	3.12	0.09	2.86	0.17	2.76

LEGEND

ATE = Along-Track Error
XTE = Crosstrack Error
VTE = Vertical Track Error

TABLE 22. SKEWNESS AND KURTOSIS FOR PARASITE APPROACH SIMULATION
FOR 45° APPROACH AT DH = 300 FT

DATE: 8/20/87

HELICOPTER-GROUP ACT140,
FAA/DOT, ATLANTIC CITY AIRPORT.

BACKGROUNDS:

- * AZ ANTENNA OPERATION IS CONICAL;
WHEN REFERENCED TO THE DTM AND CENTER LINES, ANTENNA PHASE CENTERS ARE AT:
AZ = (-13123.20 0.00 98.42)
EL = (0.00 393.70 6.56)
DME = (-12795.12 -449.47 98.42);
- * UNIT IS FT OR DEG.

DATA NORMALITY STUDIES THROUGH SKEWNESS AND KURTOSIS

PARASITE ALONG 45. DEG AT DH = 300. FT

A-TRACK DIST FROM DTM	DATA OF	GRID - OFFSET TO DTM ALONG LINE-X-DTM													
		-1500.00		-1000.00		-500.00		0.00		500.00		1000.00		1500.00	
		S	K	S	K	S	K	S	K	S	K	S	K	S	K
1000.00	ATE	-0.02	2.91					0.00	2.79	0.08	2.89	0.01	2.86	-0.07	2.99
	XTE	-0.04	2.92					-0.02	2.79	0.06	2.89	0.00	2.86	-0.09	2.99
	VTE	0.12	2.86					0.17	2.84	0.28	2.97	0.20	2.91	0.09	2.92
2000.00	ATE	0.08	3.01	-0.03	2.72	-0.08	2.80	0.08	2.98	0.07	2.74	-0.05	3.01	-0.03	2.80
	XTE	0.06	3.01	-0.04	2.72	-0.09	2.81	0.07	2.98	0.05	2.74	-0.07	3.01	-0.04	2.80
	VTE	0.17	3.05	0.06	2.74	0.03	2.80	0.20	3.01	0.17	2.75	0.06	3.02	0.05	2.81
3000.00	ATE	-0.12	2.89	0.08	2.87	-0.08	2.82	0.04	3.16	-0.13	2.81	0.12	2.83	0.00	2.76
	XTE	-0.13	2.89	0.06	2.86	-0.10	2.82	0.03	3.16	-0.14	2.82	0.11	2.83	-0.01	2.76
	VTE	-0.02	2.87	0.17	2.93	0.01	2.82	0.15	3.16	-0.04	2.79	0.20	2.86	0.07	2.75
4000.00	ATE	-0.03	2.75	-0.14	3.05	0.13	2.98	-0.15	2.92	0.07	2.63	-0.04	2.75	0.13	2.88
	XTE	-0.04	2.75	-0.15	3.06	0.12	2.97	-0.16	2.92	0.05	2.63	-0.05	2.75	0.12	2.87
	VTE	0.35	2.76	-0.05	3.02	0.21	3.01	-0.07	2.88	0.13	2.65	0.03	2.74	0.20	2.92

LEGEND

ATE = Along-Track Error
XTE = Crosstrack Error
VTE = Vertical Track Error

TABLE 23. SKEWNESS AND KURTOSIS FOR PARASITE APPROACH SIMULATION
FOR 315° APPROACH AT DH = 300 FT

DATE: 3/20/87

HELICOPTER-GROUP ACT140,
FAA/DOT, ATLANTIC CITY AIRPORT.

BACKGROUNDS:

- * AZ ANTENNA OPERATION IS CONICAL;
WHEN REFERENCED TO THE DTM AND CENTER LINES, ANTENNA PHASE CENTERS ARE AT:
AZ = (-13123.20 0.00 98.42)
EL = (0.00 393.70 6.56)
DME = (-12795.12 -449.47 98.42);
- * UNIT IS FT OR DEG.

DATA NORMALITY STUDIES THROUGH SKEWNESS AND KURTOSIS

PARASITE ALONG 315. DEG AT DH = 300. FT

A-TRACK DIST FROM DTM	DATA OF	GRID - OFFSET TO DTM ALONG LINE-X-DTM													
		-1500.00		-1000.00		-500.00		0.00		500.00		1000.00		1500.00	
		S	K	S	K	S	K	S	K	S	K	S	K	S	K
1000.00	ATE	-0.03	3.00					0.06	2.89	-0.02	2.88	0.04	3.04	-0.11	2.78
	XTE	0.01	3.00					-0.10	2.90	0.00	2.88	-0.05	3.04	0.10	2.78
	VTE	0.13	3.00					0.28	3.01	0.20	2.92	0.26	3.07	0.06	2.75
2000.00	ATE	0.06	2.87	-0.02	2.97	0.02	2.88	0.04	2.92	-0.04	2.86	0.01	3.25	-0.03	2.85
	XTE	-0.07	2.87	0.01	2.97	-0.03	2.87	-0.05	2.93	0.03	2.87	-0.02	3.25	0.02	2.85
	VTE	0.16	2.91	0.10	2.94	0.14	2.85	0.17	2.97	0.08	2.90	0.15	3.27	0.07	2.88
3000.00	ATE	-0.05	2.92	0.01	2.83	-0.01	2.69	-0.05	3.01	0.04	3.03	-0.07	2.81	-0.08	2.88
	XTE	0.04	2.92	-0.02	2.84	0.00	2.69	0.04	3.01	-0.05	3.03	0.05	2.81	0.06	2.88
	VTE	0.06	2.91	0.12	2.88	0.09	2.71	0.06	3.02	0.14	3.03	0.02	2.82	0.01	2.83
4000.00	ATE	0.09	2.99	-0.01	2.82	0.02	2.62	0.08	2.86	-0.09	2.84	0.05	2.95	0.00	3.14
	XTE	-0.11	2.99	0.00	2.82	-0.03	2.62	-0.09	2.87	0.07	2.83	-0.07	2.96	-0.02	3.15
	VTE	0.20	3.03	0.06	2.83	0.10	2.63	0.17	2.89	0.00	2.83	0.14	2.99	0.09	3.19

LEGEND

ATE = Along-Track Error
XTE = Crosstrack Error
VTE = Vertical Track Error

TABLE 24. VERTICAL POSITION ERROR (FEET) DUE TO OFFSET OF CONIC ELEVATION

Approach		3.0	4.5	6.0	9.0
DH		200 ft	250 ft	300 ft	350 ft
	0	0	0	0	0
	100	0	0	0	0
	200	0	0	1	1
	300	1	1	2	3
	400	1	2	3	6
	500	2	3	5	9
	600	2	4	7	13
	700	3	6	9	17
	800	4	8	12	22
	900	5	10	15	28
	1000	7	12	18	34
	1100	8	15	22	41
	1200	10	17	25	48
	1300	11	20	30	56
	1400	13	23	34	64
	1500	15	26	39	73
	1600	17	30	44	82
	1700	19	34	49	92
	1800	21	37	55	101
	1900	23	41	60	112
	2000	26	45	66	122
	2100	28	50	72	133
	2200	31	54	79	144
	2300	34	59	85	155
	2400	36	63	92	167
	2500	39	68	99	178

MLS RNAV SIMULATION
GP ERRORS V.S. VARIOUS EL ANTENNA OFFSETS ON 3DEG GLIDE PATH
PREPARED BY ACT140/FAA ATLANTIC CITY AIRPORT N.J. - DEC. 85

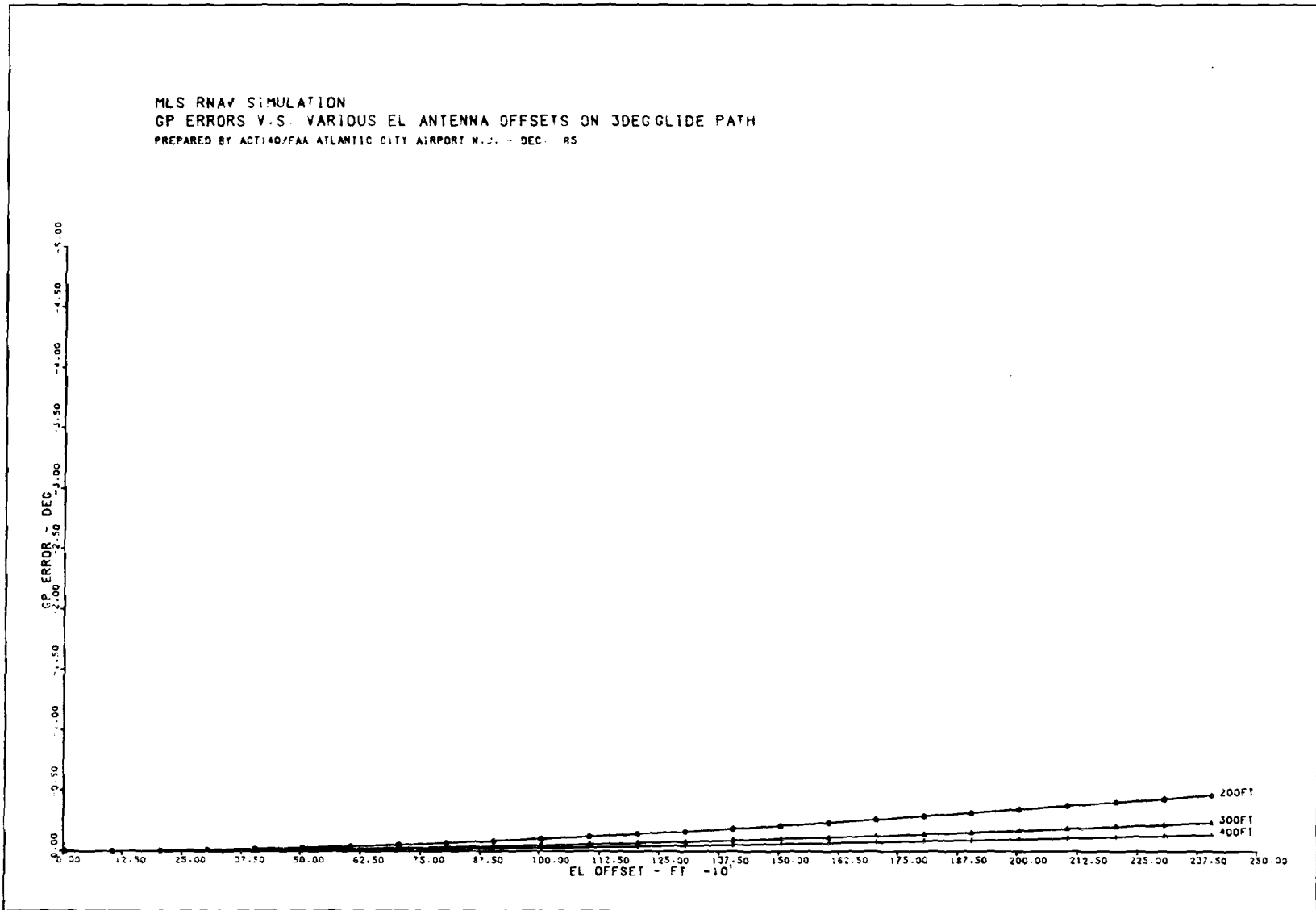


FIGURE 40. GLIDEPATH ERROR FOR OFFSET ELEVATION (EL = 3°)

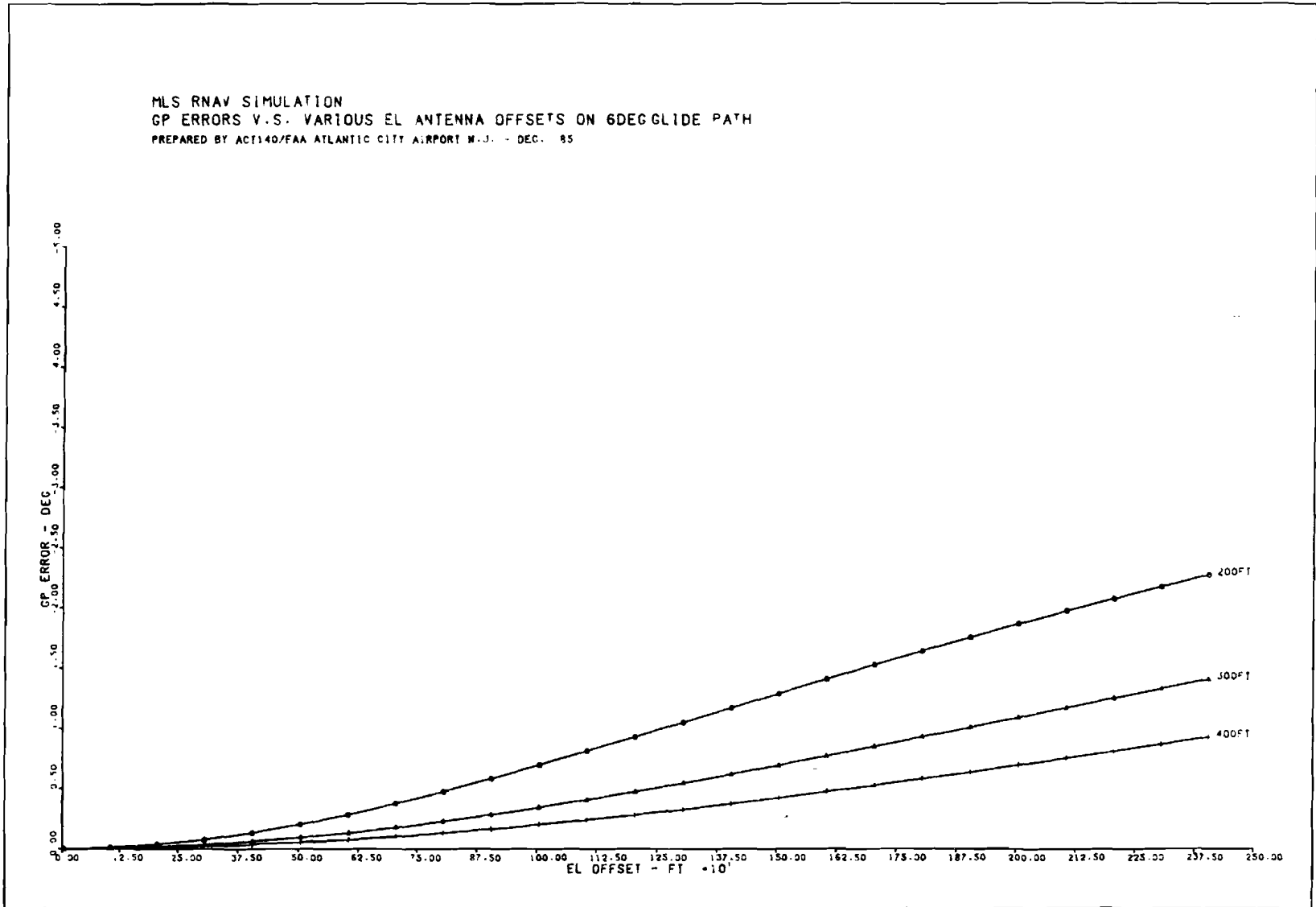


FIGURE 41. GLIDEPATH ERROR FOR OFFSET ELEVATION (EL = 6°)

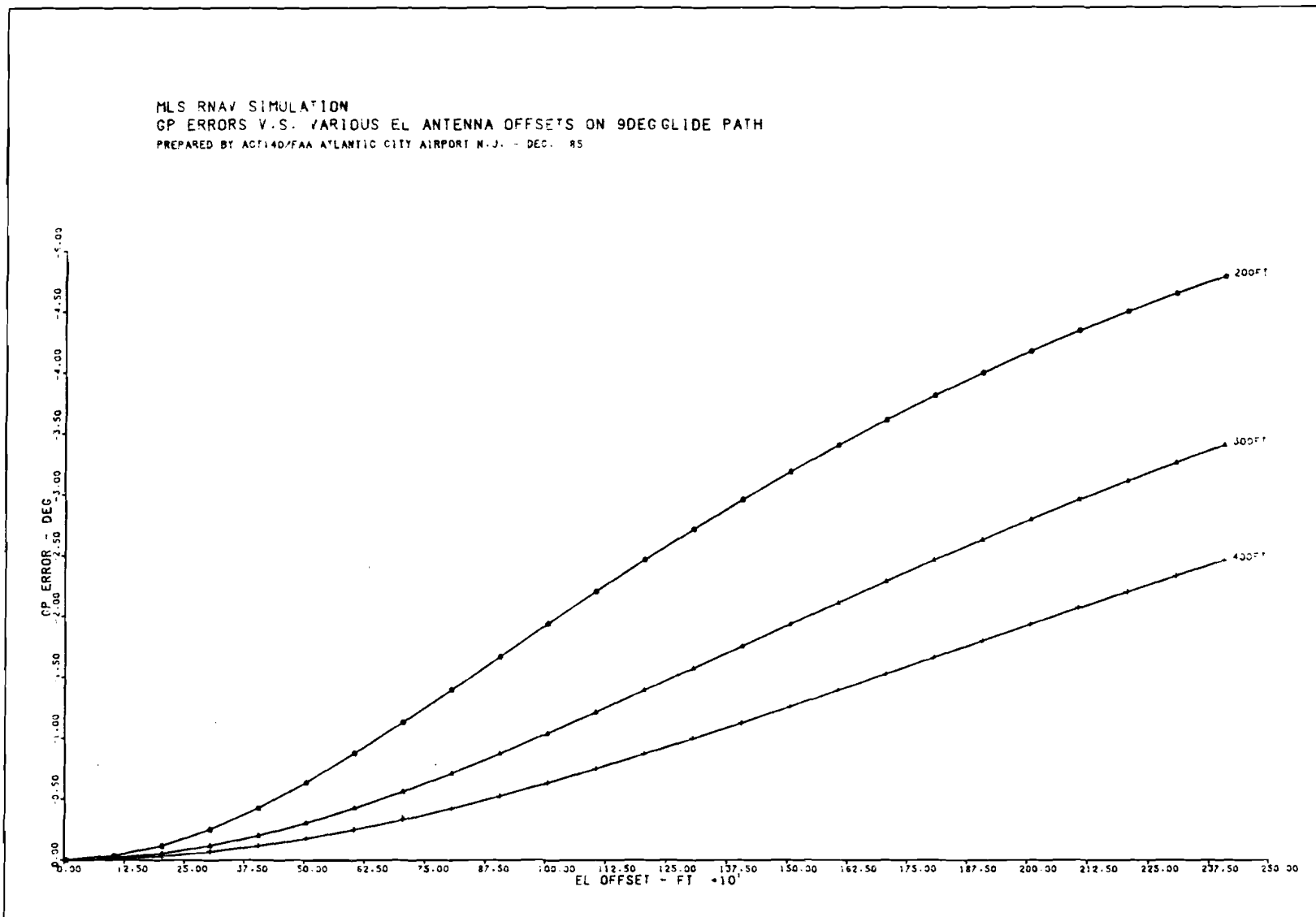


FIGURE 42. GLIDEPATH ERROR FOR OFFSET ELEVATION (EL = 9°)

In addition to those already described, other methods of presenting the errors attributable to a laterally displaced elevation transmitter were developed. The error values obtained correspond to MLS datum point referenced glidepath angles of 2.5°, 3.0°, 3.5°, and 4.0°, respectively. The results are divided into three parts. Part I, tables 25 through 28, give the vertical threshold crossing error in feet when a fixed glide angle is flown from an offset elevation transmitter whose antenna phase center is level with the datum point. Part I, tables 29 through 32, give the same vertical error for an antenna phase center located 8 feet above the MLS datum point. Part II tabulates the angular error which results at threshold when a constant elevation angle is flown. This is listed in tables 33 through 36 and is the difference between the elevation angle and the ground point of intercept (GPI) referenced glidepath angle (along the runway centerline). Part III lists the equivalent elevation angles which would have to be entered and flown in order to yield the equivalent centerline reference glidepath angle. These results are listed in tables 37 through 40.

The values tabulated in parts I, II, and III are listed as functions of elevation/GPI distance (1000, 1200, and 1500 feet) and elevation offset distance (200, 300, 400, 500, and 600 feet). It should be noted that all results have been calculated on a strictly geometric basis and, as such, do not include additional error factors such as signal source, transmission, and receiver errors. For reference purposes, a mathematical description of the methods used in calculating the elevation offset induced errors are included as appendix D.

Several conclusions can be drawn from the data generated in these analyses. First, it is apparent that the MLS threshold crossing errors which result are not insignificant. They vary from less than a foot at shallow angles and smaller elevation offsets to approximately 20 feet at the larger offsets, elevation angles, and phase center heights. Under similar conditions, the angular errors obtained varied from less than 0.05° to nearly 0.7°. It should be noted that these errors are made larger by increasing elevation angle and elevation offset distance as well as antenna height. They are decreased as the elevation to threshold distance is increased.

SUMMARY OF RESULTS

1. A total of 12 MLS to cartesian coordinate transformation algorithms were developed. These algorithms were all tested in the lab over a synthesized grid of space approximating the MLS volume of coverage and were found to converge to a solution within the specified 0.1-foot tolerance. All 12 algorithms were tested on a Digital Equipment Corporation (DEC) VAX-11/750 minicomputer and were written in VAX-11 FORTRAN. The VAX-11/750 is a 32-bit machine with floating point accelerator (FPA) support, operating under the VAX VMS operating system version 4.3. VAX-11 FORTRAN is DEC's implementation of the American National Standards Institute (ANSI) standard FORTRAN 77. Additionally, the case III algorithm was also tested on a Zenith PC-150 and a Zenith PC-248 personal computer. The PC-150 is an 8086 based microcomputer and has arithmetic

TABLE 25. PART I, MLS THRESHOLD CROSSING ERRORS (FT)
EL ANGLE = 2.5°

EL Angle = 2.5 (degrees)		EL Phase Center Height = 0.0 (ft)				
		EL Offset Distance (ft)				
		200	300	400	500	600
1000.0	EL/GPI to Threshold	0.86466	1.92242	3.36333	5.15348	7.25603
1200.0	Distance (ft)	0.72270	1.61247	2.83408	4.36609	6.18417
1500.0		0.57958	1.29699	2.28860	3.54260	5.04500

TABLE 26. PART I, MLS THRESHOLD CROSSING ERRORS (FT)
EL ANGLE = 3.0°

EL Angle = 3.0 (degrees)		EL Phase Center Height = 0.0 (ft)				
		EL Offset Distance (ft)				
		200	300	400	500	600
1000.0	EL/GPI to Threshold	1.03788	2.30755	4.03713	6.18590	8.70967
1200.0	Distance (ft)	0.86748	1.93551	3.40184	5.24078	7.42308
1500.0		0.69569	1.55682	2.74708	4.25231	6.05569

TABLE 27. PART I, MLS THRESHOLD CROSSING ERRORS (FT)
EL ANGLE = 3.5°

EL Angle = 3.5 (degrees)		EL Phase Center Height = 0.0 (ft)				
		EL Offset Distance (ft)				
		200	300	400	500	600.
1000.0	EL/GPI to Threshold	1.21126	2.69303	4.71154	7.21927	10.16464
1200.0	Distance (ft)	1.01239	2.25884	3.97013	6.11626	8.66312
1500.0		0.81191	1.81689	3.20599	4.96266	7.06731

TABLE 28. PART I, MLS THRESHOLD CROSSING ERRORS (FT)
EL ANGLE = 4.0°

EL Angle = 4.0 (degrees)		EL Phase Center Height = 0.0 (ft)				
		EL Offset Distance (ft)				
		200	300	400	500	600
1000.	EL/GPI to Threshold	1.38482	3.07892	5.38667	8.25374	11.62116
1200.0	Distance (ft)	1.15746	2.58252	4.53902	6.99268	9.90449
1500.0		0.92825	2.07724	3.66539	5.67378	8.08000

TABLE 29. PART I, MLS THRESHOLD CROSSING ERRORS (FT)
 EL ANGLE = 2.5°, EL PHASE CENTER HEIGHT = 8.0 FT

EL Angle = 2.5 (degrees)		EL Phase Center Height = 8.0 (ft)				
		EL Offset Distance (ft)				
		200	300	400	500	600
1000.0	EL/GPI to Threshold	8.86466	9.92242	11.36333	13.15348	15.25603
1200.0	Distance (ft)	8.72270	9.61247	10.83408	12.36609	14.18417
1500.0		8.57958	9.29699	10.28860	11.54260	13.04500

TABLE 30. PART I, MLS THRESHOLD CROSSING ERRORS (FT)
 EL ANGLE = 3.0°, EL PHASE CENTER HEIGHT = 8.0 FT

EL Angle = 3.0 (Degrees)		EL Phase Center Height = 8.0 (ft)				
		EL Offset Distance (ft)				
		200	300	400	500	600
1000.0	EL/GPI to Threshold	9.03788	10.30755	12.03713	14.18590	16.70967
1200.0	Distance (ft)	8.86748	9.93551	11.40184	13.24078	15.42308
1500.0		8.69569	9.55682	10.74708	12.25231	14.05569

TABLE 31. PART I, MLS THRESHOLD CROSSING ERRORS (FT)
 EL ANGLE = 3.5°, EL PHASE CENTER HEIGHT = 8.0 FT

EL Angle = 3.5 (degrees)		EL Phase Center Height = 8.0 (ft)				
		EL Offset Distance (ft)				
		200	300	400	500	600
1000.0	EL/GPI to Threshold	9.21126	10.69303	12.71154	15.21927	18.16464
1200.0	Distance (ft)	9.01239	10.25884	11.97013	14.11626	16.66312
1500.0		8.81191	9.81689	11.20599	12.96266	15.06731

TABLE 32. PART I, MLS THRESHOLD CROSSING ERRORS (FT)
 EL ANGLE = 4.0°, EL PHASE CENTER HEIGHT = 8.0 FT

EL Angle = 4.0 (degrees)		EL Phase Center Height = 8.0 (ft)				
		EL Offset Distance (ft)				
		200	300	400	500	600
1000.0	EL/GPI to Threshold	9.38482	11.07892	13.38667	16.25374	19.62116
1200.0	Distance (ft)	9.15746	10.58252	12.53902	14.99268	17.90449
1500.0		8.92825	10.07724	11.66539	13.67378	16.08000

TABLE 33. PART II, MLS THRESHOLD CROSSING ERRORS (DEGREES)
EL ANGLE = 2.5°

EL Angle = 2.5 (degrees)

	EL Offset Distance (ft)				
	200	300	400	500	600
1000.0	0.04945	0.10993	0.19231	0.29464	0.41481
EL/GPI to Threshold					
1200.0	0.03444	0.07684	0.13505	0.20804	0.29464
Distance (ft)					
1500.0	0.02210	0.04945	0.08725	0.13505	0.19231

TABLE 34. PART II, MLS THRESHOLD CROSSING ERRORS (DEGREES)
EL ANGLE = 3.0°

EL Angle = 3.0 (degrees)

	EL Offset Distance (ft)				
	200	300	400	500	600
1000.0	0.05930	0.13183	0.23063	0.35334	0.49742
EL/GPI to Threshold					
1200.0	0.04130	0.09215	0.16196	0.24948	0.35334
Distance (ft)					
1500.0	0.02650	0.05930	0.10463	0.16196	0.23063

TABLE 35. PART II, MLS THRESHOLD CROSSING ERRORS (DEGREES)
EL ANGLE = 3.5°

EL Angle = 3.5 (Degrees)

	EL Offset Distance (ft)				
	200	300	400	500	600
1000.0	0.06914	0.15370	0.26887	0.41190	0.57984
EL/GPI to Threshold					
1200.0	0.04816	0.10744	0.18881	0.29085	0.41190
Distance (ft)					
1500.0	0.03090	0.06914	0.12199	0.18881	0.26887

TABLE 36. PART II, MLS THRESHOLD CROSSING ERRORS (DEGREES)
EL ANGLE = 4.0°

EL Angle = 4.0 (degrees)

	EL Offset Distance (ft)				
	200	300	400	500	600
1000.0	0.07895	0.17551	0.30701	0.47032	0.66204
EL/GPI to Threshold					
1200.0	0.05499	0.12269	0.21561	0.33211	0.47032
Distance (ft)					
1500.0	0.03528	0.07895	0.13930	0.21561	0.30701

TABLE 37. PART III, MLS THRESHOLD EQUIVALENT ELEVATION ANGLES (DEGREES)
EL ANGLE = 2.5°

EL Angle = 2.5 (degrees)

	EL Offset Distance (ft)				
	200	300	400	500	600
1000.0	2.45451	2.39469	2.32139	2.23635	2.14409
EL/GPI to Threshold					
1200.0	2.46603	2.42545	2.37186	2.30791	2.23635
Distance (ft)					
1500.0	2.47810	2.45151	2.41569	2.37186	2.32139

TABLE 38. PART III, MLS THRESHOLD EQUIVALENT ELEVATION ANGLES (DEGREES)
EL ANGLE = 3.0°

EL Angle = 3.0 (degrees)

	EL Offset Distance (ft)				
	200	300	400	500	600
1000.	2.94185	2.87370	2.78578	2.68377	2.57310
EL/GPI to Threshold					
1200.0	2.95925	2.91058	2.84631	2.76961	2.68377
Distance (ft)					
1500.0	2.97373	2.94185	2.89888	2.84631	2.78578

TABLE 39. PART III, MLS THRESHOLD EQUIVALENT ELEVATION ANGLES (DEGREES)
EL ANGLE = 3.5°

EL Angle = 3.5 (degrees)

	EL Offset Distance (ft)				
	200	300	400	500	600
1000.0	3.43220	3.35274	3.25023	3.13127	3.00221
EL/GPI to Threshold					
1200.0	3.45249	3.39575	3.32080	3.23136	3.13127
Distance (ft)					
1500.0	3.46937	3.43220	3.38210	3.32080	3.25023

TABLE 40. PART III, MLS THRESHOLD EQUIVALENT ELEVATION ANGLES (DEGREES)
EL ANGLE 4.0°

EL ANGLE = 4.0 (DEGREES)

	EL OFFSET DISTANCE (FT)				
	200.	300.	400.	500.	600.
1000.	3.92257	3.83182	3.71474	3.57887	3.43145
EL/GPI TO THRESHOLD					
1200.	3.94575	3.88094	3.79535	3.69319	3.57887
DISTANCE (FT)					
1500.	3.96502	3.92257	3.86536	3.79335	3.71474

coprocessor support, running under Microsoft MS-DOS disk operating system version 2.0. The Zenith PC-248 is an 80286 based microcomputer that also has arithmetic coprocessor support, running under Microsoft MS-DOS disk operating system version 3.0. The programs for use on the Zenith systems were written in Microsoft Corporation's Implementation of the ANSI standard FORTRAN 77. In all cases this software was found to execute within 20 milliseconds and was within the accuracy specified for Category I operations.

2. Monte Carlo simulations of computed centerline approach operations employing a case I MLS transformation algorithm were performed. These simulations include the effects of MLS signal source error. Crosstrack errors encountered ranged from 0 to 80 feet, with the worst values occurring at large glidepath angles and elevation unit offsets from centerline. Increasing azimuth/DME/P to elevation unit spacing lowers the crosstrack error. Along-track error is fairly constant at 100 feet. A slight improvement is noted as the azimuth/DME/P to elevation unit spacing is lowered.

3. Monte Carlo simulations of generalized parasite approach operations were conducted using a case XII MLS transformation algorithm. These simulations included MLS signal source errors which varied as a function of position in MLS space. Approach angles of 45° and 315° and terminal waypoints over a 3000 by 4000-foot grid were simulated. DH's of 200, 250, and 300 feet were modeled. Crosstrack and along-track errors ranged from approximately 57 to 107 feet, the extremes of this range being observed at the extremities of the test grid. Vertical track errors were observed to vary from approximately 10 to 39 feet; again, the extremes were observed near the limits of the grid. Skewness and kurtosis studies were run on the simulation output data and indicated close conformance to a normal distribution.

4. When the MLS elevation unit is offset from the runway centerline, and vertical deviation information is not processed in the RNAV computer (but is displayed raw, as in a case I algorithm) errors due to the conicality of the elevation signal result. In the simple case of an approach along the centerline, the aircraft follows a hyperbolic rather than linear glidepath. The resulting error in feet increases with elevation offset distance, glidepath angle, and DH. Vertical errors obtained spanned the range from 0 to 178 feet. When referenced to threshold, these errors are found to increase significantly over the previous DH referenced cases since the hyperbolic and linear paths diverge more at close-in ranges (e.g., for a 3° path at 600-foot offset, the DH figure yields 2 feet vs. the threshold value of 6 to 9 feet, depending on elevation to threshold distance).

CONCLUSIONS

1. Accuracy in position determination is the prime consideration in microwave landing system area navigation (MLS RNAV). When the required site ground geometry is known, the most accurate (and general) MLS Transformation Algorithm should be employed. This will minimize error added by the transformation process. Of course this is dependent upon the availability of the necessary computer processing power.

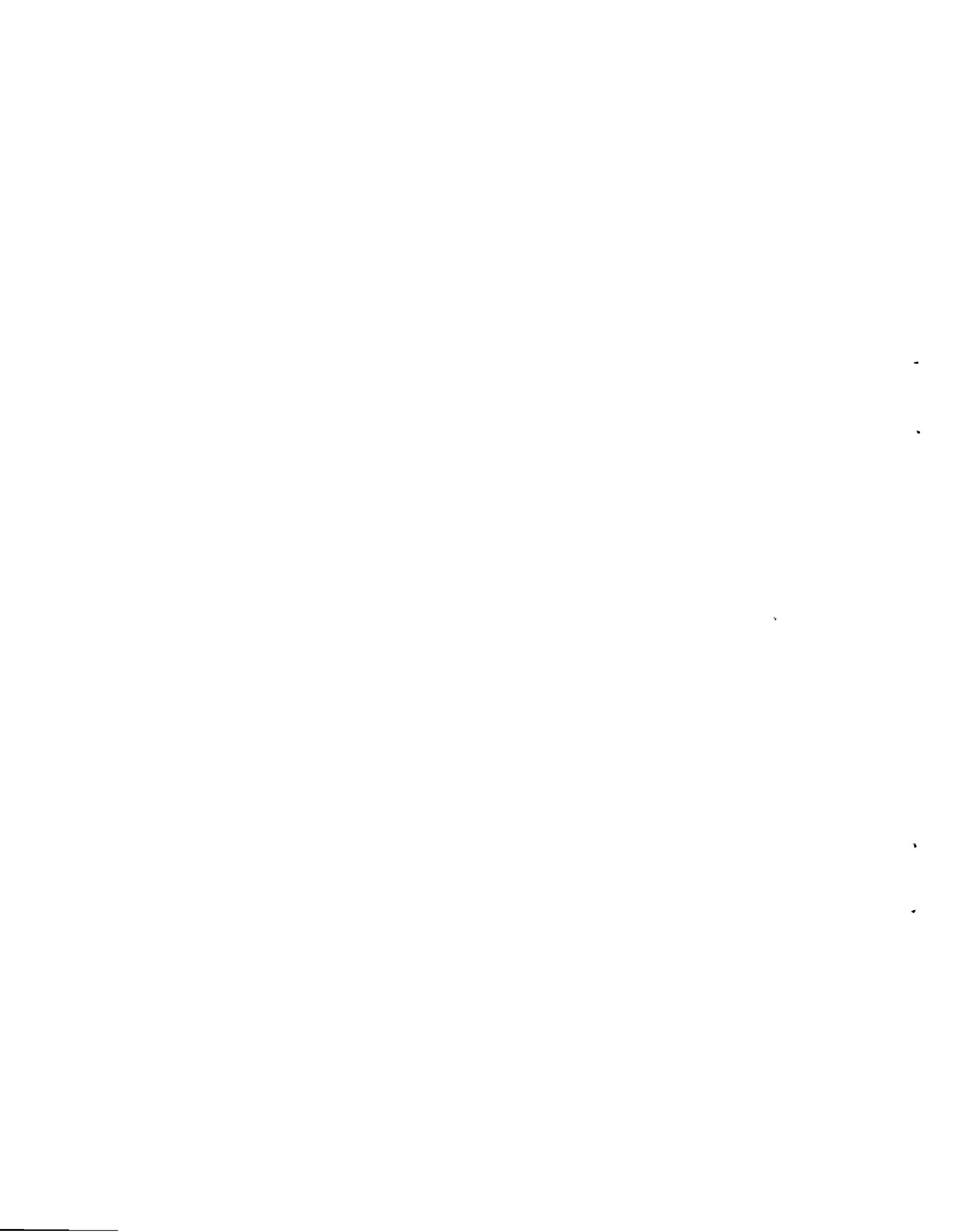
2. When the azimuth transmitter is offset due to siting restrictions category I approach minima may still be obtainable through the use of computed centerline techniques. Testing over glide slope values of 2° to 9° , azimuth transmitter to elevation transmitter distances of 3,000 to 10,000 feet and offset azimuth values of up to 2,500 feet has shown that category I approach minima are possible in some regions. However, each application must be reviewed individually since position determination accuracy is influenced by a combination of factors including azimuth transmitter offset, the distance between the azimuth and elevation transmitters and approach glide slope.

3. The ability to execute parasite approaches over a wide range of terminal waypoints, DH's and approach angles has been demonstrated analytically. However, MLS signal source error degradation over the volume of coverage, as outlined in item 4, Bibliography, results in larger error tolerances off the 0° azimuth and/or the 3° elevation. This fact causes larger across-track, vertical and along-track errors when making parasite approaches. Additionally, since DME/P accuracy heavily impacts MLS RNAV crosstrack accuracy when not paralleling the 0° azimuth, parasite approach accuracies would be considerably reduced as the final approach course biasing of the 0° reference azimuth increases.

4. Another limitation of MLS RNAV which must be considered is the error in vertical position which results from attempting to fly a linear descent path while using a raw conical elevation signal. For certain shallow angle glidepaths, small offsets, and centerline approaches it will be possible to maintain the stated minima while using the unprocessed elevation signal. However, for larger glidepath angles, elevation offset distances, and decision heights, it will be necessary to process the elevation signal using a case XI or XII algorithm to compensate for conic signal propagation and maintain required accuracy.

BIBLIOGRAPHY

1. Minimum Operational Performance Standards for Airborne MLS Area Navigation Equipment, Ninth Draft, Radio Technical Commission for Aeronautics, Special Committee 151, Washington, D.C., February 1987.
2. Redlien, Henry W. and Kelly, Robert J., Microwave Landing System: The New International Standard, Advances in Electronics and Electron Physics, Vol. 57, Academic Press Inc., New York, New York, 1981.
3. Townsend, J. E., Engineering Flights on the Bendix Small Community MLS, Runway 33, Washington National Airport, FAA Technical Center Letter Report, CT-82-100-102LR, September 1982.
4. Microwave Landing System (MLS) Interoperability and Performance Requirements, FAA-STD-022C, U.S. Department of Transportation, Federal Aviation Administration, June 1986.
5. Approval of Area Navigation Systems for Use in the U.S. National Airspace System, Advisory Circular 90-45A, U.S. Department of Transportation, Federal Aviation Administration, February 1980.



APPENDIX A
CARTESIAN TO MLS COORDINATE TRANSFORMATIONS

Sited Antenna Coordinates:

Azimuth Antenna - (Xa,Ya,Za)
DME Antenna - (Xd,Yd,Zd)

Elevation Antenna - (Xe,Ye,Ze)
MLS Datum Point - (Xm,Ym,Zm)

Aircraft Coordinates: (relative to MLS datum point)

Actual - (X,Y,Z)

Computed - (X',Y',Z')

Computed MLS Coordinates

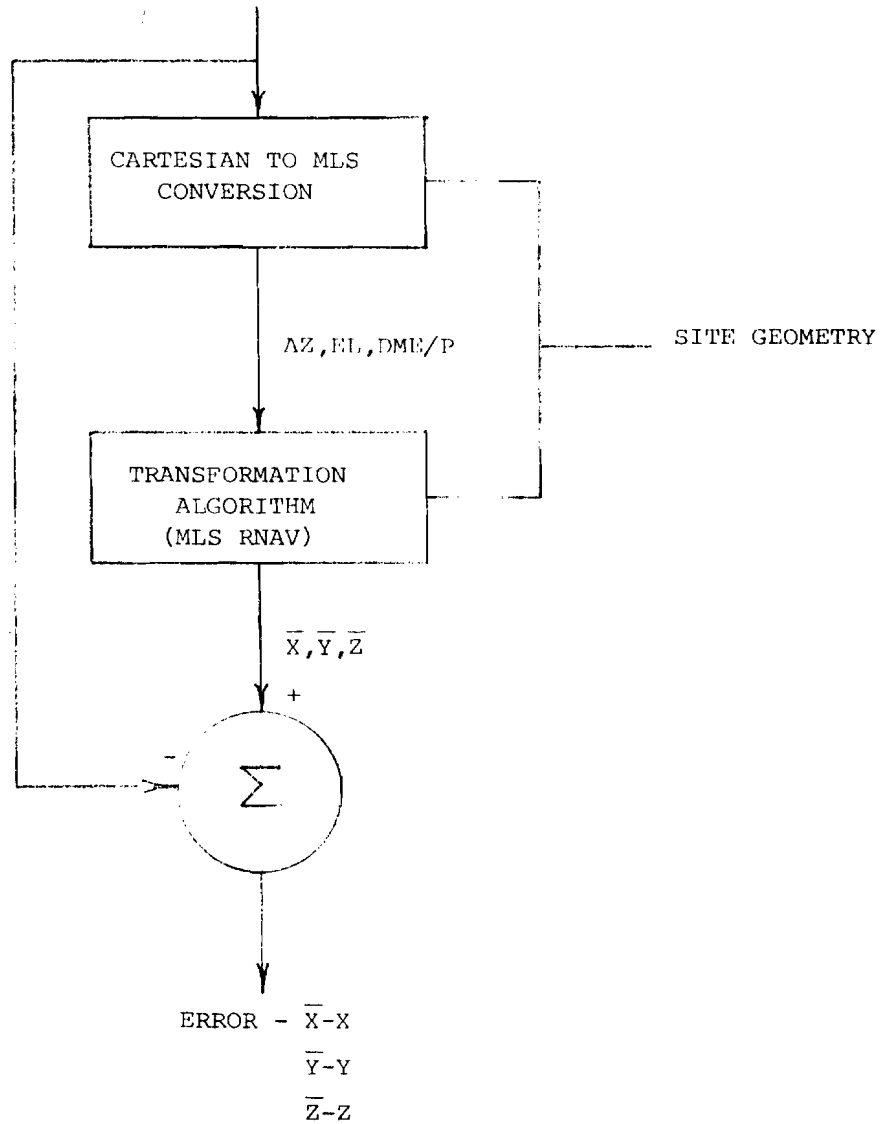
$$DME = ((X-Xd)^2 + (Y-Yd)^2 + (Z-Zd)^2)^{1/2}$$

$$AZ = \text{SIN}^{-1} \frac{-(Y-Ya)}{((X-Xa)^2 + (Y-Ya)^2 + (Z-Za)^2)^{1/2}}$$

$$EL = \text{SIN}^{-1} \frac{(Z-Ze)}{((X-Xe)^2 + (Y-Ye)^2 + (Z-Ze)^2)^{1/2}}$$

TRUTH MODEL

X, Y, Z OF AIRCRAFT



MLS TRANSFORMATION

ALGORITHM VALIDATION

FLOW CHART

APPENDIX B

MLS SIGNAL ACCURACY DEGRADATION

● Azimuth Signal Error: $\Delta\theta_{2\sigma}$ (Angular PFE in Degrees)

1. For elevation values less than 9° ($\theta < 9^\circ$)

$$\Delta\theta_{2\sigma} = \pm \text{TAN}^{-1}\left(\frac{13.5'}{R}\right) \left[1 + .5 \left| \frac{\theta}{40^\circ} \right| + .2 \left(\frac{\rho - R}{20\text{nm}} \right) \right]$$

Limited to a maximum of $\pm .25^\circ$

where:

ρ = DME/P

R = Runway centerline distance from azimuth station to MLS reference datum

θ = Azimuth angle in degrees

2. For elevation values greater than or equal to 9° , but less than or equal to 15° ($9^\circ \leq \theta \leq 15^\circ$)

$$\Delta\theta_{2\sigma} = \pm \text{TAN}^{-1}\left(\frac{13.5'}{R}\right) \left[1 + .5 \left| \frac{\theta}{40^\circ} \right| + .2 \left(\frac{\rho - R}{20\text{nm}} \right) + .5 \left(\frac{\theta - 9^\circ}{6^\circ} \right) \right]$$

Limited to a maximum of $\pm .50^\circ$

where θ = elevation angle

Use $\Delta\theta_{2\sigma}$ by generating random variables from a normal distribution having $\sigma = 2 \Delta\theta_{2\sigma}$ and then adding these values to the nominal value of θ being flown to obtain a perturbed value of θ .

● Elevation Signal Error: $\Delta\phi_{2\sigma}$ (Angular PFE in Degrees)

1. For elevation angles from 3° (or 60 percent of minimum glidepath angle, whichever is less) to the elevation coverage extreme. For purposes of simulation, this means: $0.9^\circ \leq \phi \leq 3^\circ$

$$\Delta\phi_{2\sigma} = \pm 0.133^\circ \left[1 + 0.2 \left| \frac{\theta}{40^\circ} \right| + 0.2 \left(\frac{\rho - R}{20\text{nm}} \right) + 2.0 \left(\frac{3.0^\circ - \phi}{2.1^\circ} \right) \right]$$

ρ = DME/P

R = Runway centerline distance from DME/P station to MLS reference datum

θ = Azimuth angle in degrees

ϕ = Elevation angle in degrees

2. For elevation angles from 3° to 15° , $3^\circ \leq \phi \leq 15^\circ$

$$\Delta\phi_{2\sigma} = \pm 0.133^\circ \left[1 + 0.2 \left| \frac{\theta}{40^\circ} \right| + 0.2 \left(\frac{\rho - R}{20\text{nm}} \right) + \left(\frac{\phi - 3^\circ}{12^\circ} \right) \right]$$

There are no maximum values specified for $\Delta\phi_{2\sigma}$

Use $\Delta\phi_{2\sigma}$ by generating random variables from a normal distribution having $\sigma = 2\Delta\phi_{2\sigma}$ and then adding these values to the nominal value of ϕ being flown to obtain a new value of ϕ .

• DME/P Signal Error: $\Delta\rho_{2\sigma}$ (Linear 2σ value in ft)

1. Over the volume of DME/P coverage:

$$\Delta\rho_{2\sigma} = \pm \left(\frac{820' - 100'}{20 \times 6076' - 0'} \right) (\rho - R) + 100'$$

where R = along centerline distance from DME/P ground antenna to runway threshold in feet.

ρ = DME/P distance in feet

$$\Delta\rho_{2\sigma} = \pm 0.00592 (\rho - R) + 100'$$

Use $\Delta\rho_{2\sigma}$ by generating random variables from a normal distribution having $\sigma = 2\Delta\rho_{2\sigma}$ and then adding these values to the nominal value of ρ being used at the DH point in order to obtain a perturbed value for ρ . A thousand ρ 's are obtained for each error calculation.

APPENDIX C

PARASITE APPROACH STUDIES
MEASURES OF SKEWNESS AND KURTOSIS

Skewness: The degree of asymmetry, or departure from symmetry, of a distribution. A frequency curve of a distribution is said to be skewed to the left (negative) or to the right (positive) if it has a longer tail away from the central maximum in that direction.

A measure of skewness:

Moment coefficient of Skewness:

$$= a_3 = \frac{m_3}{s^3} = \frac{m_3}{(\sqrt{m_2})^3}$$

where m_3 = The third moment about the mean

\bar{x} = the mean of the sample

x_j = jth sample value

N = Number of samples

$s = \sqrt{m_2}$ = standard deviation

$s^2 = m_2$ = the variance

$$m_3 = \frac{\sum_{j=1}^N (x_j - \bar{x})^3}{N}$$

$$s = \sqrt{\frac{\sum_{j=1}^N (x_j - \bar{x})^2}{N}} = \sqrt{\frac{\sum_{j=1}^N x_j^2}{N} - \left(\frac{\sum_{j=1}^N x_j}{N} \right)^2}$$

$$\bar{x} = \frac{\sum_{j=1}^N x_j}{N}$$

The moment coefficient of skewness = $a_3 = \frac{m_3}{s^3} = \frac{\sum_{j=1}^N (x_j - \bar{x})^3}{\left(\sqrt{\frac{\sum_{j=1}^N (x_j - \bar{x})^2}{N}} \right)^3}$

• For perfectly symmetrical curves, such as the normal curve, $a_3 = 0$

Kurtosis: Kurtosis is the degree of peakedness of a distribution relative to the normal distribution.

One measure of kurtosis uses the fourth moment about the mean expressed in dimensionless form and is given by:

$$\text{Moment coefficient of kurtosis} = a_4 = \frac{m_4}{s^4} = \frac{m_4}{m_2^2}$$

where:

m_4 = the fourth moment about the mean

\bar{x} = the mean of the sample

x_j = jth value of sample

N = Number of values in the sample

s^2 = Variance = m_2

$$m_4 = \frac{\sum_{j=1}^N (x_j - \bar{x})^4}{N}$$

$$s^4 = \left(\frac{\sum_{j=1}^N (x_j - \bar{x})^2}{N} \right)^2$$

For the normal distribution, $a_4 = 3$

APPENDIX D

CONIC ELEVATION INDUCED ERROR COMPUTATIONS

(x,y,z) = Test point coordinates based on linear glidepath

(x_c,y_c,z_c) = Test point coordinates based on conical elevation

(x_e,y_e,z_e) = Elevation unit antenna phase center coordinates

θ = Centerline (linear) glidepath angle

θ_c = Conical elevation angle

z = Height error

δ = Angular error

Assume all points referenced to MLS datum at (0,0,0)

The equation describing conical elevation is:

$$(x_c-x_e)^2 + (y_c-y_e)^2 = (z_c-z_e)^2 \cot^2 \theta_c \quad (1)$$

The equation describing a linear glidepath is:

$$z = x \tan \theta$$

Assuming $\theta_c = \theta$, $x_c = x$, $y_c = y$, (2)

Find the resulting height error:

$$(x-x_e)^2 + (y-y_e)^2 = (z_c-z_e)^2 \cot^2 \theta \quad (3)$$

From (3): $z_c = \left(\left((x-x_e)^2 + (y-y_e)^2 \right) \tan^2 \theta \right)^{1/2} + z_e$ (4)

From (4) and (2)

$$z = z_c - z_e = x \tan \theta - \left(\left((x-x_e)^2 + (y-y_e)^2 \right) \tan^2 \theta \right)^{1/2} + z_e \quad (5)$$

Assuming $(x_c,y_c,z_c) = (x,y,z)$

Find the resulting angular difference:

From (2):

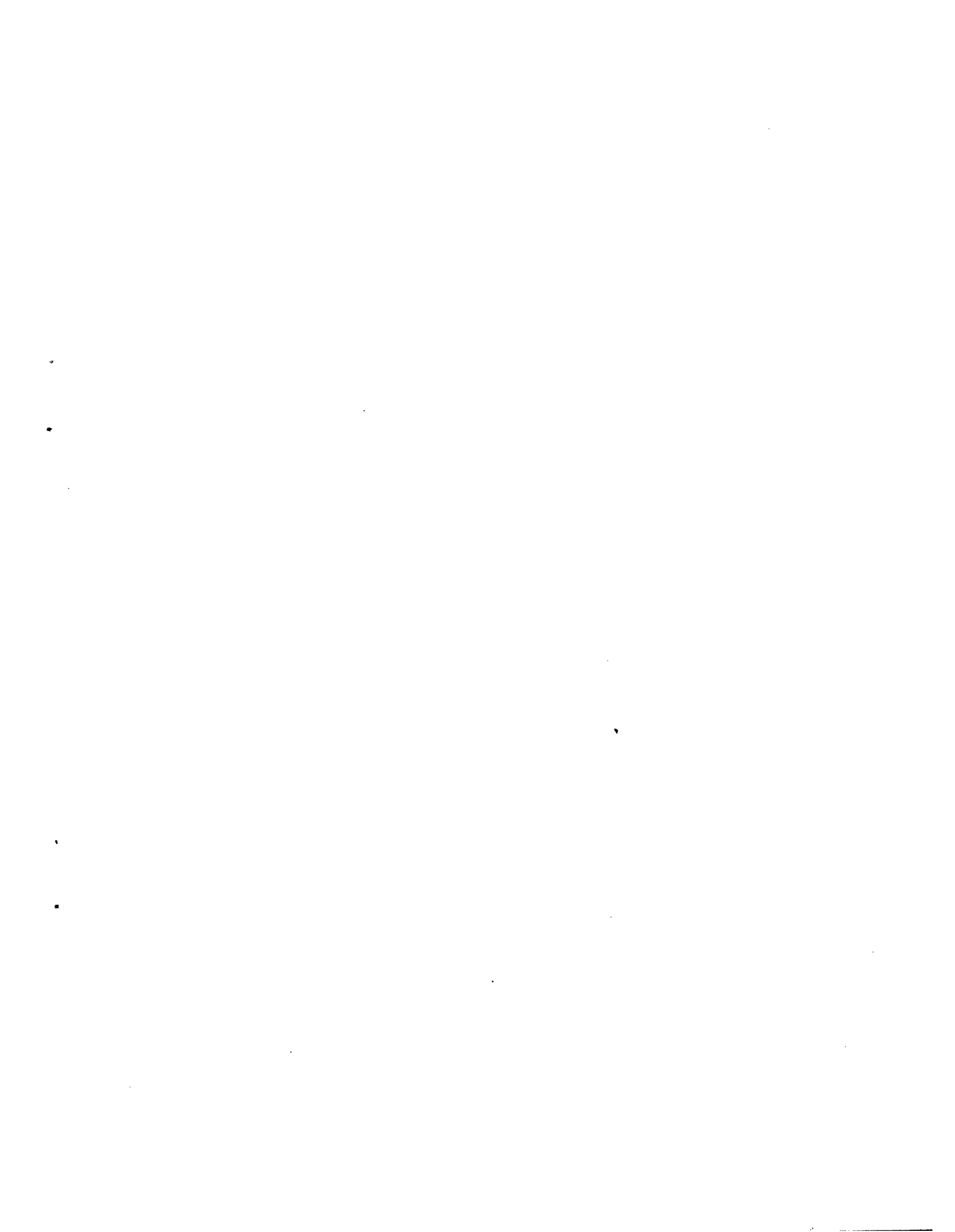
$$\theta = \tan^{-1} \frac{z}{x} \quad (6)$$

From (1)

$$\theta_c = \tan^{-1} \left(\frac{(z-z_e)^2}{(x-x_e)^2 + (y-y_e)^2} \right)^{1/2}$$

Combining (6) and (7) yields:

$$\theta = \theta - \theta_c = \tan^{-1} \frac{z}{x} = \tan^{-1} \left(\frac{(z-z_e)^2}{(x-x_e)^2 + (y-y_e)^2} \right)^{1/2}$$





•

•

•

•

11

12